

# **For Reference**

---

**NOT TO BE TAKEN FROM THIS ROOM**



Ex libris  
UNIVERSITATIS  
ALBERTAENSIS





Digitized by the Internet Archive  
in 2019 with funding from  
University of Alberta Libraries

<https://archive.org/details/Evgin1981>













THE UNIVERSITY OF ALBERTA

RELEASE FORM

NAME OF AUTHOR            ERMAN EVGIN

TITLE OF THESIS           EVALUATION OF AN ELASTO-PLASTIC MODEL

DEGREE FOR WHICH THESIS WAS PRESENTED    DOCTOR OF PHILOSOPHY

YEAR THIS DEGREE GRANTED    April 1981

Permission is hereby granted to THE UNIVERSITY OF ALBERTA LIBRARY to reproduce single copies of this thesis and to lend or sell such copies for private, scholarly or scientific research purposes only.

The author reserves other publication rights, and neither the thesis nor extensive extracts from it may be printed or otherwise reproduced without the author's written permission.

---







THE UNIVERSITY OF ALBERTA

EVALUATION OF AN ELASTO-PLASTIC MODEL

by



GERMAN EVGIN

A THESIS

SUBMITTED TO THE FACULTY OF GRADUATE STUDIES AND RESEARCH  
IN PARTIAL FULFILMENT OF THE REQUIREMENTS FOR THE DEGREE  
OF DOCTOR OF PHILOSOPHY

Civil Engineering

EDMONTON, ALBERTA

SPRING, 1981





81-170

THE UNIVERSITY OF ALBERTA  
FACULTY OF GRADUATE STUDIES AND RESEARCH

The undersigned certify that they have read, and recommend to the Faculty of Graduate Studies and Research, for acceptance, a thesis entitled EVALUATION OF AN ELASTO-PLASTIC MODEL submitted by ERMAN EVGIN in partial fulfilment of the requirements for the degree of DOCTOR OF PHILOSOPHY.





To Mireille Dubreuil





## ABSTRACT

This investigation is part of the current research effort in geotechnical engineering to integrate the deformation and stability analyses of soil structures. With the aid of recent advances made in the mathematical modelling of soil behavior, the engineering profession is now a step closer to making successful predictions for the movements of soil masses at all stages of loading up to failure. The study presented here is an attempt to evaluate the performance of Lade's work hardening stress-strain relation in an integrated analysis. Previous applications of the model carried out by others have not been fully satisfactory despite several corrections and proposed modifications.

To begin with, the original formulation of the model and subsequent modifications are re-evaluated as part of the present study. It is found that the difficulties encountered in the past are due to the nature of the hardening law of the model. For a general three dimensional problem, a unique relation between stress level and plastic work does not exist. It is shown here that, by making a suitable assumption, measured stress-strain behavior of cohesionless soils can be successfully predicted. At the same time, the problems that are created in finite element analysis can be avoided.

For further evaluation of the model, a finite element program has been developed to predict the results of passive





earth pressure tests carried out by Wong. The load-deformation response, as well as the distribution of normal stresses acting on a fully instrumented wall has been predicted with sufficient accuracy for all practical purposes. These results have shown that Lade's work hardening model works very well for the analyses of complex boundary value problems at all stages of loading. When compared with other models, such as the hyperbolic stress-strain law and the stress-dilatancy model, Lade's model gave much better results for the same wall behavior.

It is believed that the major factor in successful predictions of Lade's work hardening stress-strain relation is the reasonably accurate modelling of basic characteristics of soil behavior.





## ACKNOWLEDGMENTS

I would like to express my sincere appreciation to Professor Z. Eisenstein for suggesting this thesis topic, and for his support and understanding throughout the course of my research work.

The encouragement and help of Dr. L. Medeiros will not be forgotten. Our discussions proved very valuable.

I would also like to thank J.V. Simmons for taking the trouble to edit the thesis and A.D. Gale for his time spent in making corrections to parts of the manuscript.

Appreciation is due all my friends. Without their presence and moral support in difficult times this work would not have been completed.

Finally, I dedicate this thesis with all my love to Mireille Dubreuil whose help and understanding extend far beyond what one would expect of a friend, a wife or an intellectual companion.



## Table of Contents

Chapter	Page
<u>CHAPTER 1</u>	
INTRODUCTION .....	1
1.1 GENERAL .....	1
1.2 OBJECTIVES .....	9
1.3 ORGANIZATION OF THESIS .....	10
<u>CHAPTER 2</u>	
LADE'S ELASTO-PLASTIC WORK HARDENING MODEL .....	12
2.1 INTRODUCTION .....	12
2.2 ELASTO-PLASTIC STRESS-STRAIN RELATIONSHIP .....	13
2.2.1 Elastic Strain Increments .....	13
2.2.2 Plastic Strain Increments .....	14
2.3 LIMITATIONS .....	21
2.4 APPLICATIONS OF THE MODEL .....	22
2.5 PREVIOUS MODIFICATIONS .....	24
<u>CHAPTER 3</u>	
RE-EVALUATION OF WORK HARDENING MODEL .....	29
3.1 INTRODUCTION .....	29
3.2 VALIDITY OF PREVIOUS MODIFICATIONS .....	30
3.3 PROPOSED INTERPRETATION OF WORK HARDENING LAW ...	35
3.4 CONCLUSIONS .....	40
<u>CHAPTER 4</u>	
STRAIN SOFTENING MODEL .....	50
4.1 INTRODUCTION .....	50
4.2 STRESS-STRAIN RELATIONSHIP .....	52





4.2.1	Elastic Strain Increments .....	52
4.2.2	Plastic Strain Increments .....	53
4.2.3	Plastic Collapse Strains .....	53
4.2.4	Plastic Expansive Strains .....	56
4.3	EVALUATION OF HARDENING-SOFTENING LAW FOR PLASTIC EXPANSIVE STRAINS .....	62
4.4	REMARKS ON HARDENING LAWS FOR SOILS .....	65
4.5	CONDITIONS ESSENTIAL FOR STRAIN SOFTENING .....	66
<u>CHAPTER 5</u>		
	WORK HARDENING MODEL WITH A CAP .....	79
5.1	INTRODUCTION .....	79
5.2	TYPE OF CAP .....	79
5.3	UTILIZATION OF CAP TYPE YIELD CRITERION .....	80
5.4	JUSTIFICATION FOR WORK HARDENING MODEL WITH A CAP .....	83
5.5	PREDICTIONS OF STRESS-STRAIN BEHAVIOR .....	85
5.6	CONCLUSIONS .....	87
<u>CHAPTER 6</u>		
	FINITE ELEMENT PROCEDURES FOR WORK HARDENING MODEL ...	95
6.1	INTRODUCTION .....	95
6.2	SOLUTION METHOD FOR MATERIAL NONLINEARITY .....	96
6.3	DERIVATION OF CONSTITUTIVE MATRIX .....	97
6.4	VERIFICATION OF FINITE ELEMENT PROGRAM .....	102
6.5	CONCLUSIONS .....	107
<u>CHAPTER 7</u>		
	FINITE ELEMENT ANALYSIS OF PASSIVE EARTH PRESSURE ...	116
7.1	INTRODUCTION .....	116
7.2	EXPERIMENTAL INVESTIGATION OF PASSIVE EARTH PRESSURE PROBLEM (LITERATURE SURVEY) .....	119



7.3	EXPERIMENTAL WORK BY WONG .....	122
7.4	ANALYTICAL WORK BY WONG .....	125
7.5	PREDICTIONS BY THE FINITE ELEMENT ANALYSIS OF PRESENT STUDY .....	127
7.6	INTERPRETATION OF FINITE ELEMENT PREDICTIONS ...	134

## CHAPTER 8

	SUMMARY AND CONCLUSIONS .....	167
8.1	SUMMARY .....	167
8.2	CONCLUSIONS OF PRESENT STUDY .....	170
8.3	CLOSING REMARKS .....	174

	<u>BIBLIOGRAPHY</u> .....	175
--	---------------------------	-----

## APPENDIX A

	DERIVATION OF SOIL PARAMETERS .....	188
--	-------------------------------------	-----





## LIST OF TABLES

Table		Page
6.1	Lade's stress-strain parameters for Monterey No.0 sand .....	111
7.1	Stress-strain parameters obtained by Wong (1978) for Monterey No.0 sand. ....	147
7.2	Stress-strain parameters used in present study for Monterey No.0 sand. ....	157



## LIST OF FIGURES

Figure		Page
2.1	Elastic and plastic parts of strain in triaxial test (After Lade and Duncan (1975)) .....	27
2.2	Yield and failure surfaces in (a) principal stress space (b) loci of surfaces on octahedral plane. ....	27
2.3	Relationship between plastic work and stress level. (After Ozawa and Duncan, 1976a) .....	28
2.4	Trace of plastic potential surfaces on triaxial plane (After Duncan et al, 1977) .....	28
3.1	Stress-path with increasing deviator stress and constant confining pressure. Monterey No.0 Sand Experimental results after Lade and Duncan (1976) .....	41
3.2	Stress-path with increasing deviator stress and decreasing confining pressure. Monterey No.0 Sand. Experimental results after Lade and Duncan (1976) .....	42
3.3	Stress-path with decreasing deviator stress and decreasing confining pressure. Monterey No.0 Sand. Experimental results after Lade and Duncan (1976) .....	43
3.4	Stress-path with increasing deviator stress and increasing confining pressure. Monterey No.0 Sand. ....	44
3.5	Stress-path with decreasing deviator stress and decreasing confining pressure. Monterey No.0 Sand. ....	45





3.6	Predicted strain increment vectors .....	46
3.7	Measured Directions of Strain Increment Vectors for Different Stress-Paths in Triaxial Plane (After Lade and Duncan, 1976) .....	47
3.8	Variation of Plastic Work for Dense Monterey No.0 Sand (After Lade and Duncan, 1976) .....	48
3.9	Stress increments with a) no change in stress level b) conventional triaxial test path followed by no change in stress level. ....	49
4.1	Schematic illustration of elastic, plastic collapse and plastic expansive strains in triaxial compression test. (After Lade ,1975) .....	69
4.2	Location of yield cap relative to conical yield surface shown in triaxial plane. (After Lade ,1975) .....	70
4.3	Relation between plastic collapse work, $W_{col}$ , and the value of $f_{col}$ for loose Sacramento River sand. (After Lade ,1975) .....	71
4.4	Determination of the value of $n_1$ and $m$ involved in the failure criterion for loose Sacramento River sand. (After Lade ,1975) .....	72
4.5	Variation of total plastic work with $f_{exp}$ and $\sigma_3$ for loose Sacramento River sand. (After Lade ,1975) .....	73
4.6	Results of a stress change a) stress paths b) $W_{exp}$ versus $f_{exp}$ relationship. ....	74
4.7	Assumption used for $df_{exp}$ versus $dW_{exp}$ relationship. ....	75
4.8	Measured stress-strain and volume change behavior for loose Sacramento River sand in drained triaxial compression test. (After Lee and Seed, 1967). ....	76



4.9	Measured stress-strain and volume change behavior for dense Sacramento River sand in drained triaxial compression test. (After Lee and Seed, 1967). . . . .	77
4.10	Relationships between void ratio after consolidation and critical confining pressure. (After Lee and Seed, 1967). . . . .	78
5.1	Example of stress paths where no plastic strain increments are predicted by the work hardening model without a cap. . . . .	89
5.2	The effect of different stress paths on the expansion of yield surfaces for work hardening model (a) without a cap (b, c, d) with a cap. ....	90
5.3	The effect of different stress paths on the expansion of yield surfaces for strain softening model. . . . .	91
5.4	Hydrostatic compression of Ottawa sand. Predictions of work hardening model with and without a cap yield criterion. ( Experimental data from NSF/NSERC Workshop on Soil Plasticity, Montreal, May 1980) . . . . .	92
5.5	Proportional loading. Predictions of work hardening model with and without a cap. Loose Monterey No. 0 sand. Experimental data after Lade and Duncan (1976) . . . . .	93
5.6	Stress path with increasing deviator stress and constant $\sigma_3$ after previous loading to a higher stress level (Experimental data after Lade and Duncan, 1976) . . . . .	94
6.1	Single degree of freedom representation of incremental-iterative procedure. . . . .	108
6.2	Results of plane strain analysis and experimental data for loose Monterey No 0 sand. (Experimental data after Ozawa, 1973) . . . . .	109





6.3	Plane strain analysis and experimental data for dense Monterey No 0 sand. (Experimental data after Ozawa, 1973) .....	110
6.4	Predictions of stress state under $K_0$ -Loading condition for loose Monterey No. 0 sand. ....	112
6.5	Predictions of stress state under $K_0$ -Loading condition for dense Monterey No. 0 sand. ....	113
6.6	Boundary conditions for the hypothetical retaining wall and the assumed initial state of stress at different depths before wall movement. .	114
6.7	Predictions of passive earth pressure for dense Monterey No. 0 sand and finite element calculations. ....	115
7.1	Relation between wall rotation and earth pressure for different densities (After Terzaghi, 1954). ....	142
7.2	Shear strain contours for dense and loose sand (After James and Bransby, 1970). ....	143
7.3	Rupture planes observed on radiographs exposed at three stages of wall rotation (After James and Bransby, 1970). ....	144
7.4	Instrumented wall for passive pressure test (After Wong, 1978). ....	145
7.5	Gradation curves for Monterey No.0 sand (After Wong, 1978). ....	146
7.6	Observed rupture planes at 10 degree wall rotation (After Wong, 1978). ....	148
7.7	Experimental results for dense sand. Vari stresses and passive earth pressure coefficient with the angle of wall rotation. (After Wong, 1978). ....	149



7.8	Experimental results for medium dense sand. Variations of average normal and shear stresses and passive earth pressure coefficient with the angle of wall rotation. (After Wong, 1978). ....	150
7.9	Experimental results for dense sand. Distribution of normal and shear stresses on four panels of the wall. (After Wong, 1978). ....	151
7.10	Experimental results for medium dense sand. Distribution of normal and shear stresses on four panels of the wall. (After Wong, 1978). ....	152
7.11	Summary of Wong's work for dense sand. Comparisons of measured normal stresses with finite element calculations. (After Wong, 1978). ....	153
7.12	Summary of Wong's work for medium dense sand. Comparisons of measured normal stresses with finite element calculations. (After Wong, 1978). ....	154
7.13	Relation between active and passive earth pressure coefficient and horizontal strain. ....	155
7.14	Predictions for $\sigma_{vert} = \text{const.}$ tests with $\sigma_{horz.}$ increasing to failure. ....	156
7.15	Experimental results and predictions of present study for dense Monterey No.0 sand in plane strain tests. (Experimental data after Lade, 1972) ....	158
7.16	Finite element mesh and boundary conditions for the analysis of rigid wall. ....	159
7.17	Variation of average normal stress with wall rotation for dense Monterey No.0 sand. ....	160
7.18	Distribution of normal stresses along the wall for dense Monterey No.0 sand. ....	161
7.19	Zones of high stress level as a function of wall rotation for dense Monterey No. 0 sand. ....	162



7.20	Variation of average normal stress with wall rotation for medium dense Monterey No.0 sand. ...	163
7.21	Distribution of normal stresses along the wall for medium dense Monterey No.0 sand. ....	164
7.22	Zones of high stress level as a function of wall rotation for medium dense Monterey No. 0 sand. ..	165
7.23	Contours of cumulative shear strains and volumetric strains at 2 degree wall rotation for medium dense Monterey No. 0 sand. ....	166
A.1	Three drained conventional triaxial compression tests for dense Monterey No.0 sand. (After Lade, 1972) .....	192
A.2	Derivation of parameters for elastic strains ....	193
A.3	Variation of $K_2$ with stress level for dense Monterey No.0 sand. ....	194
A.4	Variation of plastic work with stress level for dense Monterey No.0 sand. ....	195
A.5	Transformed plastic work curves for dense Monterey No.0 sand. ....	196
A.6	Variation of initial slope of plastic curves with confining pressure for dense Monterey No.0 sand. ....	197





## LIST OF SYMBOLS

### Roman Letters

- $A, A_1, A_2$  -Plastic potential parameters for Lade's work hardening model
- $C$  -Parameter in hardening law for plastic collapse strains
- $[C^e]$  -Elastic stress-strain matrix
- $[C^{ep}]$  -Elastic-plastic stress-strain matrix
- $D_r$  -Relative density
- $E$  -Young's modulus
- $E_{ur}$  -Unloading-reloading modulus
- $F$  -Yield function
- $f$  -Stress level in work hardening model
- $f_{col}$  -Stress level for cap yield surface
- $f_{exp}$  -Stress level for cone yield surface
- $f_t$  -Treshold stress level
- $g$  -Plastic potential function in work hardening model
- $g_{col}$  -Plastic potential function associated with plastic collapse strains
- $g_{exp}$  -Plastic potential function associated with plastic



expansive strains

$I_1, I_2, I_3$  -Stress invariants

$K_1$  -Failure parameter in work hardening model

$K_0$  -Coefficient of earth pressure at rest

$K_p$  -Coefficient of passive earth pressure

$K_{ur}$  -Elastic unloading-reloading parameter

$l$  -(First use)Hardening parameter in Lade's work hardening law

$l$  -(Second use)Parameter for plastic work at peak stress level

$m$  -Parameter responsible for the curvature of yield surface in strain softening model

$M$  -Hardening parameter in Lade's work hardening law

$n$  -Elastic unloading-reloading parameter

$n_1$  -Stress level at failure for strain softening model

$n_2$  -Parameter in plastic potential function

$p$  -Parameter in hardening law for plastic collapse strains

$P$  -Parameter for plastic work at peak stress level

$P_a$  -Atmospheric pressure

$R$  -Parameter in plastic potential function





$r_f$	-Asymptotic ratio in Lade's work hardening model
$S$	-Parameter in plastic potential function
$t$	-Parameter in plastic potential function
$W_p$	-Total plastic work
$W_{col}$	-Total plastic work due to plastic collapse strains
$W_{exp}$	-Total plastic work due to plastic expansive strains

### Greek Letters

$\alpha$	-(First use)Plastic potential parameter in Lade's work hardening model
$\alpha$	-(Second use)Parameter used in hardening law of strain softening model
$\beta$	-Parameter used in hardening law of strain softening model
$\Delta\epsilon$	-Strain increment
$\Delta\sigma$	-Stress increment
$\lambda$	-Proportionality constant
$\lambda_{col}$	-Proportionality constant for plastic collapse strains
$\lambda_{exp}$	-Proportionality constant for plastic expansive strains



$\epsilon$	-Total strains
$\epsilon_{col}$	-Plastic collapse strains
$\epsilon^e$	-Elastic strains
$\epsilon_{exp}$	-Plastic expansive strains
$\epsilon^p$	-Plastic Strains
$\epsilon_v$	-Total volumetric strains
$\nu$	-Poisson's ratio
$\sigma_1 \sigma_2 \sigma_3$	-Principal stresses
$\sigma_{ij}$	-Stress tensor
$\phi$	-Friction angle



## CHAPTER 1

### INTRODUCTION

#### 1.1 GENERAL

In classical soil mechanics, the problems of deformation and stability are treated separately. Combined with experience, these methods provide satisfactory results for most geotechnical engineering problems. However, the response of a soil mass to loading is one continuous process, and the classical approach is therefore artificial. In some deformation problems, it is quite possible to have local yielding even at high factors of safety. Similarly, when collapse takes place, not all elements of a soil mass are in a state of failure; some regions may still be undergoing loading or even unloading. Considering that the aim of a stability analysis, at least for some problems, is to find the most economical way of avoiding failure, the collapse load needs to be predicted as accurately as possible. Further, the mechanism of failure is mainly a function of the stress distribution which can only be found, in general, by using a deformation analysis capable of simulating all loading stages prior to instability.

One of the principal requirements for an integrated analysis of deformations and failure is a constitutive relationship suitable for modelling the stress-strain behavior of soil correctly up to and beyond the peak





strength. This challenge has been taken by a growing number of researchers since the first establishment of the Cam-clay model (Roscoe et al, 1958) which marked the beginning of a modern approach to modelling and fundamental understanding of the mechanical behavior of soils.

Soil behavior under controlled laboratory conditions has been investigated in great detail and is well documented in the literature. Even under these ideal conditions soil behavior is extremely complicated in comparison to other engineering materials. Consequently, constitutive laws which aim to model most aspects of soil behavior tend to become highly complex. Considering that the behavior of natural soils is affected by many other factors such as anisotropy, non-homogeneity, time and temperature effects, the task of developing mathematical models becomes very demanding if every aspect of soil behavior is to be accounted for.

While the importance of developing constitutive models is indicated and the complexity of the developer's work is acknowledged, the size of the remaining work required to complete the analysis of an engineering structure should not be underestimated. The analysis of any continuum mechanics problem requires that the field equations must be solved subject to the appropriate boundary conditions. Also, the effects of the initial state of stress and the stress history of in-situ soils have to be considered in a realistic analysis. Finite element techniques employing elastic or nonlinear elastic models have been used widely in



the past for the analysis of important soil structures, and considerable experience has already been accumulated in this area. But much more effort is required to use the complicated constitutive models in finite element analysis with the same level of confidence gained so far for linear and nonlinear elastic solutions. It should be noted that nonlinear analysis by the finite element method is still an ongoing research area requiring a high level of expertise.

In the following, the stress-strain laws which attempt to model the essential features of soil behavior such as nonlinearity, inelasticity, shear dilatancy and path dependency are referred to as "non-classical" models. This term is used in this thesis not only to point out the remarkable abilities of these models to predict the stress-strain behavior of soils, but also to suggest that their application to the analysis of soil structures may not be straight forward but full of difficulties.

It would seem that sufficiently accurate answers can be found to any geotechnical problem once the finite element programs for non-classical stress-strain laws are developed. However, one should be cautious about reaching this conclusion too quickly. Not too long ago Wroth (1976) stated that:

"It might be thought that any boundary value problem in foundation engineering, such as the behavior of



the ground around an excavation could now be completely and accurately solved by a deformation analysis using the finite element method. But it is my contention that is not so; I intend to show that the finite element method as developed at present is unable to represent in an adequate manner the discontinuous nature of the behavior of soils at failure..."

In addition to our inability to introduce the development of failure surfaces into finite element analysis, geotechnical engineering practice is also troubled in determining accurately the state of stress and the stress history of in-situ soils. This vital information is the starting point to any analysis.

Knowing that no single constitutive law describes adequately all features of soil behavior, the analyst has to make a choice of the most appropriate model which inevitably becomes a compromise. Therefore the finite element method of analysis will be useful to engineering practice only if the limitations of particular soil model and solution method are recognized.

It should also be noted that the appreciation of all the refinements of recently developed constitutive laws and the understanding of the limitations of finite element analysis are not the only issues the user or practicing





engineer has to deal with. As pointed out by Morgenstern (1975),

"Stress-strain relations for soils, either theoretical or empirical, constitute only one element in the total design procedure that involves at the very least calculations, judgement, quality control and monitoring of performance."

In relation to the application of stress-strain laws there are several important points to be considered. Some of them are discussed below.

1. So far, there has not been any comparative study available as a guideline to the users to show the capabilities and limitations of non-classical models. Not only predictions of laboratory test results but also analyses of the same engineering structures by all models considered are necessary before the true value of each model can be assessed. Therefore it is difficult to decide among a dozen or more different constitutive models which one to choose for a particular problem in hand, unless information on comparative performance, cost, availability etc has been provided.
2. For each model, testing techniques required and difficulties involved to obtain soil parameters should



be the first questions to be asked. While some models require several different types of tests, for others conventional triaxial tests are sufficient for deriving soil parameters.

3. Due to the difficulties associated with representative sampling and sample disturbance, laboratory tests often are of limited value (Lambe, 1973). Therefore the existence of a correlation between the results of present day in-situ testing techniques and the parameters of a stress-strain model has practical importance.
4. Some of the non-classical constitutive models depend heavily on curve fitting techniques to obtain soil parameters from laboratory test results. However, due to the nature of soils, it is difficult to duplicate the test results for the same type of soil even under ideal laboratory conditions. Therefore the sensitivity of each soil parameter to any slight variation in soil properties and also to the accuracy of the soil testing technique should be fully investigated. For those that vary significantly and have a considerable effect on the results of an analysis have to be determined and the analysis has to be carried out accordingly.
5. It is not always necessary to use the most complete stress-strain model in every analytical problem. The significance of modelling certain soil characteristics depends on the type of boundary value problem and the



nature of the in-situ soils. For example in some problems the time factor becomes important. For some others cyclic loading does not exist. A constitutive law capable of modelling strain softening may be attractive but a work hardening model may well be satisfactory for some problems. The use of a non-associated flow rule does not necessarily produce better results over an associated flow rule for all problems. Similarly, a failure criterion which has a curved envelope in the triaxial plane and can also account for the effect of intermediate principal stress may not be significantly superior to the Mohr-Coulomb failure criterion. So far there has not been any systematic study of real soil structures demonstrating the advantages of the effort involved to include the refinements mentioned above in an analysis. A parametric study using the type and the size of soil structure, the boundary conditions, and the kind and the state of soil as variables would be valuable for engineering practice.

6. Although some models are claimed to account for most characteristics of soil behavior, they are developed mostly on the basis of laboratory tests on kaolinite or uniform sand ("university materials"). The application of such models to the analysis of soil structures where natural materials exist may be a good test for those models.
7. Once the type of model to be used has been decided, the





availability of the finite element program specifically written for the model has to be ascertained. At this point, the difficulties involved in its use have to be determined. If modifications are required or problems are encountered during analysis, it is usually necessary to consult the developer of the program or even the developer of the model itself. These processes may greatly complicate the application of a model.

8. The cost and the time required to run a finite element program depend on the complexity of the model adopted and the refinement necessary to solve that particular problem. This can be a decisive factor in choosing a soil model for analysis depending on the size and the importance of the project.
9. Sometimes the accuracy of the results of a finite element program becomes questionable. Depending on the numerical technique used to solve the nonlinear problem, there are always approximations introduced into the analysis.
10. The reliability of the finite element program at hand should be checked carefully. For any situation different from a previous successful use, the program should be treated as suspect until proven otherwise. Every program has to go through a testing period before its results are relied upon.

The points made in this introductory section form the general framework of present study. An attempt is made to



find answers to some of the questions discussed above by using a model which is one of the most advanced stress-strain laws presently proposed. The model was developed for sand and its capabilities were demonstrated by Lade (1972). Subsequent development by Ozawa (1974) and Wong (1978) to apply the model to geotechnical engineering problems was not fruitful for reasons which will be discussed as they arise during presentation.

## 1.2 OBJECTIVES

The research effort presented here is directed towards the following objectives:

1. To find out the significance of using an elasto-plastic stress-strain law for modelling the behavior of cohesionless soils in a deformation analysis. This is accomplished:
  - a) by reviewing critically the characteristics and the limitations of the selected model as well as the modifications introduced subsequently by others.
  - b) by analyzing a well documented boundary value problem using the finite element method.
2. To investigate the reasons why the previous finite element applications of the model to geotechnical problems were not successful.
3. To compare the measured collapse load for a passive earth pressure problem against the predictions of a finite element analysis. The present day finite element



models are not capable of simulating the propagation of a thin rupture zone in a previously undetermined direction. In the selected model the soil mass which has discrete rupture surfaces at failure is approximated by a continuum with averaged deformation properties.

### 1.3 ORGANIZATION OF THESIS

In Chapter 2, the original formulation of Lade's model and the modifications suggested by others are introduced.

Chapter 3 is partly devoted to the re-evaluation of the modified form of the model. A shortcoming of the model is indicated and a new way of interpreting Lade's original formulation is proposed as part of the present study.

Although it is not used directly in any of the analyses introduced in this thesis, Lade's strain-softening model is presented in Chapter 4. One reason for its presentation is that, part of it is utilized in Chapter 5 in connection with the work hardening model. Also the problems attached to the work hardening laws of both models are found to be common. Therefore a clarification is considered to be useful for future work.

The significance of a cap-type yield surface is elaborated in Chapter 5. The cap yield surface used by Lade in his strain softening model has been selected for use in his work hardening model, which had only a cone shaped yield surface. By this means one of the major criticisms concerning unsatisfactory modelling under increasing hydrostatic stresses has been eliminated.





The development of a finite element program using Lade's work hardening model without a cap is introduced in Chapter 6.

Chapter 7 deals with the predictions of the finite element analysis of a boundary value problem. Results obtained by using finite element method are compared with the passive earth pressure tests carried out by Wong (1978).

Finally, in Chapter 8 the conclusions of this research are stated and the recommendations for future research are presented.



## CHAPTER 2

### LADE'S ELASTO-PLASTIC WORK HARDENING MODEL

#### 2.1 INTRODUCTION

The model was developed by Lade (1972) to account for several aspects of the stress-strain and strength characteristics of cohesionless soils under general three-dimensional stress conditions. To a certain extent, it has the capability for modeling:

1. Nonlinearity
2. Shear dilatancy
3. Inelasticity
4. Stress path dependency
5. Influence of intermediate principal stress
6. Coincidence of strain increment and stress increment axes at low stress levels with transition to coincidence of strain increment and stress axes at high stress levels.

The theory is based on experimental data from cubical triaxial tests on sand, and uses the concepts of the incremental theory of plasticity.

In the following sections, the theory, as introduced by Lade and Duncan (1975), is summarized, and the degree of success in its application is reviewed. The limitations of the model and modifications to overcome these limitations are also indicated.



## 2.2 ELASTO-PLASTIC STRESS-STRAIN RELATIONSHIP

For the purpose of the development of this theory, it is assumed that the total strain increments  $\{d\epsilon_{ij}\}$  can be divided into an elastic part  $\{d\epsilon_{ij}^e\}$  and a plastic part  $\{d\epsilon_{ij}^p\}$  as shown in Eqn. 2.1.

$$\{d\epsilon_{ij}\} = \{d\epsilon_{ij}^e\} + \{d\epsilon_{ij}^p\} \quad \dots\dots\dots \text{Eqn. 2.1}$$

Each part is then calculated separately. A schematic illustration of this concept is given in Figure 2.1 for a triaxial compression test.

### 2.2.1 Elastic Strain Increments

The elastic strain increments are calculated from Hooke's law, using the unloading-reloading modulus,  $E_{ur}$ , defined by Duncan and Chang (1970):

$$E_{ur} = K_{ur} \times p_a \times \left( \frac{\sigma_3}{p_a} \right)^n \quad \dots\dots\dots \text{Eqn. 2.2}$$

where  $K_{ur}$  and  $n$  are elastic unloading-reloading parameters (dimensionless) and  $p_a$  is the atmospheric pressure expressed in the same units as  $E_{ur}$  and  $\sigma_3$ . The evaluation of these parameters from triaxial tests is explained in Appendix A.

The value of Poisson's ratio is assumed to be zero. This assumption is based on triaxial test data where the





axial and volumetric strains are very nearly equal for the first increment of load.

As a result, the incremental stress-strain relationship for an elastic isotropic material takes the following form:

$$\begin{Bmatrix} d\epsilon_x^e \\ d\epsilon_y^e \\ d\epsilon_z^e \\ d\epsilon_{xy}^e \\ d\epsilon_{yz}^e \\ d\epsilon_{zx}^e \end{Bmatrix} = \begin{bmatrix} \frac{1}{E_{ur}} & & & & & \\ 0 & \frac{1}{E_{ur}} & & & & \\ & 0 & \frac{1}{E_{ur}} & & & \\ & 0 & 0 & \frac{1}{E_{ur}} & & \\ & 0 & 0 & 0 & \frac{1}{E_{ur}} & \\ & 0 & 0 & 0 & 0 & \frac{1}{E_{ur}} \\ & 0 & 0 & 0 & 0 & 0 \end{bmatrix} \begin{Bmatrix} d\sigma_x \\ d\sigma_y \\ d\sigma_z \\ d\tau_{xy} \\ d\tau_{yz} \\ d\tau_{zx} \end{Bmatrix} \quad \text{Eqn. 2.3}$$

### 2.2.2 Plastic Strain Increments

For the calculation of plastic strain increments, the model follows the basic requirements of plasticity theory as summarized by Lade and Duncan (1975) :

"There are three basic requirements for a plastic stress-strain theory:

1. There must exist a yield surface such that if the soil is subjected to changes in stress represented by points inside that surface, the soil will deform elastically, whereas if the changes in stress tend to cross the yield surface, it will simultaneously yield plastically and deform elastically. The yield surface expands as the soil is loaded to



successively higher stress levels, and at failure the yield surface coincides with the failure surface.

2. A flow rule is also required. The flow rule is a law which relates the relative magnitudes of the strain increments to the stresses. The flow rule is derived from the requirement that the plastic strain increment direction should be normal to the plastic potential surface. There are an infinite number of such surfaces, and one passes through every point in stress space. In so-called "perfect plasticity," the plastic potential surface is assumed to be the same as the yield surface. As mentioned previously, this implies much higher rates of dilation than are observed in tests on real soils. When the plastic potential surface is assumed to differ from the yield surface, i.e. when the flow rule is "non-associated," much better agreement between theory and experiment can be achieved.
3. A work-hardening law is needed, from which the magnitudes of the plastic strain increments caused by a given stress increment can be determined."



The details of Lade's model in relation to those requirements are given below:

### 1. Yield surface

The yield surface is assumed to have the shape of a cone with the apex at the coordinate center of the principal stress space as shown in Figure 2.2. It is expressed as a function of the first and third stress invariants as follows:

$$f = \frac{I_1^3}{I_3} \quad \dots\dots\dots \text{Eqn. 2.4}$$

$f$  denotes the stress level and its value varies from 27 for hydrostatic stress conditions up to a value  $K_1$  at failure. With increasing values of  $f$ , the yield surface expands continuously, and becomes identical with the failure surface at its outermost shape.

### 2. Flow Rule

A non-associated flow rule is used for this model in which the plastic potential surface is no longer assumed to be the same as the yield surface. In doing so, much better predictions for the rate of dilation are expected.

The plastic potential is a function of the state of stress, from which the relative, but not the absolute





magnitudes of the components of the plastic strain increments can be determined by differentiating with respect to stresses. The function incorporated in the theory is expressed by Lade and Duncan (1975) in a form:

$$g = I_1^3 - K_2 \times I_3 \quad \dots\dots\dots \text{Eqn. 2.5}$$

where:

$g$  is the value of the plastic potential and

$K_2$  is a constant for a given value of  $f$ . It is calculated from

$$K_2 = A \times f + 27 \times (1 - A) \quad \dots\dots\dots \text{Eqn. 2.6}$$

$A$  is a material constant and its evaluation from triaxial compression tests is given in Appendix A.

Eqn. 2.5 describes a series of surfaces which are normal to the plastic strain increment directions.

In the theory of plasticity, see for example Hill (1950), the relation between the plastic strain increments and the plastic potential function is given by an expression as follows:

$$d\epsilon_{ij}^p = \lambda \frac{\partial g}{\partial \sigma_{ij}} \quad \dots\dots\dots \text{Eqn. 2.7}$$

in which  $\lambda$  is called the proportionality constant. The value of  $\lambda$  is the same for all components of plastic



strain increments and is determined by the work hardening law as explained next.

### 3. Work hardening law

The work hardening law adapted for the model is an experimentally determined relationship between the plastic work  $W_p$  and the stress level  $f$ . The increment of plastic work done per unit volume due to a strain increment  $\{d\epsilon_{ij}^p\}$  is calculated from  $\{\sigma_{ij}\}^T \{d\epsilon_{ij}^p\}$  and is added to the previous values to find the total plastic work.

Test data by Lade (1972) have indicated that the plastic work was very small for a range of  $f$  starting with 27 at hydrostatic state of stress up to a certain value which was called the threshold stress level  $f_t$ . As a convenience in fitting curves to the experimental data, it has been assumed that, for values of  $f$  between 27 and  $f_t$ , no plastic strains occur and no plastic work is done. Therefore, the relations between  $W_p$  and  $(f - f_t)$  have been approximated by hyperbolae for which Eqn. 2.8 has been proposed.

$$(f - f_t) = \frac{W_p}{a + b \times W_p} \quad \dots\dots\dots \text{Eqn. 2.8}$$

The initial slope of a curve representing  $W_p$  versus  $(f - f_t)$  relationship is the reciprocal of the parameter  $a$  as shown in Figure 2.3.

The value of  $a$  increases with confining pressure, and this



variation has been expressed as in Eqn. 2.9.

$$a = M \times p_a \times \left( \frac{\sigma_3}{p_a} \right)^l \quad \dots\dots\dots \text{Eqn. 2.9}$$

where:

$p_a$  is atmospheric pressure express the same units as  $a$  and  $\sigma_3$ .

$M$  and  $l$  are dimensionless numbers. Their evaluation from test data is given in Appendix A.

The parameter  $b$  in Eqn 2.8 is the reciprocal of the ultimate value of  $(f-f_t)$  which the hyperbola approaches asymptotically with increasing values of  $W_p$ . This relationship is given by Eqn. 2.10.

$$b = \frac{1}{(f-f_t)_{ult}} \quad \dots\dots\dots \text{Eqn. 2.10}$$

Since the value  $(f-f_t)_{ult}$  determined from the curve fitting procedure is always larger than the value of  $(f-f_t)$  at failure for all finite values of  $W_p$ , a new parameter  $r_f$  was introduced to relate the asymptotic value of  $(f-f_t)$  to its value at failure.

$$r_f = \frac{(K_1-f_t)}{(f-f_t)_{ult}} \quad \dots\dots\dots \text{Eqn. 2.11}$$





The determination of the proportionality constant  $\lambda$  follows the development outlined by Hill (1950) and is given as:

$$\lambda = \frac{dW_p}{3g} \quad \dots\dots\dots \text{Eqn. 2.12}$$

The increment of plastic work  $dW_p$  is expressed as:

$$dW_p = \frac{a \times df}{\left(1 - r_f \times \frac{f - f_t}{K_1 - f_t}\right)^2} \quad \dots\dots\dots \text{Eqn. 2.13}$$

The plastic strain increments expressed in suffix notation in Eqn. 2.7, can now be written in matrix form:

$$\begin{Bmatrix} d\epsilon_x^p \\ d\epsilon_y^p \\ d\epsilon_z^p \\ d\epsilon_{xy}^p \\ d\epsilon_{yz}^p \\ d\epsilon_{zx}^p \end{Bmatrix} = \frac{a \times df}{3g \left(1 - r_f \times \frac{f - f_t}{K_1 - f_t}\right)^2} \begin{Bmatrix} 3I_1^2 - K_2(\sigma_y \sigma_z - \tau_{yz}^2) \\ 3I_1^2 - K_2(\sigma_z \sigma_x - \tau_{zx}^2) \\ 3I_1^2 - K_2(\sigma_x \sigma_y - \tau_{xy}^2) \\ 2K_2(\sigma_z \tau_{xy} - \tau_{yz} \tau_{zx}) \\ 2K_2(\sigma_x \tau_{yz} - \tau_{xy} \tau_{zx}) \\ 2K_2(\sigma_y \tau_{zx} - \tau_{yz} \tau_{xy}) \end{Bmatrix} \quad \text{Eqn. 2.14}$$

Therefore, the elastic and plastic parts of strain increments are fully described. Substitution of Eqn. 2.3 and



Eqn. 2.14 into Eqn. 2.1 allows the total strain increments to be calculated if the state of stress and the stress increments are known.

There are nine soil parameters required to characterize the soil behavior according to this theory, and their values can be derived from the results of conventional triaxial compression tests.

### 2.3 LIMITATIONS

The theory, as recapitulated in the previous section, is not able to model all aspects of soil behavior.

1. Strain softening cannot be handled. If the conditions for strain softening specified in Chapter 4 prevail, then the predictions may deviate from measured results considerably depending on the degree of softening.
2. According to the theory, no plastic straining takes place as a result of a proportional loading. This is due to the fact that the model does not have a yield cap. For example in hydrostatic compression tests which follow a proportional loading path, the model predicts recoverable strains only. This is in contradiction with measured behavior. The degree of discrepancy between the predicted and measured results depends mainly on the relative density of the soil and the stress level.
3. Although the Mohr envelope is curved for most cohesionless soils, the failure envelope in the triaxial plane for this model is linear. The effects of this



limitation apply more to soils under low mean normal stresses where the curvature of failure envelope is appreciable.

4. The value of Poisson's ratio for elastic deformations was assumed to be equal to zero. Therefore the terms multiplied by its value will disappear in formulae to calculate strain increments. Consequently, no straining should be expected in any other direction but that of the stress increment.

#### 2.4 APPLICATIONS OF THE MODEL

Applications of the model to laboratory tests and engineering problems are reviewed next.

1. Predictions of laboratory testing results:

To assess the ability of the model to predict soil behavior, a variety of tests with different stress paths were conducted and the comparative results were published by Lade and Duncan (1975,1976). Their conclusions were:

"The generally good agreement between the calculated and measured strains indicated that the conditions of primary loading, unloading, and reloading implied in plasticity theory for isotropically work-hardening materials is reasonably accurate for cohesionless soils. The strains calculated...are in reasonable agreement with those measured, but some discrepancies do





occur. The largest differences between measured and calculated strains occur for proportional loading with increasing stresses and for unloading and reloading at constant confining pressure. Considering that the strains observed in these cases are relatively small, the calculated strains may be close enough for many purposes. The analyses thus demonstrate the usefulness of elastoplastic stress strain theory for calculating strains... during complex stress changes..."

The effectiveness of the theory in modeling stress strain behavior along several different stress paths was also confirmed by Medeiros (1979).

## 2. Engineering Problems:

Ozawa (1973) was the first to use the model for the analysis of stresses and movements in earth masses. His results of finite element analyses of passive earth pressure problems were published later by Ozawa and Duncan (1976a). Due to errors in the analysis of this published data, and the problems related to the formulation of the model, (see Section 2.5), the results were not suitable for determining the usefulness of the model.

The second attempt to find the effectiveness of the model for engineering problems was made by Wong (1978). Using the modifications summarized in the following



section, the predictions of a finite element analysis were compared with experimental results from passive pressure tests on sand. The calculated values of average stresses on the wall exceeded those measured by a considerable amount. Attention was then drawn to the limitations of the model as possible reasons for the discrepancies. For the same problem, Wong has also provided calculated results obtained by using simpler relationships, such as the nonlinear elastic hyperbolic model. The predictions made by using Lade's model were not as impressive as the others, yet the simpler stress-strain relationships have more severe limitations.

## 2.5 PREVIOUS MODIFICATIONS

Modifications and corrections for the model were first proposed by Ozawa and Duncan (1976b) as follows:

1. The plastic potential function was found to be mathematically inconsistent with the expressions for plastic strain increments and a new equation was proposed as:

$$g = I_3 \times (f - 27)^\alpha \quad \dots\dots\dots \text{Eqn. 2.15}$$

where:



$\alpha$  is a constant for a particular material and is defined as:

$$\alpha = \frac{1}{1-A}$$

where A is the same as in Eqn. 2.6

2. Due to the error in the calculation of derivatives of plastic potential function with respect to shear stresses, the shear strain increments were in an error by a factor of 2.0. Therefore on the right hand side of Eqn. 2.14, the multiplier 2.0 of each term related to plastic shear strain increments has to be removed.
3. The parameter a of Eqn. 2.8 varies with  $\sigma_3$  according to Eqn. 2.9. This variation was neglected in calculating  $\partial f / \partial \{\sigma\}$  which is used in the finite element formulation to form the elasto-plastic constitutive matrix  $[C^{ep}]$ .

Having made these corrections, the authors then presented the elasto-plastic constitutive relation in matrix notation, suitable for use in a finite element analysis. Wong's predictions were based on this form of the model and therefore utilized all previous modifications.

The same corrections were again published by Duncan et al (1977) with an illustration of the new plastic potential surface which has an unsymmetrical bullet





shape in principal stress space. The intersections of the plastic potential surfaces with the triaxial plane are shown in Figure 2.4.



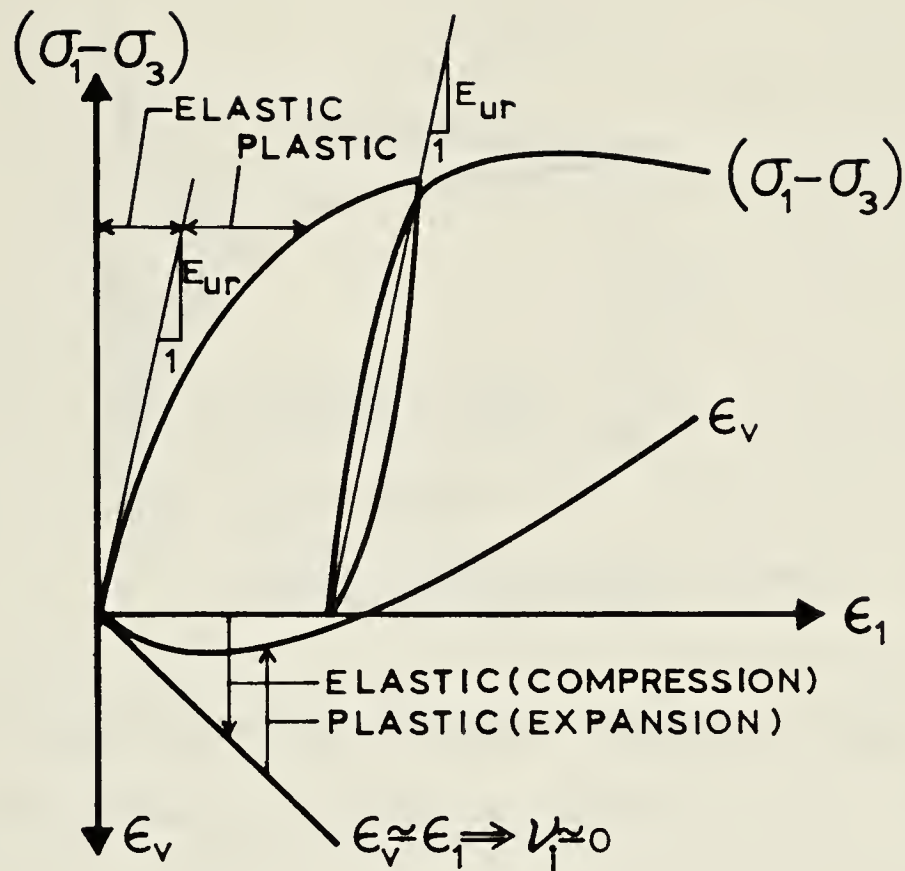


Figure 2.1 Elastic and plastic parts of strain in triaxial test (After Lade and Duncan (1975))

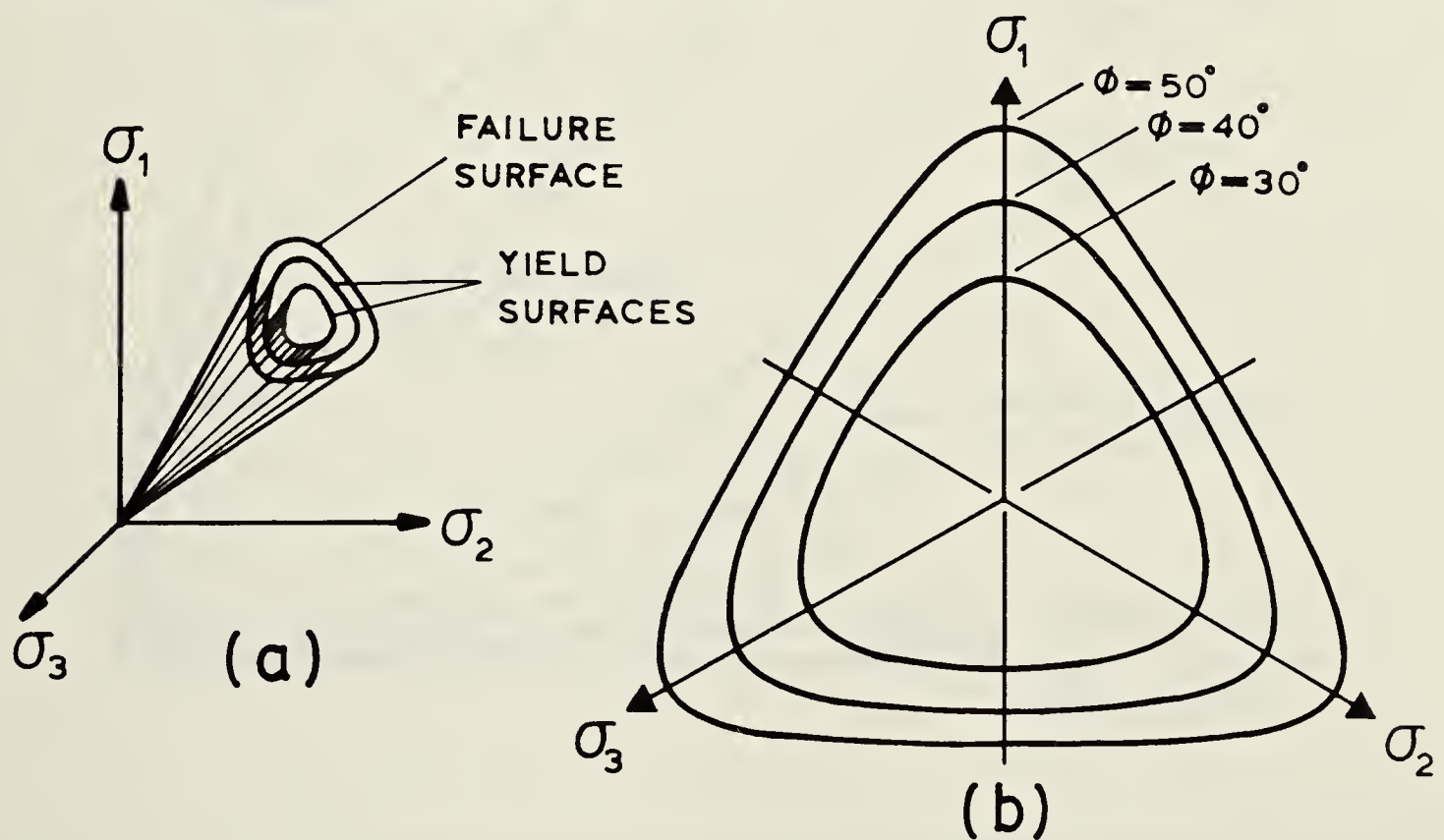


Figure 2.2 Yield and failure surfaces in (a) principal stress space (b) loci of surfaces on octahedral plane.



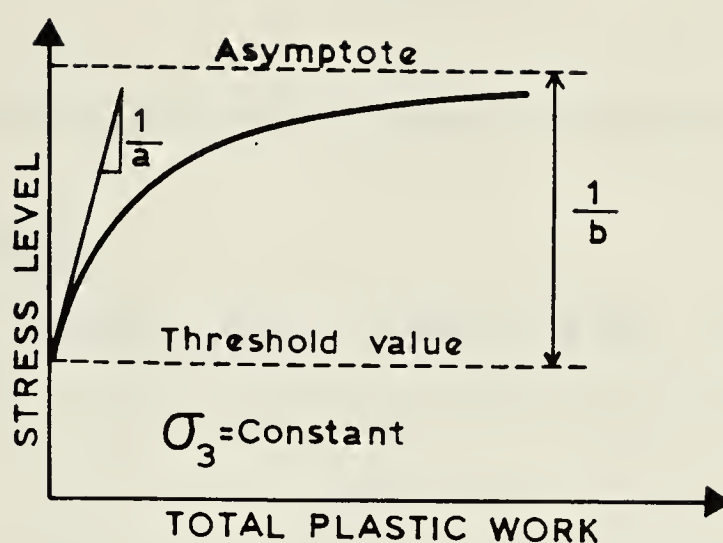


Figure 2.3 Relationship between plastic work and stress level. (After Ozawa and Duncan, 1976a)

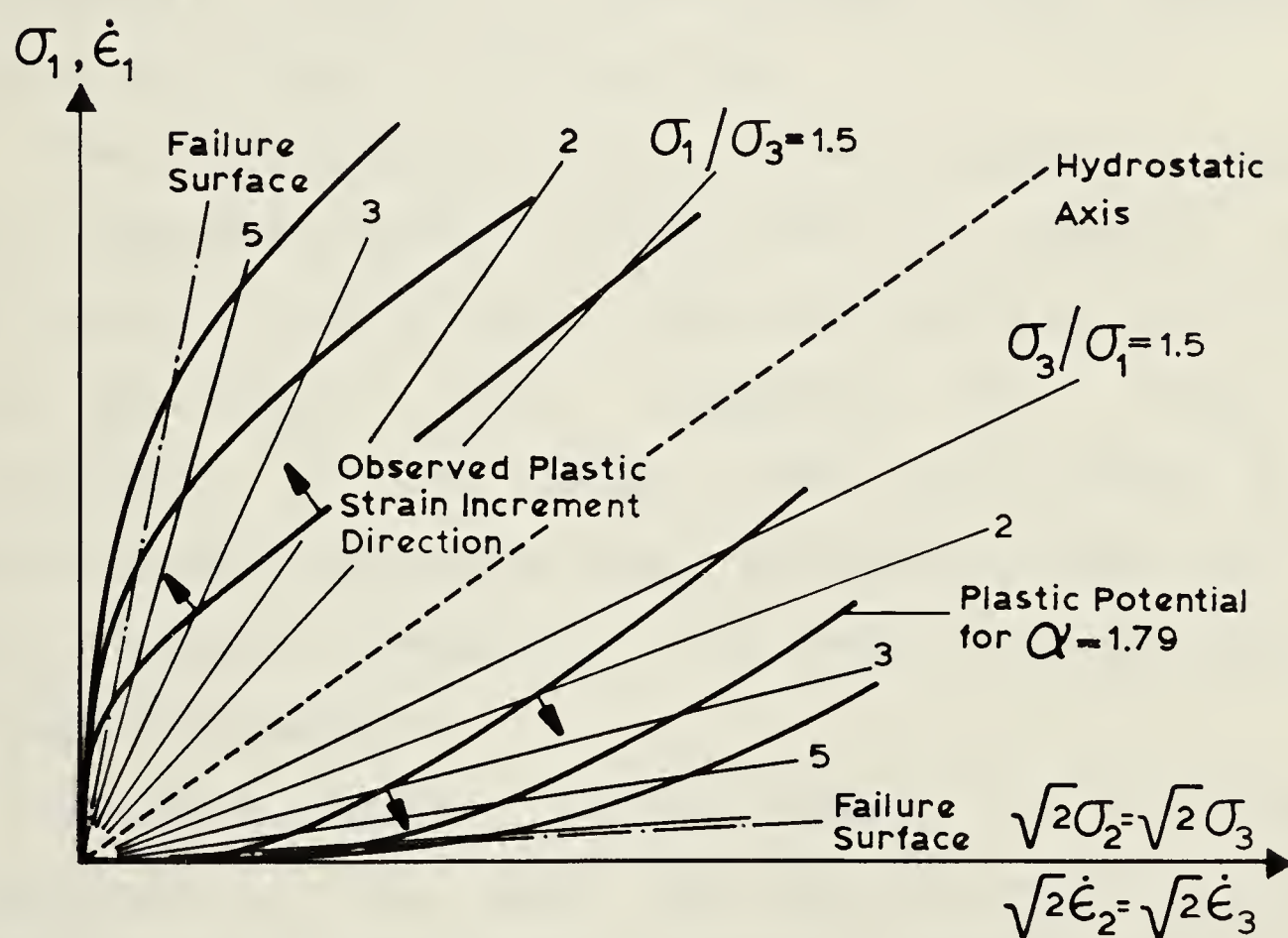


Figure 2.4 Trace of plastic potential surfaces on triaxial plane (After Duncan et al, 1977)





## CHAPTER 3

### RE-EVALUATION OF WORK HARDENING MODEL

#### 3.1 INTRODUCTION

For most stress paths, Lade's model has been shown to be effective in its predictions of stress strain behavior of cohesionless soils in laboratory tests. However finite element applications of the model have not reached the same level of success so far. In the past, difficulties were encountered with regard to the formulation of the model, and consequently a number of modifications were proposed by others as reviewed in Section 2.5.

The discouraging results of finite element analyses of earth pressure problems by Wong (1978) as opposed to the satisfactory predictions of laboratory tests by Lade (1972), Lade and Duncan (1976), suggested that either the limitations of the model were too severe or the modifications proposed by Ozawa and Duncan (1976b) have not been effective enough for the model to become useful in engineering practice.

In this Chapter, certain aspects of the original formulation of the model and previous modifications are examined. The significance of correct interpretation of the laws used in Lade's original theory is demonstrated by comparing the test results of Lade (1972) with predictions by the previously modified and presently re-evaluated forms



of the model.

The adaptation of the suggestions made here to finite element analysis is dealt with in Chapter 6.

### 3.2 VALIDITY OF PREVIOUS MODIFICATIONS

Any alteration to the original formulation of the model affects its ability to predict stress-strain behavior of soils. To evaluate the effect of modifications on the existing capabilities of the model, predictions have to be compared with laboratory test results. The calculations made by using the original form of the model (Lade, 1972) and the form with previous modifications (Ozawa and Duncan, 1976) are presented next with some test data.

Ozawa and Duncan (1976) have proposed that the variation of parameter  $a$  with respect to  $\sigma_3$  has to be included in the calculation of  $\partial f / \partial \{\sigma\}$  which is used in the finite element formulation to form the elasto-plastic constitutive matrix  $[C^{ep}]$ . If this proposal is used in the finite element analysis, the results will be equivalent to that of a simple stress analysis where the parameter  $a$  is used as a variable in the calculation of plastic work increments. Therefore, realizing that the parameter  $a$  of Eqn. 2.8 has to be treated as a variable rather than a constant and using the new plastic potential function given by Eqn. 2.15, the constitutive relationship in modified form can be written as:



$$\begin{Bmatrix} d\epsilon_x^p \\ d\epsilon_y^p \\ d\epsilon_z^p \\ d\epsilon_{xy}^p \\ d\epsilon_{yz}^p \\ d\epsilon_{zx}^p \end{Bmatrix} = \text{MULT} \times \begin{Bmatrix} 3I_1^2 - K_2(\sigma_y \sigma_z - \tau_{yz}^2) \\ 3I_1^2 - K_2(\sigma_z \sigma_x - \tau_{zx}^2) \\ 3I_1^2 - K_2(\sigma_x \sigma_y - \tau_{xy}^2) \\ K_2(\tau_{xy} \sigma_z - \tau_{yz} \tau_{zx}) \\ K_2(\tau_{yz} \sigma_x - \tau_{zx} \tau_{xy}) \\ K_2(\tau_{zx} \sigma_y - \tau_{xy} \tau_{yz}) \end{Bmatrix} \quad \text{Eqn. 3.1}$$

where:

$$\text{MULT} = \left[ \frac{(M+bh)^2(\sigma_3)^l (df) + Ml\sigma_3^{l-1} h(d\sigma_3)}{3Mg} \right] \left( \alpha^{f-27} \right)^{\alpha-1}$$

$$K_2 = A_1 f + A_2$$

$$A_1 = 1 - 1/\alpha$$

$$A_2 = 27/\alpha$$

$$\alpha = 1/(1 - A)$$

$$h = W_p / (\sigma_3^l)$$

Notes: 1)  $W_p$  has to be updated at each loading step

2) The column vector on the right hand side of Eqn.

3.1 will be denoted by  $\{\text{COLUMN}\}$  and the left hand side by  $\{d\epsilon^p\}$  in the following as required.

3)  $M, g, b, l$  are all defined in Chapter 2.

Several stress-strain curves following different stress paths were reproduced by substituting Eqn. 3.1 into Eqn. 2.1, and are presented with the test results, if available, in Figures 3.1 to 3.5. The predictions by using Lade's approach are also plotted in the same figures. Although the





predicted curves of the previously modified approach are as good as the curves produced by using Lade's approach for Figure 3.1 and 3.2, the gap between these curves rapidly opens up for large changes in  $\sigma_3$  but relatively small changes in  $f$ . Figures 3.3 to 3.5 demonstrate that the modified approach may produce significantly different results from Lade's approach, even resulting in different signs for strains as shown in Figure 3.5.

Although there are no measured test results to be plotted in Figures 3.4 and 3.5 to support either one of the predictions, it can be concluded that the use of Eqn. 3.1 alters the abilities of the model for certain stress paths.

Figure 3.6 shows the strain increment vectors for two different stress paths in the triaxial plane as predicted by the previously modified form and the presently re-evaluated approach which is described later in this chapter.

For similar stress paths, Lade and Duncan (1976) provided measured test results which are reproduced on Figure 3.7. A comparison of measured and predicted strain increment vectors shows that the re-evaluated procedure predicts the increments of strain reasonably well for both stress paths, while the modified approach fails to do so for the stress path with decreasing deviator stress and decreasing confining pressure.

To find out which one of the previous modifications is responsible for altering the abilities of the model, the effect of each modification to the original formulation is



investigated separately. The modification related to the plastic potential function is treated first, with the parameter  $\alpha$  held constant in calculating the plastic work increment. Rather than reproducing the stress-strain curves, the following proof is provided to show that the modified plastic potential function (Eqn. 2.15) does not change the stress-strain relation in incremental form.

To differentiate between the original and modified plastic potential functions,  $g$  of Eqn. 2.5 and Eqn. 2.15 are renamed here as  $g_o$  and  $g_m$  respectively. Substituting Eqn. 2.12 into Eqn. 2.7 and using Eqn. 2.5 for the plastic potential function results in the following plastic strain increment values:

$$\left\{ d\epsilon^p \right\} = \left( \frac{dW}{3g_o} \right) \left\{ \text{COLUMN} \right\} \dots\dots\dots \text{Eqn. 3.2}$$

where:  $\left\{ d\epsilon^p \right\}$  and  $\left\{ \text{COLUMN} \right\}$  are defined in the notes for Eqn. 3.1.

If Eqn. 2.15 is used rather than Eqn. 2.5, the set of equations for calculating the plastic strain increments becomes:

$$\left\{ d\epsilon^p \right\} = \left( \frac{dW_p}{3g_m} \times \alpha (f-27)^{\alpha-1} \right) \left\{ \text{COLUMN} \right\} \dots \text{Eqn. 3.3}$$

If the multipliers on the righthand side of Eqn. 3.2 and



Eqn. 3.3 have the same values, then  $d\epsilon_{ij}^p$  calculated by either way are identical. This can readily be shown:

Ignoring the common multiplier  $(dW_p/3.0)$ , and writing  $f$ ,  $g_o$  and  $g_m$  in terms of stress invariants gives:

Reduced multiplier for Eqn. 3.2:

$$\frac{1}{g_o} = \frac{1}{I_1^3 - K_2 I_3} = \frac{1}{I_1^3 - [A \frac{I_1^3}{I_3} + 27(1-A)] I_3}$$

$$\frac{1}{g_o} = \frac{1}{I_1^3 - A I_1^3 - 27 I_3 + 27 A I_3} \quad \dots\dots\dots \text{Eqn. 3.4}$$

Reduced multiplier for Eqn. 3.3:

$$\frac{1}{g_m} \times \alpha (f - 27)^{\alpha-1} = \frac{1}{1-A} \times \frac{(f-27)^{\alpha-1}}{I_3 (f-27)^\alpha} = \frac{1}{(1-A)(f-27) I_3}$$

$$\frac{1}{g_m} \times \alpha (f-27)^{\alpha-1} = \frac{1}{I_1^3 - A I_1^3 - 27 I_3 + 27 A I_3} \quad \dots\dots\dots \text{Eqn. 3.5}$$

where  $\alpha = 1/(1 - A)$

Eqn. 3.4 and Eqn. 3.5 have equal values, therefore, the use of Eqn. 2.15 for the modified plastic potential function will produce results identical to those obtained from Lade's original formulation. If this modification is used, it improves the formulation of the model in the sense of mathematical integrity. The explanation for this statement is as follows: when the derivatives of the plastic potential function are needed for the flow rule, the use of Eqn. 2.5





requires that  $K_2$  be held constant in the derivation process. Yet  $K_2$  is a function of  $f$  which is in turn a function of stresses. The use of Eqn. 2.15 does not require such an assumption.

In the light of the above observations regarding the plastic potential function, the cause for large discrepancies between the predictions by Lade's approach and the results of the modified formulation, as plotted in Figure 3.3 to Figure 3.6, seems to be related to the parameter  $a$ , in other words, to the work hardening law of the theory.

### 3.3 PROPOSED INTERPRETATION OF WORK HARDENING LAW

The work hardening law and its modification are re-evaluated here to establish a correct method for its use.

Lade's test results from which the work hardening law was obtained are reproduced in Figure 3.8. The results show that there is a unique relationship between  $f$  and  $W_p$  for tests where  $\sigma_3$  is held constant. This relationship is expressed by Lade and Duncan (1975) in mathematical form (see Eqn. 2.8). Figure 3.8 also shows some data points for various  $b$  values [ $b = \frac{\sigma_2 - \sigma_3}{\sigma_1 - \sigma_3}$ ] obtained from tests where  $\sigma_3$  was still kept constant. These results allowed Lade and Duncan (1975) to state that "the relationship between  $W_p$  and  $f$  ... depends on the confining pressure,  $\sigma_3$ , but it is essentially the same for all values of  $b$ ". There are no other test results with plastic work calculations to support



the validity of Eqn. 2.8 for stress paths with varying  $\sigma_3$ . Therefore, this equation is applicable strictly for stress changes for which  $\sigma_3$  remains constant.

In order to use Eqn. 2.8 in the analysis of a general three dimensional problem where  $\sigma_3$  generally changes during loading, an assumption has to be made. The theory which was first published by Lade and Duncan (1975) does not elaborate on this point, but simply treats the parameter  $a$  as a constant when Eqn. 2.8 is used to derive an expression for the increment of plastic work. However, in an attempt to use Eqn. 2.8 in its true sense, Lade (1972) calculated the stress dependent parameter  $a$  for an average  $\sigma_3$  value which was obtained from initial and final values of  $\sigma_3$  for a given stress increment. Some of his predictions of laboratory tests can be found in the publication by Lade and Duncan (1976). Unfortunately the importance of the non-generality of Eqn. 2.8 for changing  $\sigma_3$  values has never been emphasized, nor has the basic assumption which allows its use in such problems been clearly stated. In the publications by Ozawa and Duncan (1976, 1976b), Eqn. 2.8 remained as a three dimensional representation of the work hardening law. Subsequently, as a deviation from Lade's original work, Duncan et al. (1977) and Wong (1978) treated the parameter  $a$  as a variable when a differentiation was needed on Eqn. 2.8.

The consequences of assuming that Eqn. 2.8 is unique for general three dimensional problems are as follows:



Case I:

Referring to Figure 3.9a, the initial state of stress is assumed to be on the current yield surface as indicated by point A with a total plastic work value equal to  $W_A$ . An increment of stress is applied such that the stress path follows the route from A to B without travelling outside the current yield surface. The limits of the elastic region are not exceeded, so there are no plastic deformations, and no increment in plastic work. Therefore, the total plastic work done is the same for points A and B. But since the value of  $\sigma_3$  has changed, and with it, the value of parameter  $a$ , the Eqn. 2.8 is no longer satisfied for point B.

Case II:

Figure 3.9b illustrates three different stress paths, all of which start from the hydrostatic axis. All three follow the stress path of the conventional triaxial test up to the new yield surface, then, without leaving that surface end at point F. The change in  $f$  value in going from the hydrostatic axis to the new yield surface is the same for all points A, B and C. But the parameter  $a$  calculated for point A will be the smallest of all, and the plastic work increment for path A to D will be smaller than for path B to E or C to F. Therefore, depending on which path is followed, the total plastic work at point F will have a different value. Although all these work values as well as an infinite number of others are possible for point F, only one of them satisfies Eqn. 2.8. Subsequent increments of stress from







point F with increasing stress level will create problems for any total plastic work value other than the one which satisfies Eqn. 2.8. The reason for this is that Eqn. 2.8 will become an inequality and cannot be used any further to calculate the increments of plastic work, which are needed for Eqn. 2.12.

Case III:

This case is related to the use of Eqn. 2.8 in its modified form, in which the parameter  $a$  is treated as a function of  $\sigma_3$  in calculating the increment of plastic work, as formulated below:

$$dW_p = \frac{1}{M} \left[ (M + bh)^2 (\sigma_3^l) (df) + M \sigma_3^{l-1} h (d\sigma_3) \right] \quad \dots \text{Eqn. 3.6}$$

The problem does not surface with this formulation until the term with  $d\sigma_3$  becomes larger in absolute value with a negative sign than the term with  $df$  on the right hand side of the equation as in stress paths with decreasing  $\sigma_3$  and increasing  $f$  values. As a result of this,  $dW_p$  will have a negative value. As long as the plastic deformation is an irreversible process from which the energy cannot be recovered, a negative  $dW_p$  will contradict the laws of the theory of plasticity.

Due to the lack of generality as demonstrated by Case I and II, Eq. 2.8 is not assumed here as a work hardening law applicable for all problems. Instead the following procedure



is adopted:

Rather than searching for a general relationship between  $f$  and  $W_p$ , and then differentiating that function to find a relation between  $df$  and  $dW_p$ , the following assumption is made to establish a criterion about how the yield surface will expand as the plastic work is done. Using Figure 3.8, the tangent to the related experimental curve specified by  $\sigma_3$ , at the point corresponding to known  $f$ , defines the relation between the increments of  $f$  and  $W_p$  without any regard for the actual value of  $W_p$ . As it is shown earlier, depending on the loading history of the soil, the accumulated value of  $W_p$  may vary for the same values of  $f$  and  $\sigma_3$ . However, the increments of plastic work will always be unique for a given state of stress and stress increment. In mathematical form this statement is equivalent to the expression given by Eqn. 2.13, which is Lade's original equation for plastic work increments. Therefore, it can be concluded that the re-evaluated approach makes full use of the experimental data and Eqn. 2.8 without influencing adversely what has been formulated so far.

To find out the results of such an approach the stress-strain curves of Figures 3.1 to 3.6 were reproduced and plotted as "re-evaluated" predictions on the same figures. These results show that the curves obtained by the re-evaluated approach follow closely the original predictions which were provided by Lade (1972) for the verification of his model.



### 3.4 CONCLUSIONS

As the calculations provided here indicate, the measured stress-strain behavior of cohesionless soils can be successfully predicted by using the newly proposed interpretation without making the previous modifications of Ozawa and Duncan (1976). At the same time, the problems that are created in finite element analysis by using Eqn. 2.8 as the work hardening law can be avoided .





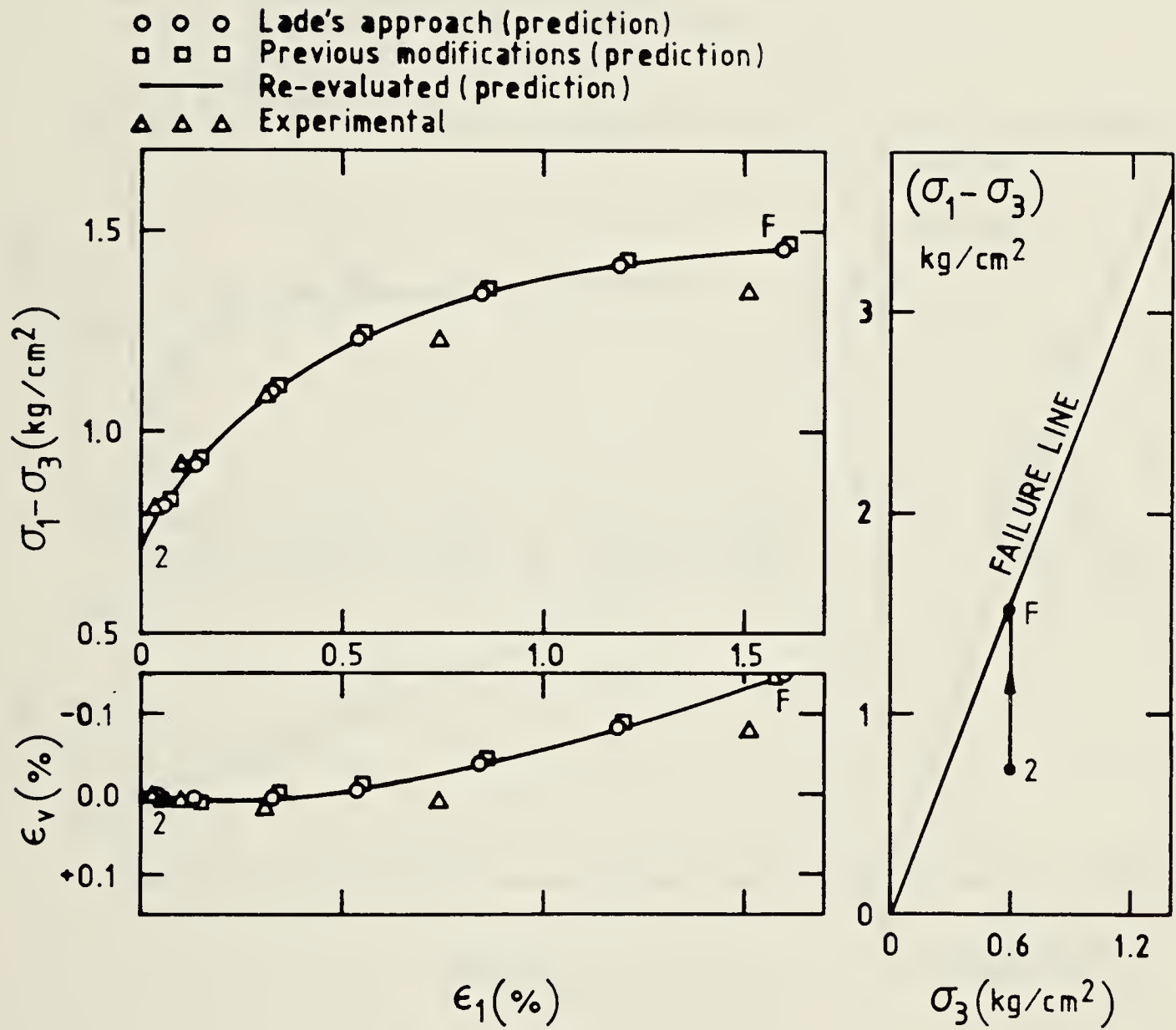


Figure 3.1 Stress-path with increasing deviator stress and constant confining pressure. Monterey No.0 Sand  
Experimental results after Lade and Duncan (1976)



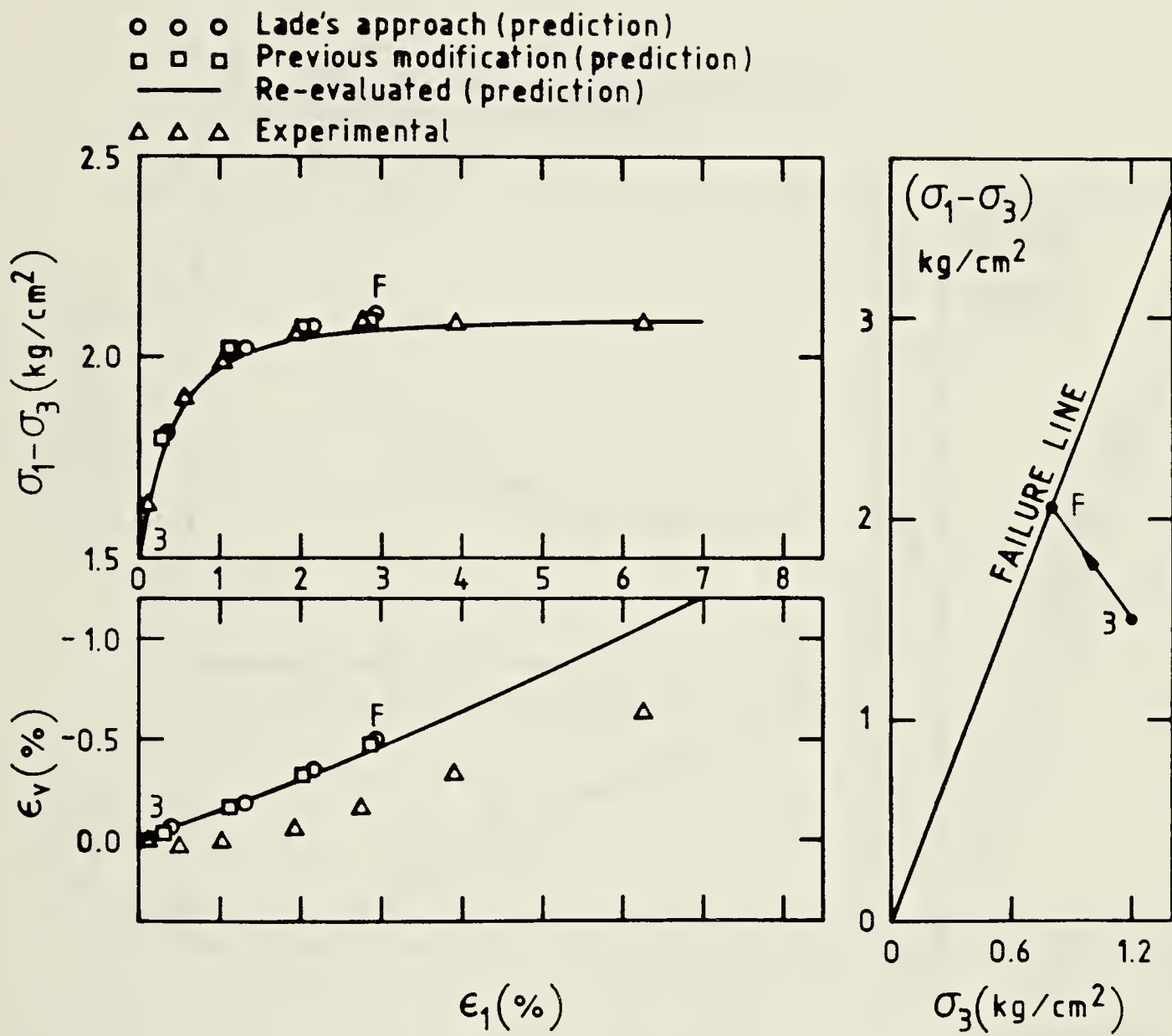


Figure 3.2 Stress-path with increasing deviator stress and decreasing confining pressure. Monterey No.0 Sand. Experimental results after Lade and Duncan (1976)



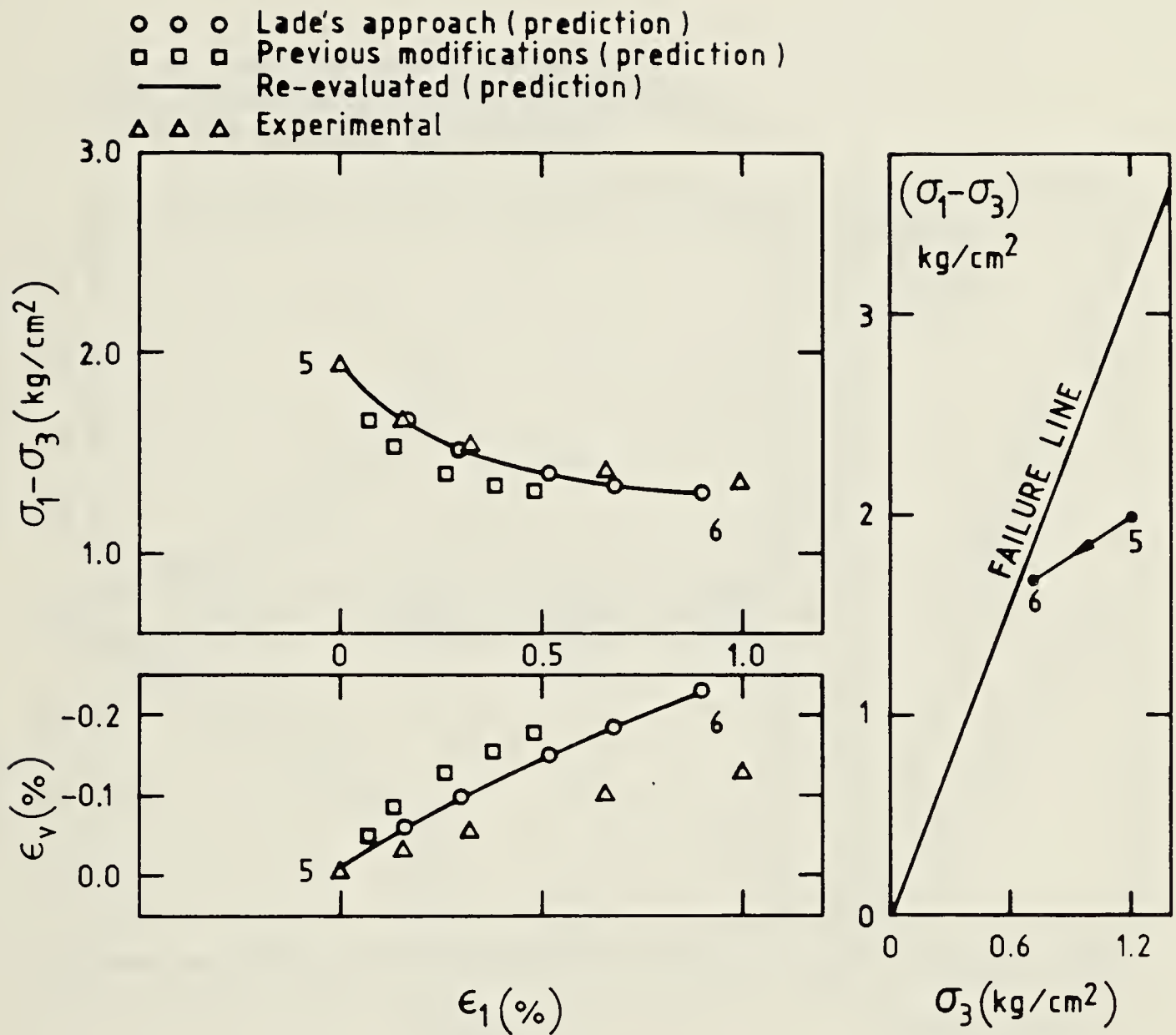


Figure 3.3 Stress-path with decreasing deviator stress and decreasing confining pressure. Monterey No.0 Sand. Experimental results after Lade and Duncan (1976)





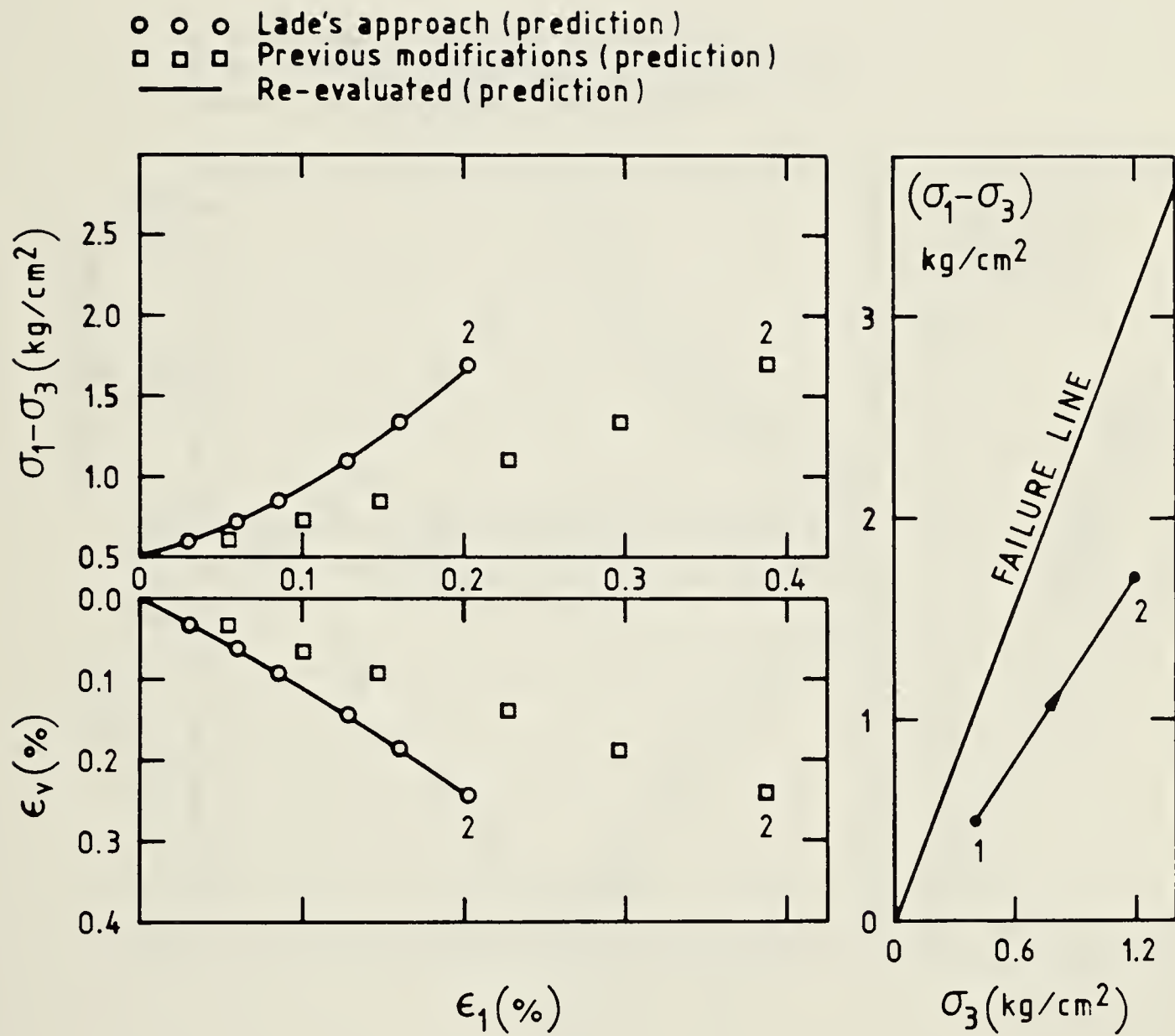


Figure 3.4 Stress-path with increasing deviator stress and increasing confining pressure. Monterey No.0 Sand.



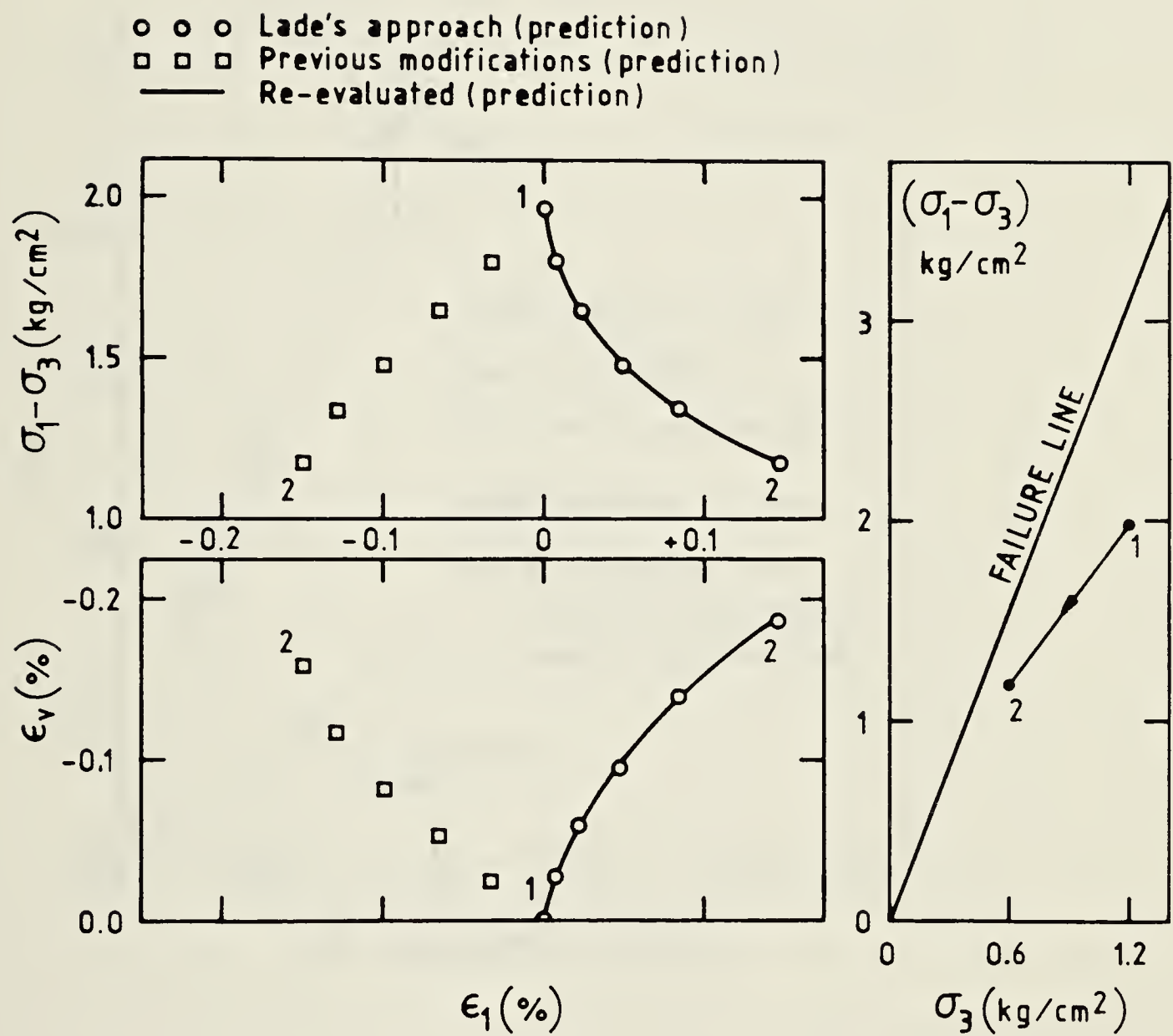


Figure 3.5 Stress-path with decreasing deviator stress and decreasing confining pressure. Monterey No.0 Sand.



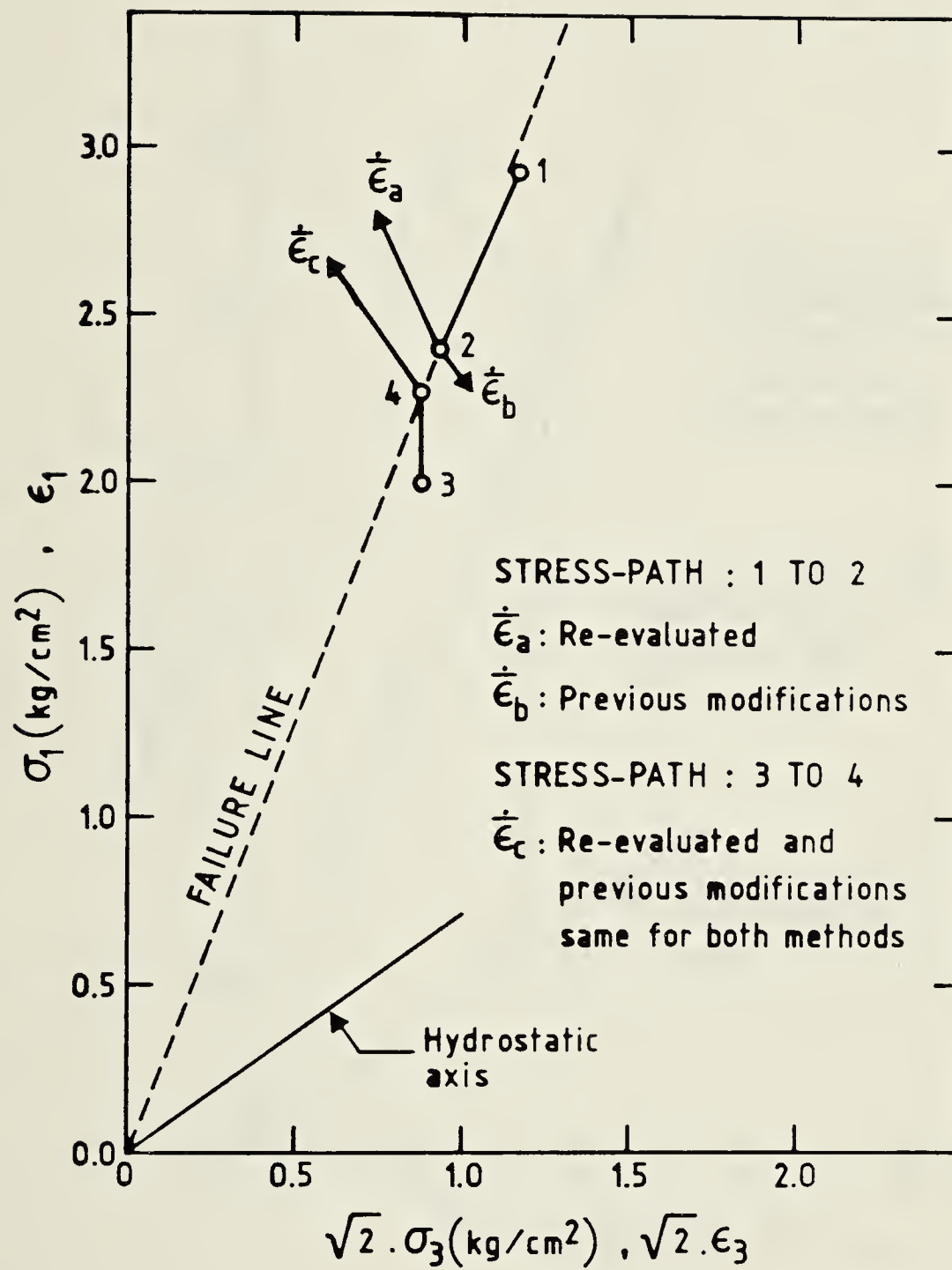


Figure 3.6 Predicted strain increment vectors





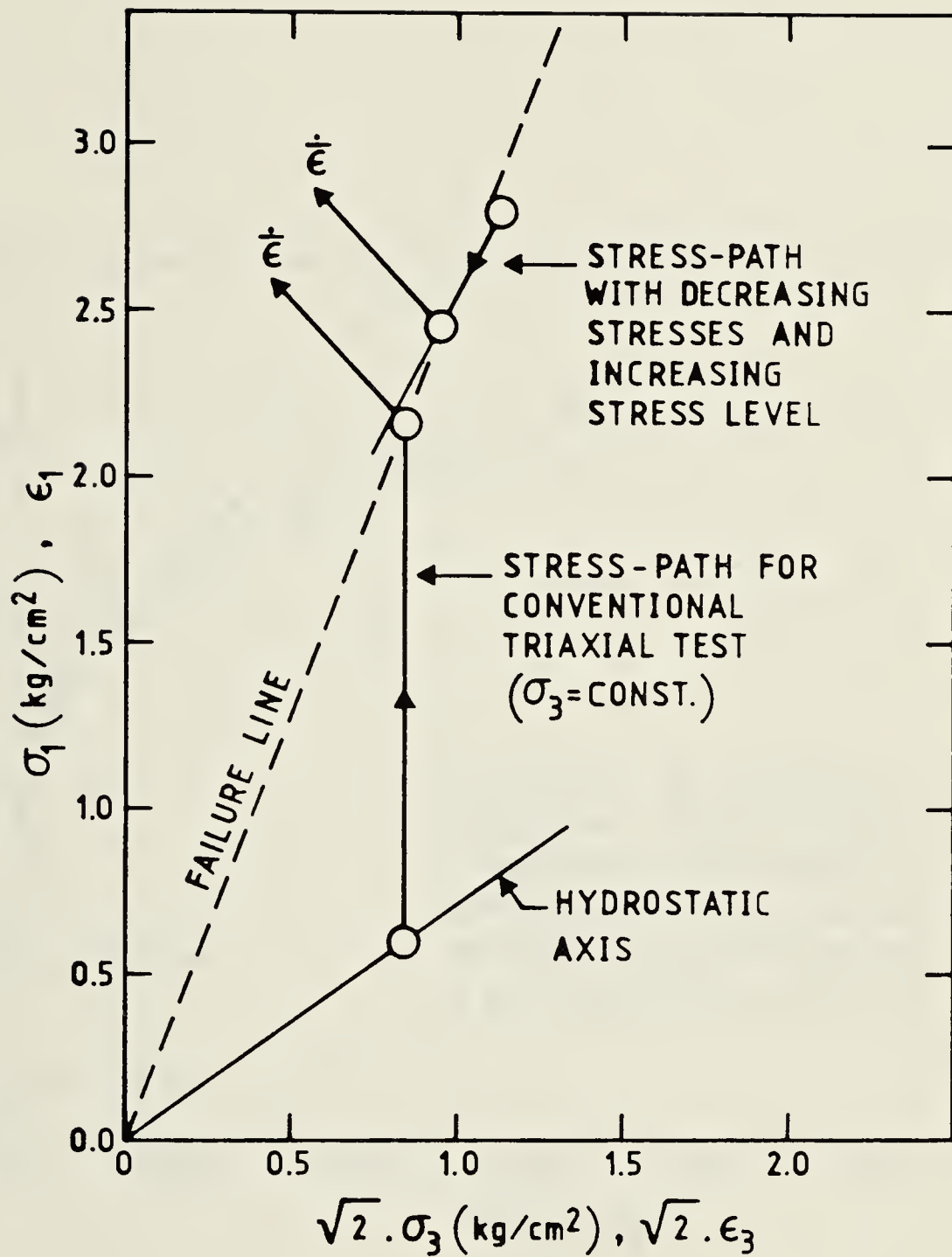


Figure 3.7 Measured Directions of Strain Increment Vectors for Different Stress-Paths in Triaxial Plane (After Lade and Duncan, 1976)



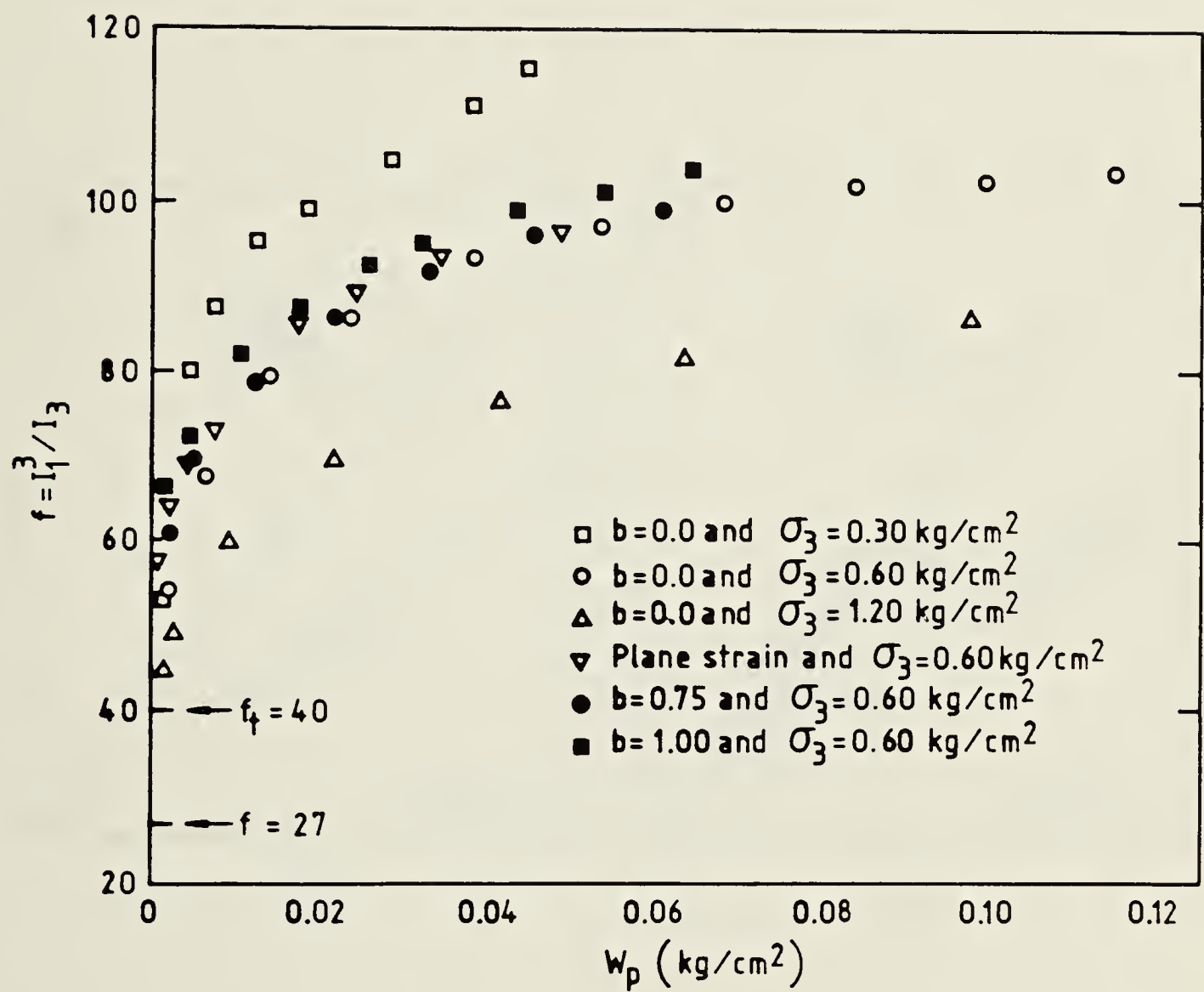


Figure 3.8 Variation of Plastic Work for Dense Monterey No.0 Sand (After Lade and Duncan, 1976)



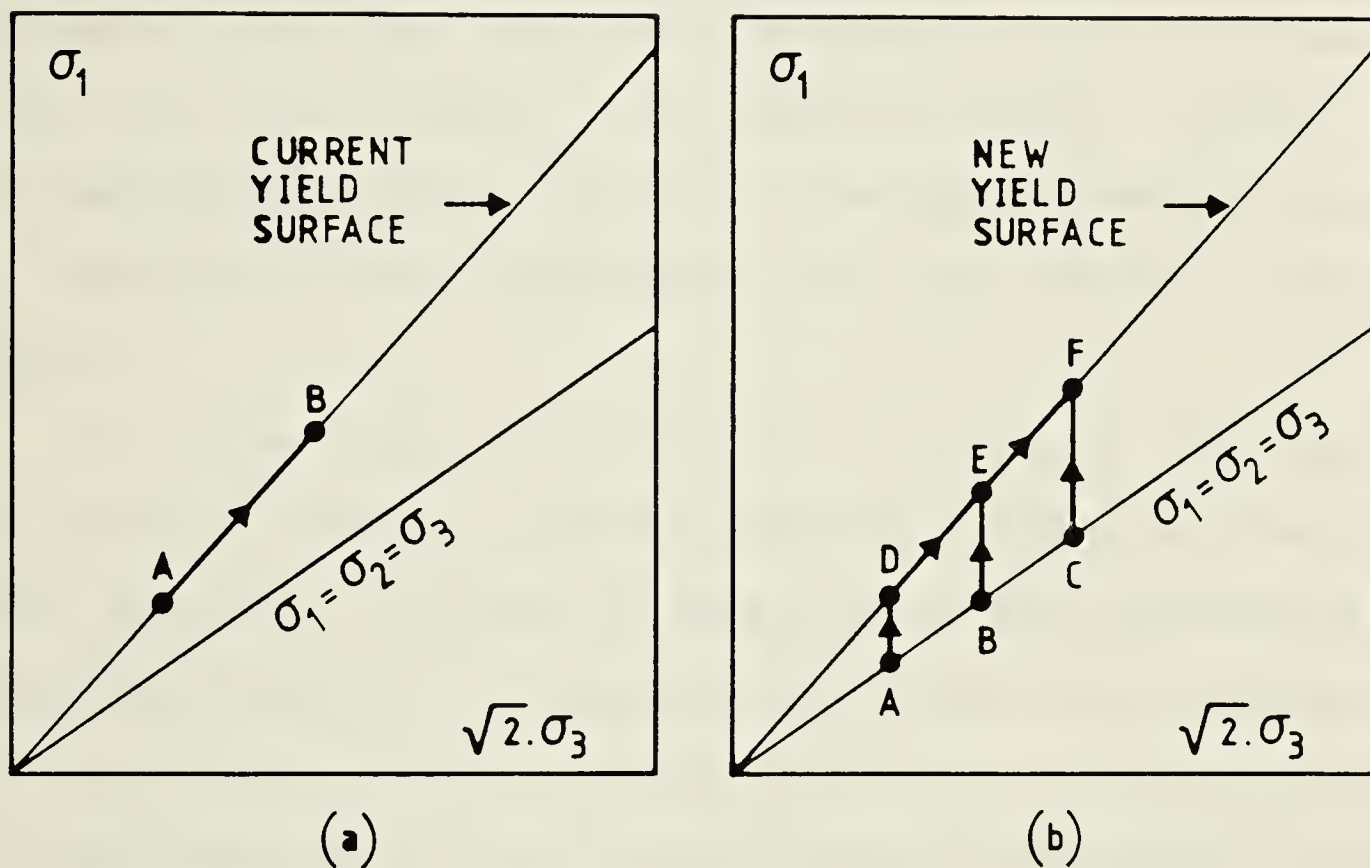


Figure 3.9 Stress increments with a) no change in stress level b) conventional triaxial test path followed by no change in stress level.





## CHAPTER 4

### STRAIN SOFTENING MODEL

#### 4.1 INTRODUCTION

In his continuing work on soil plasticity Lade (1977) developed a strain softening model to overcome the limitations of his work hardening model. Those limitations are presented in Section 2.3. Although some of the general concepts used for the work hardening model remained the same, the formulation of the conical yield surface, the corresponding plastic potential, and the hardening law were all modified in the development of the strain softening model.

In this model the cone has a curvature like a bullet and not only expands as work hardening takes place but can also contract in order to model the strain softening after the failure surface is reached. Since the failure surface is the outermost yield surface which has a curvature, the failure envelope in the triaxial plane is no longer straight but curvilinear.

In addition to the strain softening feature, a cap type yield surface was added to the open end of the conical yield surface to account for the plastic strain increments due to proportional loading.

Elastic strains were calculated using a non-zero Poisson's ratio (zero was used for the work hardening model)



and therefore a general improvement was expected in predictions of elastic deformations.

The strain softening model has been used so far mainly for the analysis of laboratory tests. The modelling of stress-strain curves was reasonably accurate and the pore pressure calculations in undrained loading were satisfactory. The model was developed for sand but its application to cohesive soils was also a success (Lade and Musante, 1976). The finite element application of this model has not been popular yet even among researchers. At present, the only published data is by Aubry and Des Croix, (1979), and the correctness of their results is not beyond doubt.

The present research work essentially deals with the work hardening model. The reasons for introducing the strain softening model in this thesis are as follow.

1. Part of the strain softening model is used in Chapter 5 to improve the capabilities of the work hardening model.
2. The suggestions made for the use of the hardening law given in Section 3.3 are also valid for the strain softening model. It is believed that a critical evaluation of the hardening-softening law of the strain softening model will be useful for future developments in the subject.

In this chapter the strain softening model is presented first as developed by Lade (1977). Then, by following a similar line of thought to that expressed in Chapter 3, the generality of the hardening-softening law is evaluated.



Essential conditions for strain-softening to take place in cohesionless soils are also examined, and reference will be made to this when the finite element results of passive earth pressure tests are evaluated in Chapter 7.

## 4.2 STRESS-STRAIN RELATIONSHIP

In the strain softening model, it was assumed that the total strain increments  $\{d\epsilon_{ij}\}$ , can be divided into an elastic,  $\{d\epsilon_{ij}^e\}$ , a plastic collapse,  $\{d\epsilon_{ij}^{col}\}$ , and a plastic expansive part,  $\{d\epsilon_{ij}^{exp}\}$ , such that

$$\{d\epsilon_{ij}\} = \{d\epsilon_{ij}^e\} + \{d\epsilon_{ij}^{col}\} + \{d\epsilon_{ij}^{exp}\} \quad \dots\dots\dots \text{Eqn. 4.1}$$

The parts of the total strain are illustrated schematically in Figure 4.1. The calculation of each part is discussed in the following.

### 4.2.1 Elastic Strain Increments

The elastic strain increments,  $\{d\epsilon_{ij}^e\}$ , are calculated using Hooke's law. The unloading-reloading branch of a stress-strain curve is used to determine the elastic modulus as presented for the work hardening model in section 2.2.1. Poisson's ratio is chosen equal to 0.2 based on the work by Duncan and Chang (1970), Calladine (1973).





#### 4.2.2 Plastic Strain Increments

Plastic strain increments are divided into two parts: plastic collapse strains and plastic expansive strains. These parts are calculated from two distinct stress-strain relationships. The yield criterion, flow rule and hardening law used for each part are formulated separately. The shape of the yield surfaces related to different parts of plastic straining are illustrated in Figure 4.2.

#### 4.2.3 Plastic Collapse Strains

Contrary to the assumption made for metals in the classical theory of plasticity, soils behave in such a way that part of the strain increment due to hydrostatic compression is irrecoverable. Similarly, under proportional loading part of the strain increment is plastic in nature. It is believed that the plastic collapse strains are produced by re-arrangement of the grain structure and this results in a volumetric reduction. The development of the stress-strain relationship is as follows.

##### 1. Yield Criterion

The cap yield surface used by Lade (1975) is a sphere with the center in the origin of the principal stress space as shown in Figure 4.2, and is described by the function





$$f_{col} = I_1^2 + 2 \times I_2 \quad \dots\dots\dots \text{Eqn. 4.2}$$

where  $I_1$  and  $I_2$  are the first and second stress invariants respectively.

If a stress increment results in an increase in the value of the yield function  $f_{col}$ , i.e.,  $df_{col} > 0$ , then the soil will undergo elasto-plastic deformation while work hardening takes place. This type of yielding does not result in eventual failure. The type of yielding which causes the conical yield surface to expand is responsible for soil failure.

## 2. Flow Rule

An associated flow rule is used for the calculation of plastic collapse strain increments. Hence, the plastic potential function is identical to the yield function and is expressed as:

$$g_{col} = I_1^2 + 2 \times I_2 \quad \dots\dots\dots \text{Eqn. 4.3}$$

The relation between the plastic collapse strain increments and the plastic potential function is given as:



$$d\epsilon_{ij}^{col} = \lambda_{col} \frac{\partial g_{col}}{\partial \sigma_{ij}} \quad \dots\dots \text{Eqn. 4.4}$$

$\lambda_{col}$  is the proportionality constant and its value is determined by the work hardening law.

### 3. Work Hardening Law

The work hardening law, required for the calculation of the magnitudes of the plastic strain increments, is expressed as an experimentally determined relation between the total plastic work,  $W_{col}$  due to collapse strains, and the value of the yield function  $f_{col}$ .

$$W_{col} = C \times p \times \left( \frac{f_{col}}{p_a^2} \right)^p \quad \dots\dots \text{Eqn. 4.5}$$

where  $p_a$  is the atmospheric pressure, and  $C$  and  $p$  are constants which can be determined from a  $(W_{col}/p_a)$  versus  $(f_{col}/p_a^2)$  plot in log-log scale, as shown in Figure 4.3. It is assumed that the work hardening relationship is independent of the stress path.

The value of  $\lambda_{col}$  can be determined from the following expression.



$$\lambda_{col} = \frac{dW_{col}}{2 \times g_{col}} \quad \dots\dots \text{Eqn. 4.6}$$

where

$$dW_{col} = C \times p_a \times p \left( \frac{p_a^2}{f_{col}} \right)^{1-p} \times d \left( \frac{f_{col}}{p_a^2} \right) \quad \dots\dots \text{Eqn. 4.7}$$

The derivation of Eqn. 4.6 is given by Lade (1975) and will not be repeated here.

By substituting Eqn. 4.6 into Eqn. 4.4 and calculating the partial derivatives of the plastic potential function, the final form of the stress-strain relationship for plastic collapse strains becomes

$$\begin{Bmatrix} d\epsilon_x^{col} \\ d\epsilon_y^{col} \\ d\epsilon_z^{col} \\ d\epsilon_{xy}^{col} \\ d\epsilon_{yz}^{col} \\ d\epsilon_{zx}^{col} \end{Bmatrix} = \frac{dW_{col}}{f_{col}} \begin{Bmatrix} \sigma_x \\ \sigma_y \\ \sigma_z \\ \tau_{xy} \\ \tau_{yz} \\ \tau_{zx} \end{Bmatrix} \quad \dots\dots \text{Eqn. 4.8}$$

where  $dW_{col}$  is given by Eqn. 4.7.

#### 4.2.4 Plastic Expansive Strains

This part of the strain increment is calculated according to a stress-strain theory which resembles the





theory presented previously for the work hardening law.

### 1. Yield Surface

The yield surface is assumed to have the same shape as the failure surface and is expressed by Eqn. 4.9.

$$f_{exp} = \left( \frac{I_1^3}{I_3} - 27 \right) \left( \frac{I_1}{p_a} \right)^m \quad \dots\dots \text{Eqn. 4.9}$$

where  $f_{exp}$  is the stress level

$m$  is a material constant which is responsible for the curvature of the yield surface.

$I_1$  ,  $I_3$  are the stress invariants.

It should be noted that the expression for stress level given here is different from that of Eqn. 2.4 . In the work hardening model the yield surface does not have curvature.

As the value of  $f_{exp}$  increases, the yield surface expands symmetrically around the hydrostatic axis. When the stress level is increased to its peak value, i.e.,  $f_{exp} = n_1$  the failure state is reached. Beyond this point soil can not support any further increase in stress level, and is not capable of sustaining previous stress levels under continued straining.

The parameters  $n_1$  and  $m$  can be found by plotting  $(I_1^3/I_3 - 27)$  versus  $(p_a/I_1)$  at failure in a log-log scale. In Figure 4.4,  $n_1$  is shown as the intercept of



the straight line with  $(p_a/I_1)=1$  and  $m$  as its slope.

The effect of  $\sigma_2$  is included in this failure criterion.

## 2. Flow Rule

A non-associated flow rule is employed in the development of the stress-strain relationship to calculate the plastic expansive strain increments. Consequently, the plastic potential function which is given by Eqn. 4.10 is different from the yield function,

$$g_{exp} = I_1^3 - \left[ 27 + n_2 \left( \frac{p_a}{I_1} \right)^m \right] \times I_3 \quad \dots\dots \text{Eqn. 4.10}$$

where  $g_{exp}$  is the value of the plastic potential and

$n_2$  is a constant for given values of  $f_{exp}$  and  $\sigma_3$ . The value of  $n_2$  can be found by using the following expression.

$$n_2 = S \times f_{exp} + R \left( \frac{\sigma_3}{p_a} \right)^{0.5} + t \quad \dots\dots \text{Eqn. 4.11}$$

in which  $S$ ,  $R$  and  $t$  are material constants.

The stress-strain relationship for plastic expansive strains is then derived according to Eqn. 4.12 in incremental form.



$$d\epsilon_{ij}^{\text{exp}} = \lambda_{\text{exp}} \frac{\partial g_{\text{exp}}}{\partial \sigma_{ij}} \quad \dots\dots \text{Eqn. 4.12}$$

The magnitude of  $\lambda_{\text{exp}}$  is determined from the hardening-softening law.

### 3. Hardening-Softening Law

An experimentally determined relation between plastic work and stress level is used as the hardening-softening law for the strain softening model. The term stress level is defined in Eqn. 4.9. The plastic work is calculated from

$$W_{\text{exp}} = \int \sigma_{ij} \cdot d\epsilon_{ij}^{\text{exp}} \quad \dots\dots \text{Eqn. 4.13}$$

where  $\sigma_{ij} d\epsilon_{ij}^{\text{exp}}$  is the plastic work done per unit volume during a strain increment  $d\epsilon_{ij}^{\text{exp}}$ .

Figure 4.5 shows the variation of the total plastic work,  $W_{\text{exp}}$ , with the stress level,  $f_{\text{exp}}$ , and the confining pressure,  $\sigma_3$ , as obtained from triaxial tests. It is assumed that the peaks of all  $f_{\text{exp}}$  versus  $W_{\text{exp}}$  curves occur at  $f_{\text{exp}} = n_1$ . The amount of plastic work required to reach the peaks is dependent on the confining pressure. Since there are two  $W_{\text{exp}}$  values for a single  $f_{\text{exp}}$  on each curve, the value of  $W_{\text{exp}}$  at the peak stress level is used to distinguish between the



points on the ascending and descending parts.

Experimental results shown on Figure 4.5 are approximated by exponential functions and the following expression gives this relationship.

$$f_{\text{exp}} = a \times e^{-bW_{\text{exp}}} \times \left( \frac{W_{\text{exp}}}{p_a} \right)^{\frac{1}{q}} \quad \dots\dots \text{Eqn. 4.14}$$

The parameters  $a$ ,  $b$  and  $q$  are constants for a given value of the confining pressure  $\sigma_3$ . As a limitation to Eqn. 4.14, Lade (1975) indicated that the value of  $f_{\text{exp}}$  decreases asymptotically to zero for very large values of  $W_{\text{exp}}$ .

The variation of the total plastic work at peak stress level is approximated by Eqn. 4.15 as a function of confining pressure  $\sigma_3$ .

$$W_{\text{peak}} = P \times p_a \left( \frac{\sigma_3}{p_a} \right)^l \quad \dots\dots \text{Eqn. 4.15}$$

where  $P$  and  $l$  are constants and

$p_a$  is the atmospheric pressure.

The values of  $q$ ,  $a$  and  $b$  can be calculated from the following expressions:

$$q = \alpha + \beta \frac{\sigma_3}{p_a} \quad \dots\dots \text{Eqn. 4.16}$$





where  $\alpha$  and  $\beta$  are constants,

$$a = n_1 \left( \frac{e^{\alpha p_a}}{W_{peak}} \right)^{\frac{1}{q}} \quad \dots\dots \text{Eqn. 4.17}$$

where  $e$  is the base for natural logarithms and  $n_1$  is the value of peak stress level.

$$b = \frac{1}{q \times W_{peak}} \quad \dots\dots \text{Eqn. 4.18}$$

Based on Eqn. 4.14, the increment of plastic work is expressed as

$$dW_{exp} = \frac{df_{exp}}{f_{exp}} \left( \frac{1}{\frac{1}{q \cdot W_{exp}} - b} \right) \quad \dots\dots \text{Eqn. 4.19}$$

The expression for the evaluation of the proportionality constant  $\lambda_{exp}$  is given by Eqn. 4.20 and its derivation can be found in Lade (1975).

$$\lambda_{exp} = \frac{dW_{exp}}{3g_{exp} + m \cdot n_2 \left( \frac{p_a}{I_1} \right)^m \cdot I_3} \quad \dots\dots \text{Eqn. 4.20}$$



### 4.3 EVALUATION OF HARDENING-SOFTENING LAW FOR PLASTIC EXPANSIVE STRAINS

The test results shown in Figure 4.5 indicate the dependence of  $W_{exp}$  versus  $f_{exp}$  relationship on the confining pressure  $\sigma_3$ . Accordingly, Eqn. 4.14 which is the expression for this relationship is valid only for cases where the confining pressure is kept constant. Generalization of Eqn. 4.14 into problems with varying  $\sigma_3$  is not possible, as can be shown next.

Referring to Figure 4.6, it is assumed that the initial state of stress of a soil element is on the current yield surface as indicated by point A, with total plastic work value equal to  $W_A$ . A stress increment is applied such that the state of stress moves to point B without exceeding the limits of the current yield surface. No plastic deformations take place for this stress increment and therefore the total plastic work remains the same, i.e.  $W_B = W_A$ . Since the value of  $\sigma_3$  has changed, the value of the parameters  $a$ ,  $b$ , and  $q$  have also changed due to this stress increment. Looking at Figure 4.6b point B is on a curve for which the parameters are based on the new  $\sigma_3$  and the stress level  $f_{exp}$  corresponds to point B of Figure 4.6a. The only value of the total plastic work which can satisfy Eqn. 4.14 for point B is indicated by  $W_{Btrue}$ . Since the plastic work value for point B attained at the end of the stress increment going from A to B as in Figure 4.6a is not equal to  $W_{Btrue}$ , Eqn. 4.14 is no longer valid. Therefore, a unique



relationship between  $f_{exp}$  and  $W_{exp}$  does not exist, except for tests with  $\sigma_3$  constant.

In order to use this hardening-softening relationship established for  $\sigma_3 = \text{constant}$  tests in the analysis of general three dimensional problems an assumption has to be made. This assumption is as follows:

Considering Figure 4.7, at any stress level  $f_{exp}$ , a tangent to the  $f_{exp}$  versus  $W_{exp}$  curve for  $\sigma_3 = \text{constant}$  at a known state of stress provides the relationship between  $df_{exp}$  and  $dW_{exp}$ . It should be noted that for each  $f_{exp}$  versus  $W_{exp}$  curve there exist two points with the same  $f_{exp}$  value, one before and the other after the peak. Lade's approach to differentiate between the hardening and the softening parts of these curves is to compare the current values of  $W_{exp}$  and  $W_{peak}$ . If  $W_{exp}$  is less than  $W_{peak}$ , hardening is taking place and therefore  $f_{exp}$  is still on the ascending part of the curve. If  $W_{exp}$  is greater than  $W_{peak}$ , the descending part of the curve which corresponds to strain softening has to be used. This rule can no longer be accepted valid within the context of the new approach as explained next.

In general,  $W_{exp}$ ,  $f_{exp}$  and  $\sigma_3$  are not uniquely related to each other. The total plastic work  $W_{exp}$  at any point, for example at point D on Figure 4.6b, may have any value including the larger values than  $W_{peak}$  for the corresponding confining pressure,  $\sigma_3$ . This situation may arise for certain stress paths leading to point D. As an





example of this, a stress path is considered which results in no change to the stress level  $f_{exp}$  but a large decrease in confining pressure. In Figure 4.6 the results of such a stress change, i.e., from point C to D is shown. At point C the total plastic work is  $W_{exp}^C$  which has a larger value than  $W_{peak}^{(\sigma_3^a)}$ . During the stress increment, the stress point remains on the current yield surface as shown on Figure 4.6a. Therefore, when point D is reached, there will not be any change in total plastic work and  $W_{exp}^D$  will have the same value as  $W_{exp}^C$ . Since  $W_{exp}^C > W_{peak}^{(\sigma_3^a)}$ ,  $W_{exp}^D$  is also larger than  $W_{peak}^{(\sigma_3^a)}$ . It should be noted that at point D the soil element has not yet failed and before the peak stress level is reached more hardening has to take place and more plastic work has to be done. Therefore,  $W_{peak}$  values can not give a correct indication of whether the ascending or descending section of  $f_{exp}$  versus  $W_{exp}$  curves to be used.

It seems that the only way to decide which part of a curve is to be employed is to keep track of the stress level at all times. Once the peak stress level is attained, further loading will always require the strain softening sections of  $f_{exp}$  versus  $W_{exp}$  curves to be utilized.



#### 4.4 REMARKS ON HARDENING LAWS FOR SOILS

One of the hardening hypotheses in plasticity theory is stated as: the amount of hardening depends on the total plastic work (Mendelson, 1968). The yield criterion is written as

$$F(\sigma_{ij}) = f(w^P) \quad \dots\dots\dots \text{Eqn. 4.21}$$

with the implication that the resistance to further yielding depends only on the amount of work which has been done on the material. The work hardening and also the strain softening models presented here adopt this hypothesis. In both models the stress level, confining pressure and total plastic work form a unique relationship, hence the plastic strain increments can be found uniquely for a given stress increment if the state of stress in soil is known. In this Chapter and also in Chapter 3, it has been shown that such a unique relationship for  $f$ ,  $\sigma_3$  and  $w_p$  does not exist. For the same state of stress, the total plastic work,  $w_p$ , may assume almost any value. It appears that the work hardening hypothesis used in the classical theory of plasticity does not apply to soils and the subject requires further study.

To secure the uniqueness of plastic strain increments an interpretation of the hardening laws of Lade is proposed in this thesis. Although satisfactory results are obtained,



there is no real reason why a relationship between  $df$  and  $dW_p$  obtained from a conventional triaxial test data should apply to strongly path dependent soil behavior in any other loading conditions. Yet it is a common practice in metal plasticity to use a hardening relationship obtained from one type of test to predict material behavior under other test conditions. This is in fact one of the basic assumptions of the classical plasticity theory (see Hill, 1950). Similarly, by using the same approach, good predictions for laboratory tests on soils were obtained as shown in Chapter 3. With the interpretations presented here for the hardening and softening laws, Lade's models can now be employed for the solution of boundary value problems. Consequently, the evaluation of these models can be completed with their application to practical problems.

#### 4.5 CONDITIONS ESSENTIAL FOR STRAIN SOFTENING

Strain softening behavior of material may play an important role in both movements and instability of soil structures. The progressive loss of strength with increased deformation may cause a significant redistribution of the stress and eventually a progressive failure of the structure. The key points which play an important role in the development of strain softening are discussed next by using conventional triaxial test results. Figure 4.8 and 4.9 show stress-strain-volume change data for loose and dense





sands. As illustrated on these figures:

1. The behavior of soil during the shear stage is dependent on the relative density of the specimen attained at the end of all-round pressure application. Under continued straining after the peak resistance is reached, large decrease in resistance is mostly related to dense sand.
2. An increasing confining pressure decreases the tendency to dilate, increases the strain to failure and reduces the brittle characteristics of the stress-strain curves. For high confining pressures even dense sand does not exhibit any significant softening, and the volume changes are entirely compressive. When sheared at low pressures, dense sands are allowed to dilate, and softening becomes apparent. On the other hand, sands with any initial density can be sheared without any volume change at failure by applying an appropriate cell pressure. This pressure, corresponding to zero volume change, is called the critical confining pressure. An example of it is given in Figure 4.10 for samples of Sacramento River sand tested at different void ratios (Lee and Seed, 1967). Points between the origin of the coordinate axes and the curve shown on this figure indicate the state of soil which is most likely to display strain softening characteristics. It appears then, only the combined effects of relative density and confining pressure can reveal the nature of post peak behavior.





Evidently, for strain softening to take place, the stress level should go high enough to reach the peak value. Also, strains should be large enough to pass well beyond the values corresponding to the peak strength before the effect of softening becomes appreciable.

These conditions are not satisfied in all boundary value problems. When they do, they might be confined to a small portion of the structure and therefore might not affect the overall behavior. When widespread areas of a soil mass are affected, or the deformations are concentrated in discrete zones then the problem requires a realistic analysis. The effects of strain softening can be studied only by analyzing the complete soil structure under load. The soil type and triaxial test data alone are not enough for making judgment.



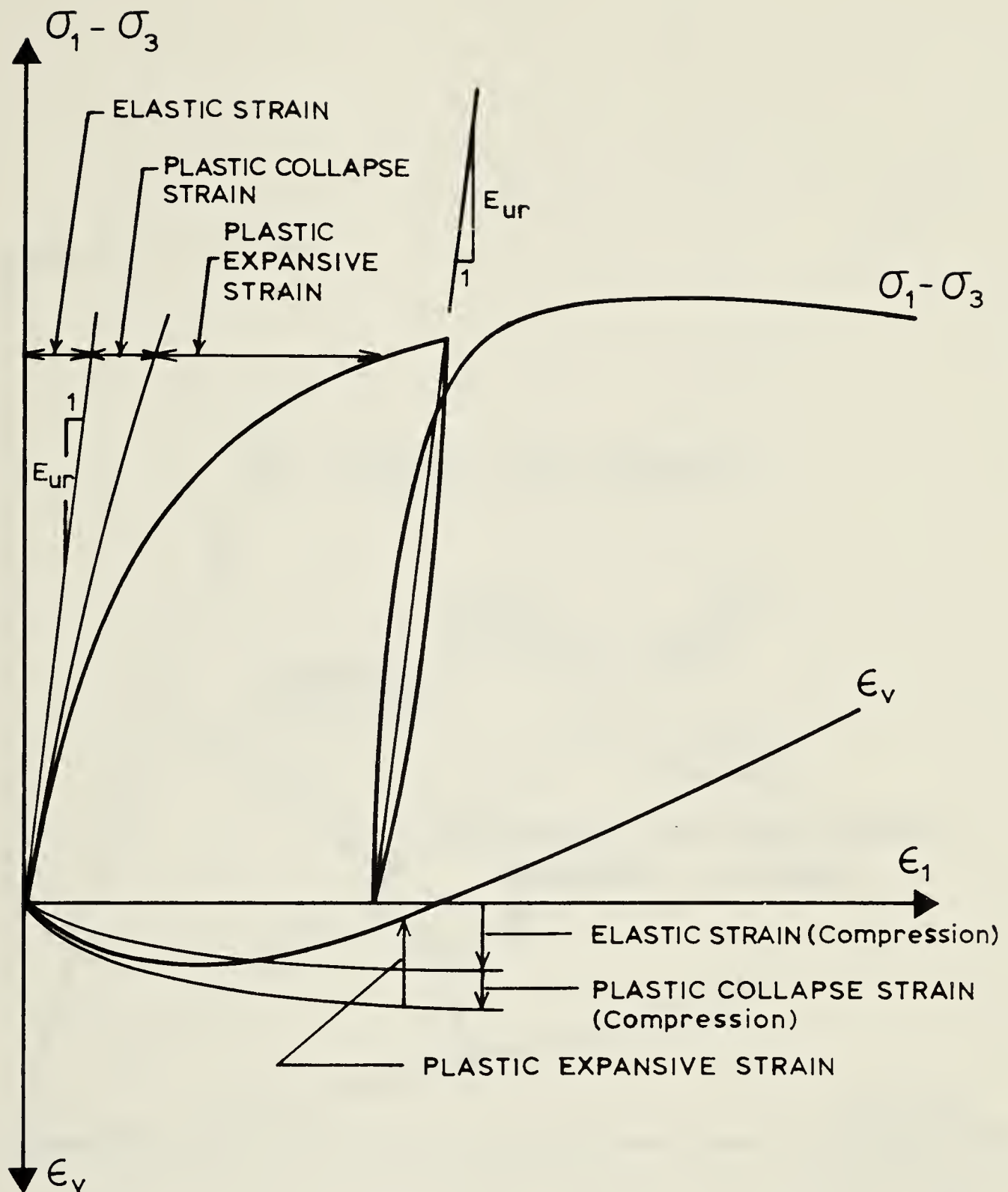


Figure 4.1 Schematic illustration of elastic, plastic collapse and plastic expansive strains in triaxial compression test. (After Lade ,1975)



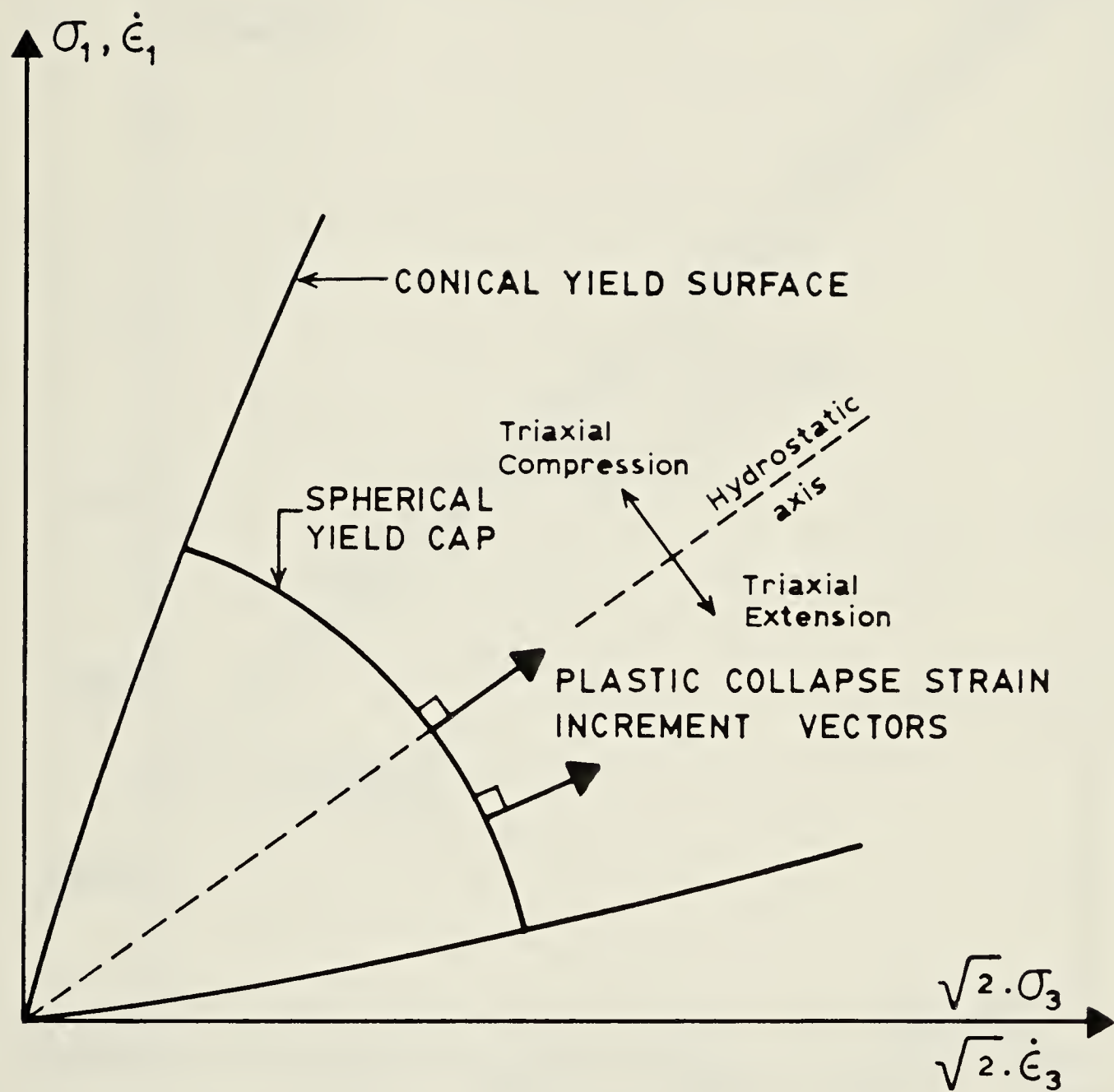


Figure 4.2 Location of yield cap relative to conical yield surface shown in triaxial plane. (After Lade ,1975)





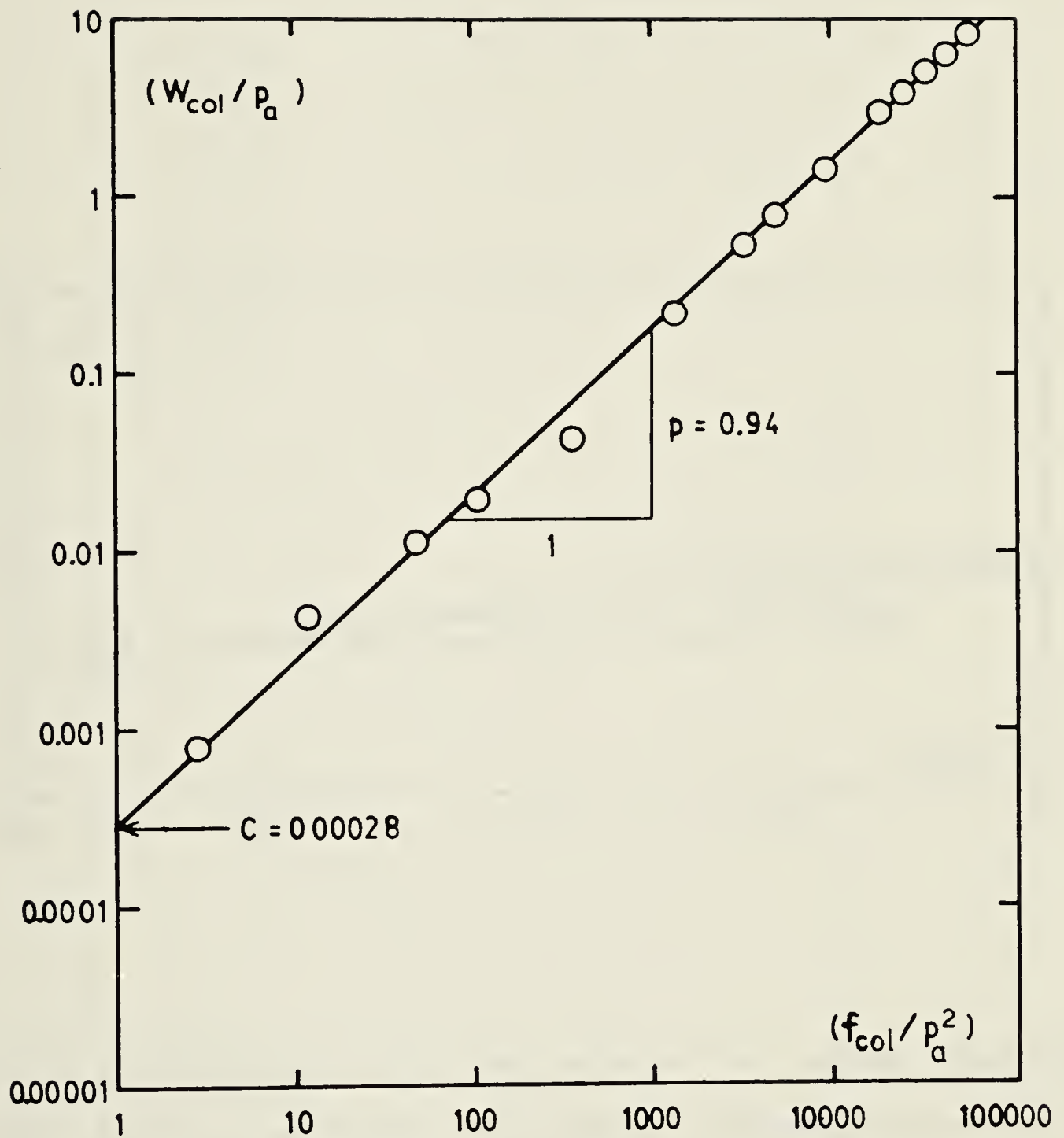


Figure 4.3 Relation between plastic collapse work,  $W_{col}$ , and the value of  $f_{col}$  for loose Sacramento River sand. (After Lade, 1975)



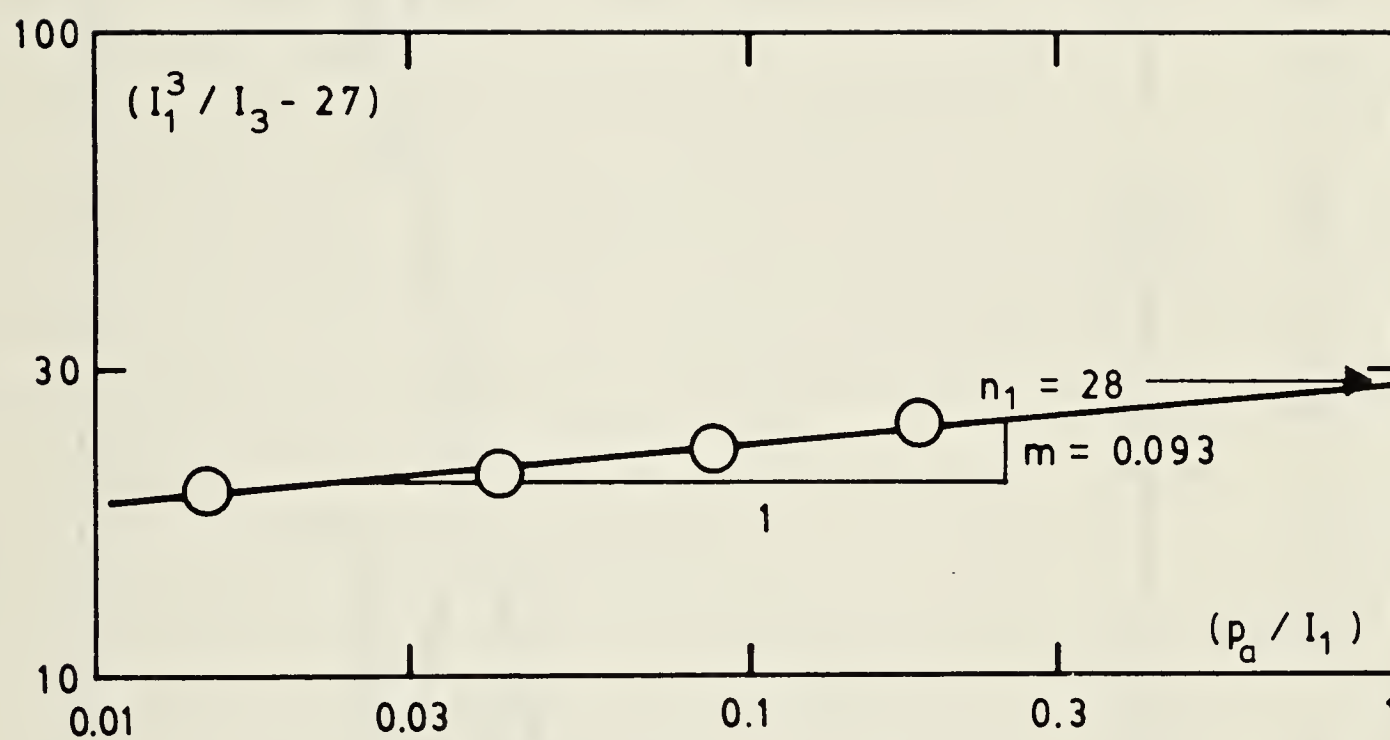


Figure 4.4 Determination of the value of  $n_1$  and  $m$  involved in the failure criterion for loose Sacramento River sand. (After Lade, 1975)



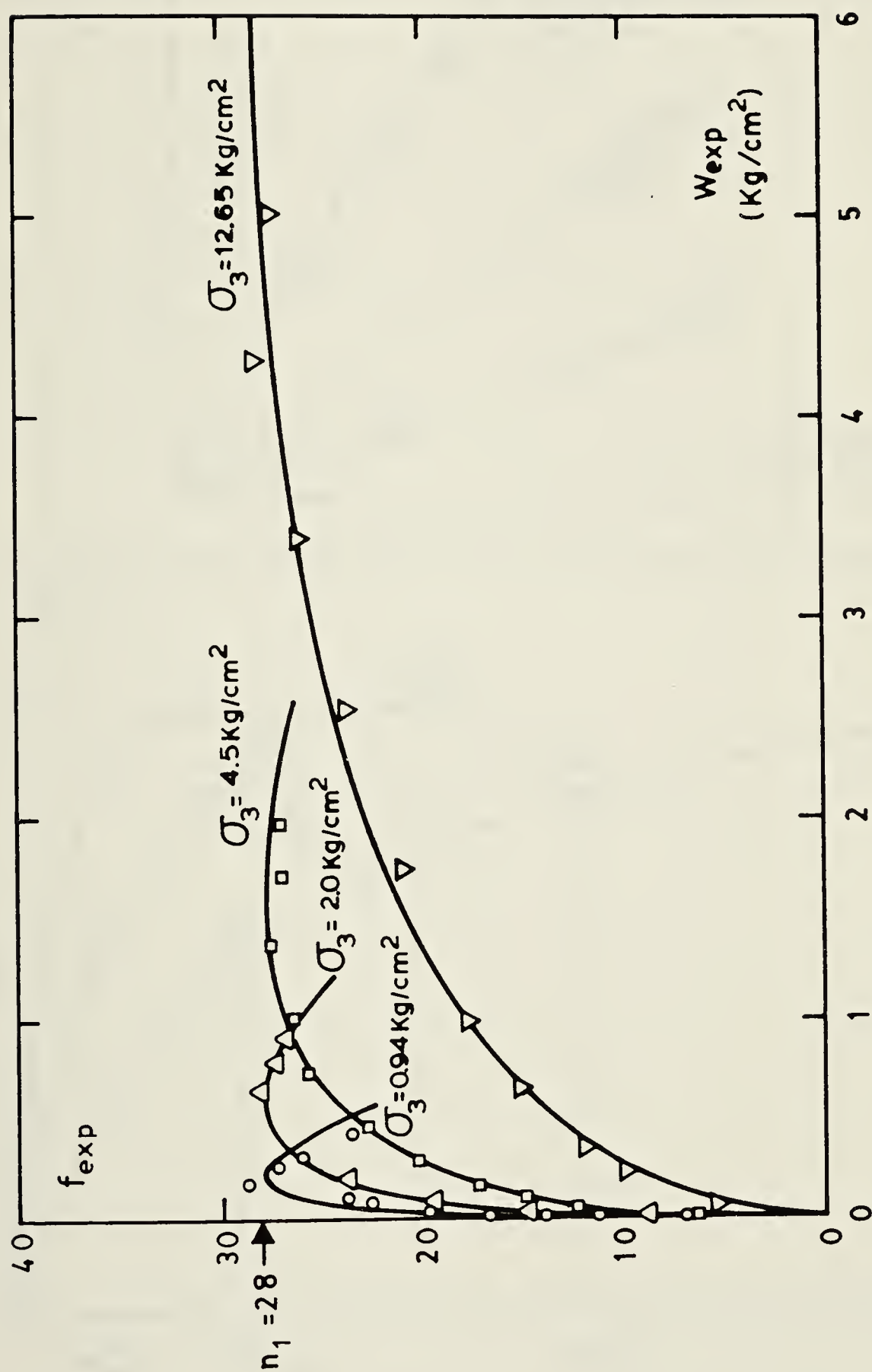


Figure 4.5 Variation of total plastic work with  $f_{exp}$  and  $\sigma_3$  for loose Sacramento River sand. (After Lade, 1975)



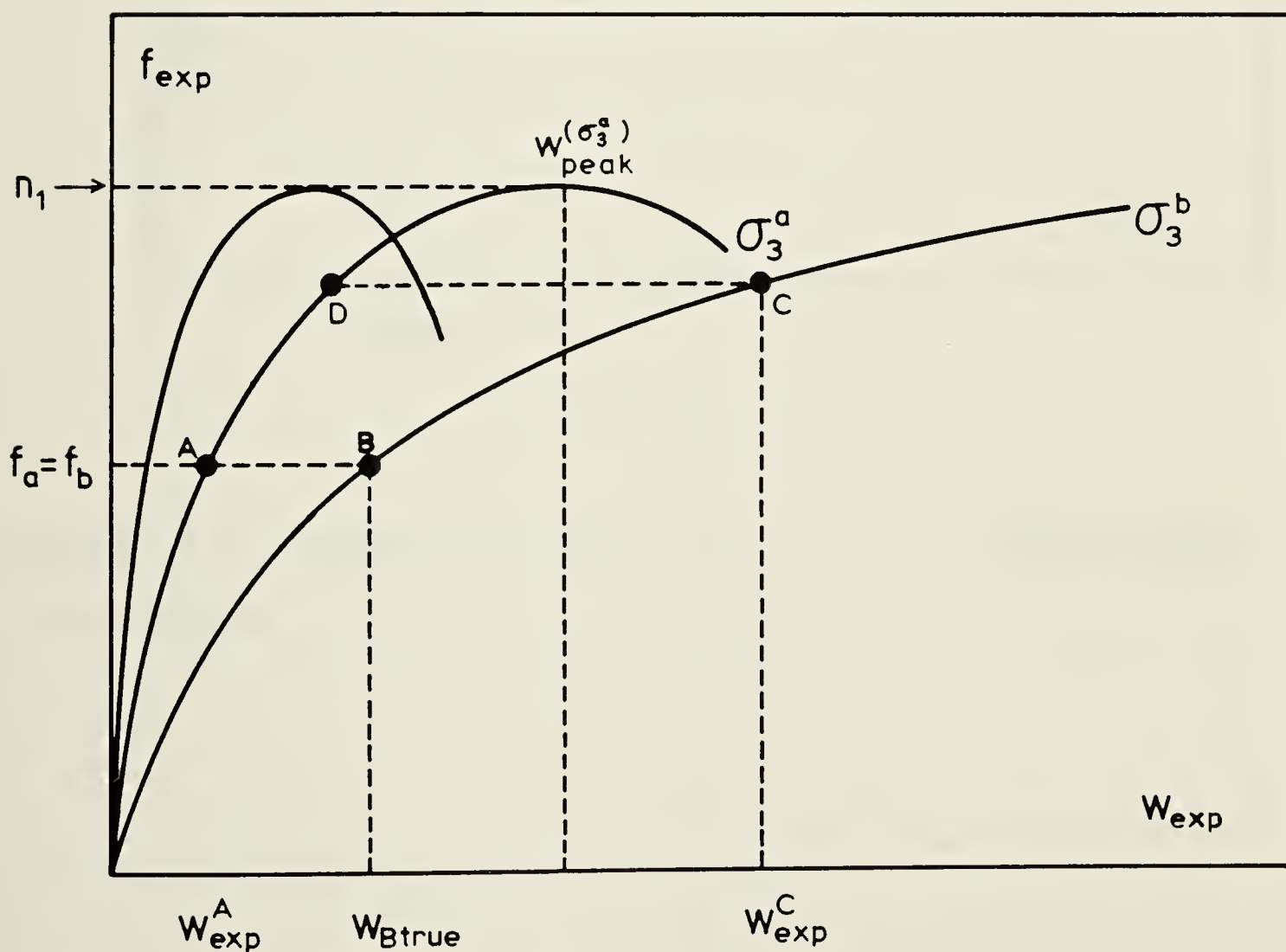
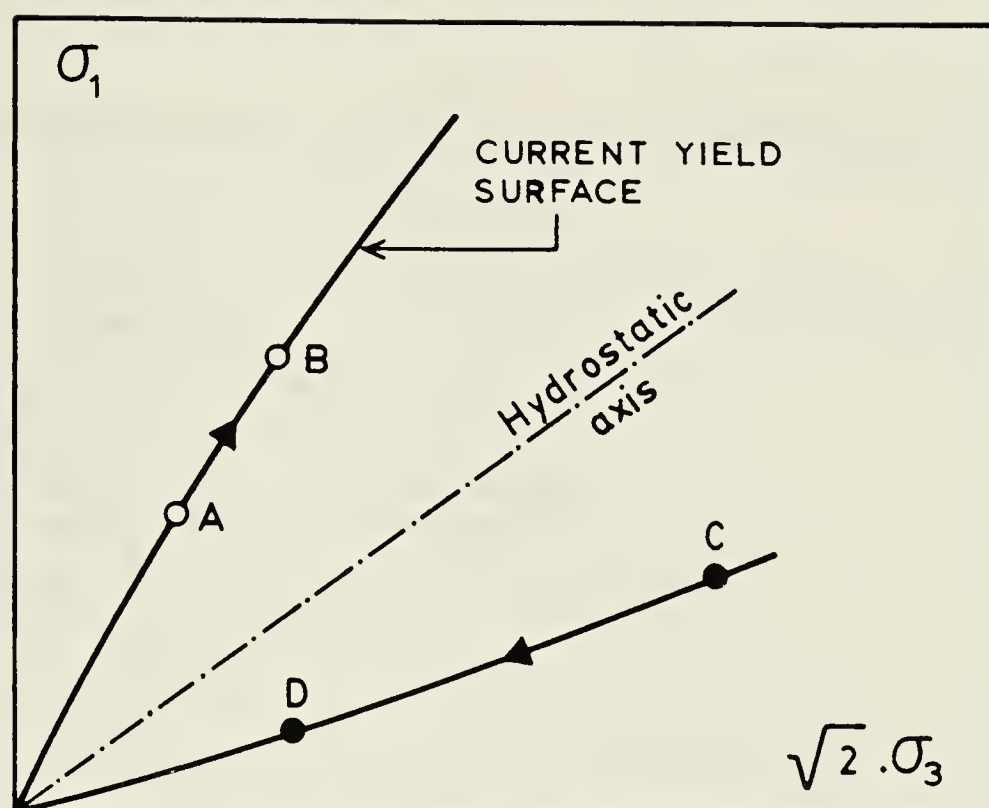


Figure 4.6 Results of a stress change a) stress paths  
b)  $W_{exp}$  versus  $f_{exp}$  relationship.





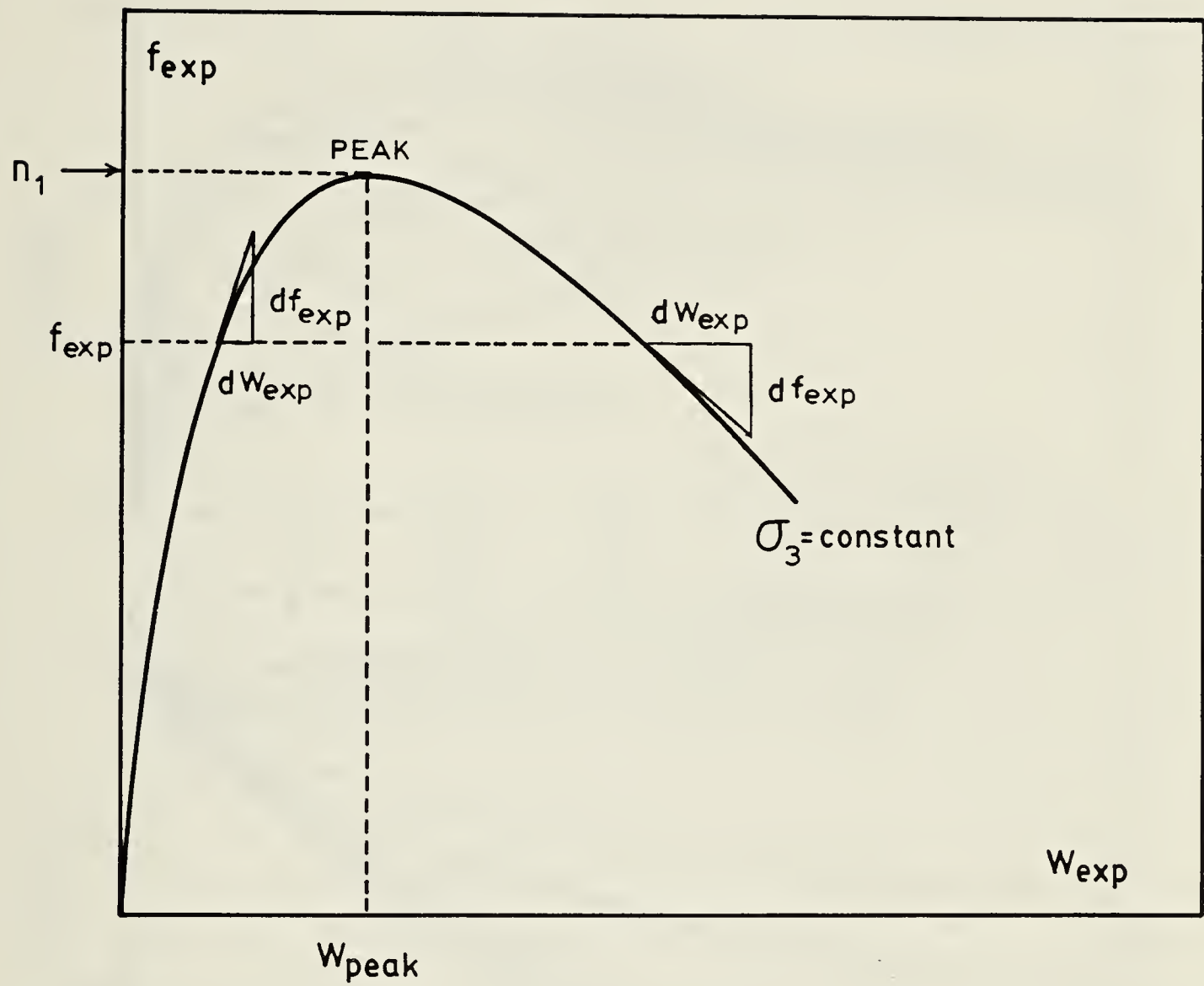


Figure 4.7 Assumption used for  $df_{\text{exp}}$  versus  $dW_{\text{exp}}$  relationship.



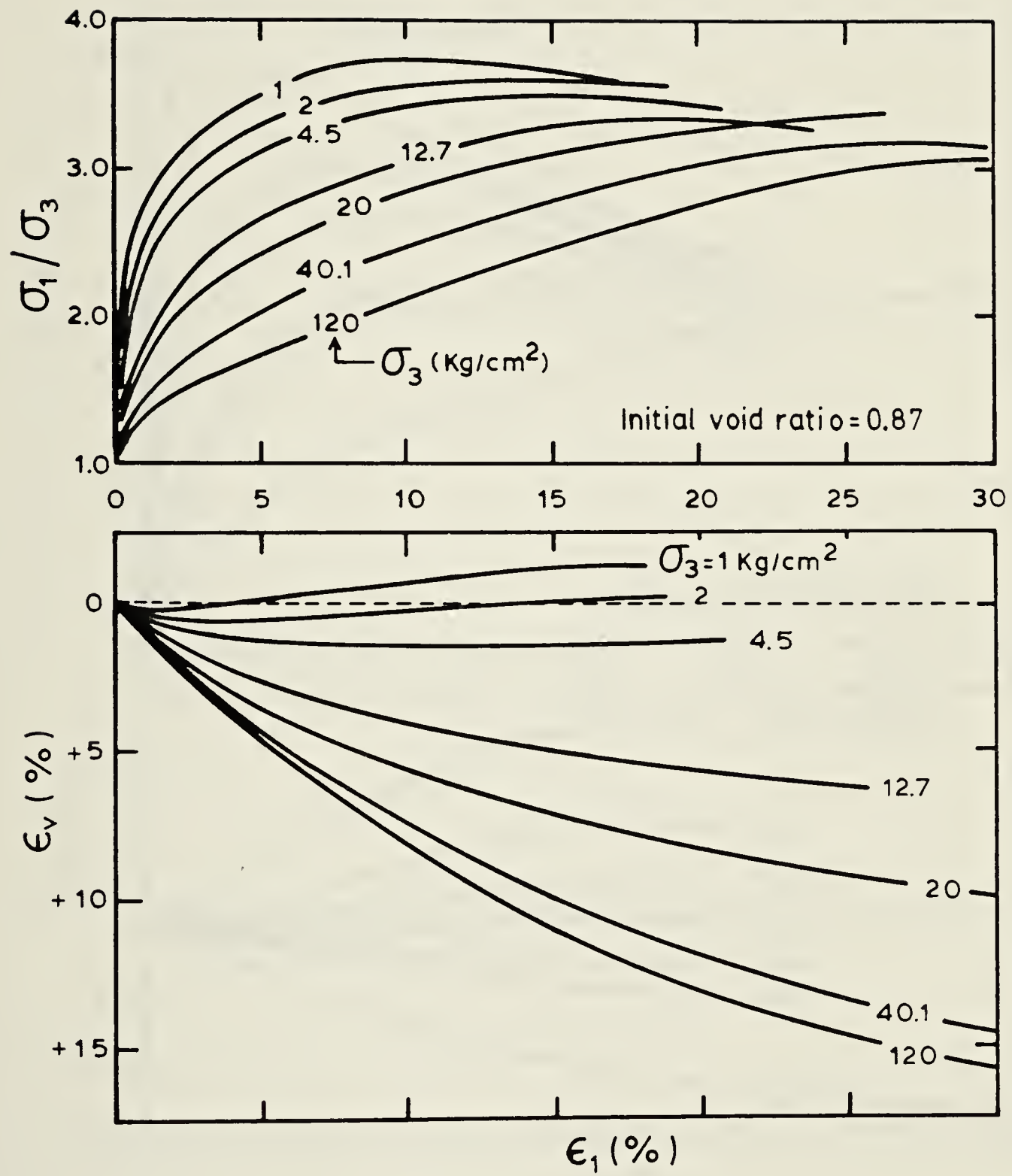


Figure 4.8 Measured stress-strain and volume change behavior for loose Sacramento River sand in drained triaxial compression test. (After Lee and Seed, 1967).



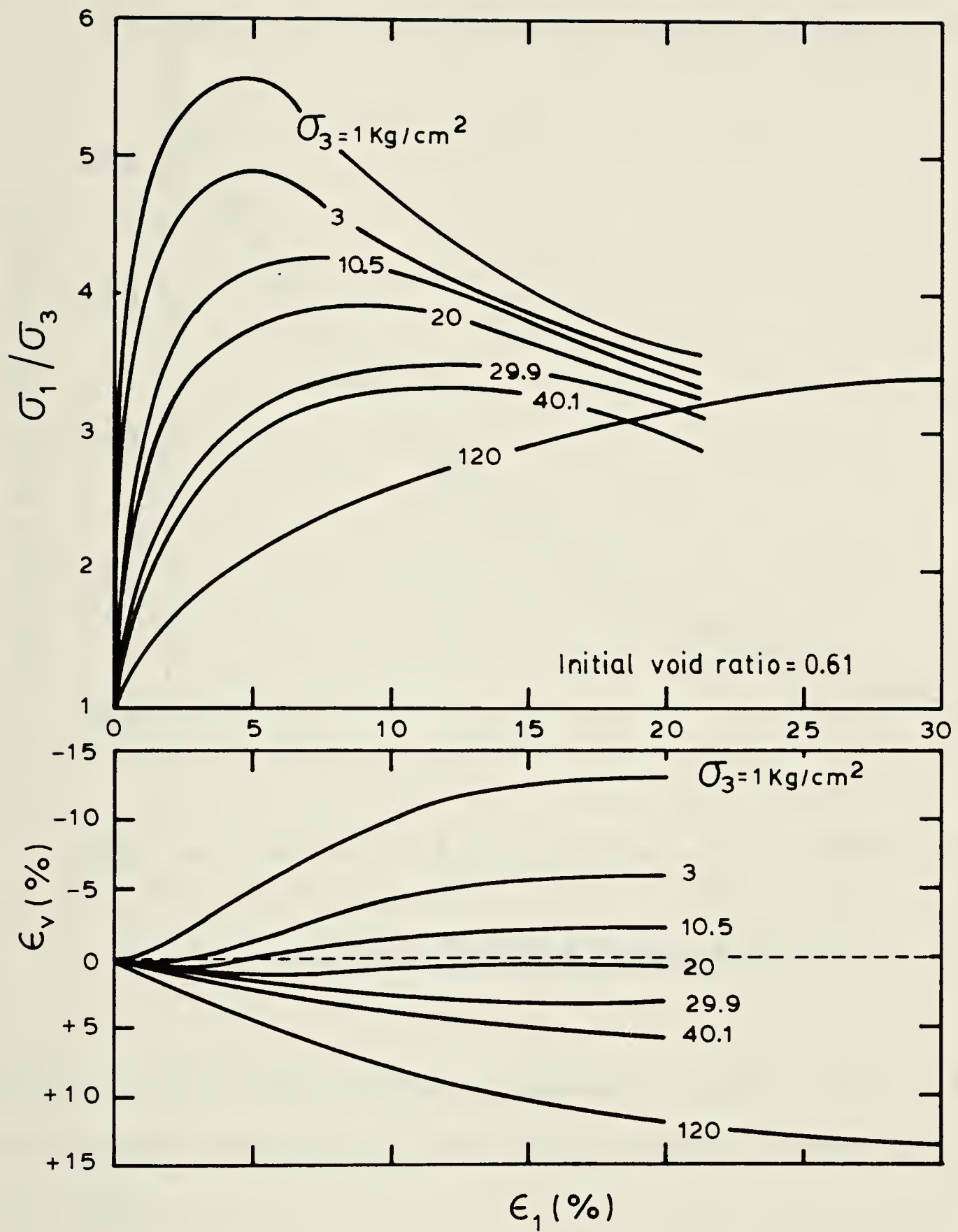


Figure 4.9 Measured stress-strain and volume change behavior for dense Sacramento River sand in drained triaxial compression test. (After Lee and Seed, 1967).





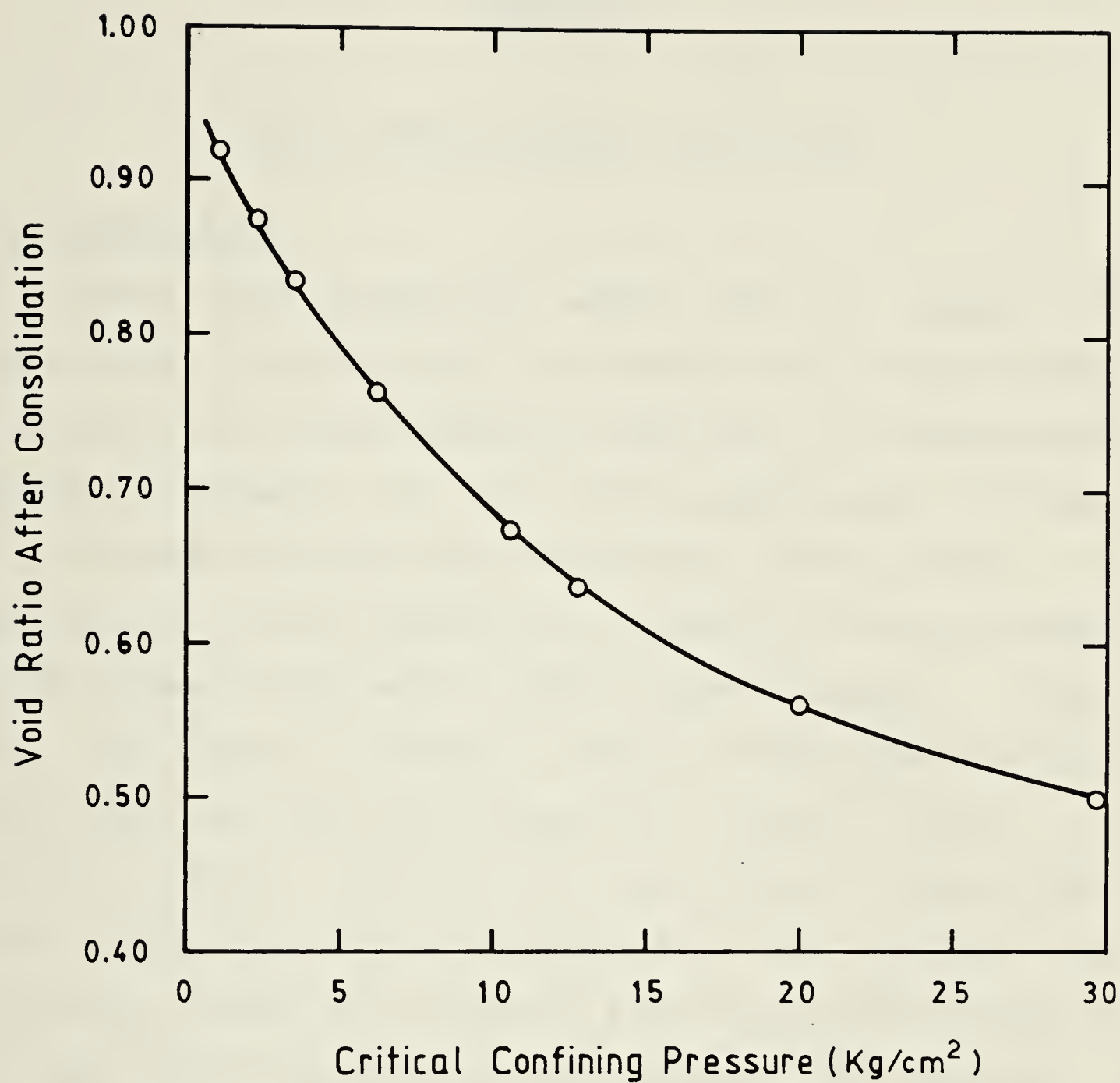


Figure 4.10 Relationships between void ratio after consolidation and critical confining pressure. (After Lee and Seed, 1967).



## CHAPTER 5

### WORK HARDENING MODEL WITH A CAP

#### 5.1 INTRODUCTION

Lade's work hardening model has a number of limitations. As discussed in Section 2.3, one of these limitations is unsatisfactory modelling in proportional loading. Similarly, for all stress paths shown in Figure 5.1, the model predicts only recoverable strains which is in contradiction with observed soil behavior. The cone shaped yield surface of the model without a cap is shown in Figure 5.2a. Any stress increment along a stress path remaining within that cone does not produce any plastic strains. In reality, plastic strains may take place for some stress paths in that zone. It is proposed here to overcome this limitation alone by attaching a cap type yield surface to the open end of the conical yield surface. The details of the type of cap used and the improvements obtained in predictions are presented in this Chapter.

#### 5.2 TYPE OF CAP

In order to model soil behavior more correctly cap type yield surfaces have been proposed in the past by many researchers starting with Drucker et al., (1957). Depending on the model, a spherical or some other convex shape yield surface is employed as a cap. If the state of stress changes



such that this cap is pushed out as in Figure 5.2b, then plastic strains are predicted. Among several cap type yield surfaces available in the literature, the cap yield surface used by Lade (1975) as part of his strain softening model was selected as a cap for the present work, and is used in connection with his work hardening model. The corresponding flow rule and the work hardening law are also taken from his work without any change. The details of the yield criterion are given in Section 4.2.3.

### 5.3 UTILIZATION OF CAP TYPE YIELD CRITERION

Although the cap yield surface of Lade's strain softening model was chosen without any change in its formulation, as the desired cap for the work hardening model, the conditions under which it is used are not the same in the present development. In order to clarify the differences in using the same cap yield criterion for these two models, it is necessary first to elaborate on the corresponding sections of the strain softening model.

In the strain softening model total strain increments are calculated as the sum of elastic, plastic collapse and plastic expansive parts. It is assumed that each part can be calculated separately and then superposed. An important point here is that any stress change causing the yield cap to expand, see Figure 5.3a and 5.3b, will produce  $\{d\epsilon_{ij}^{col}\}$  without any condition on where the conical yield surface is located at that moment. For example the stress paths from A





to B and from P to D of Figure 5.3a and 5.3b respectively, require that the plastic collapse strains be calculated and superposed on the other parts of strain as indicated by Eqn. 4.1. The significance of the stress path from A to B is that it causes only the cap yield surface to expand while the conical yield surface stays where it was before. On the other hand the stress path from P to D results in expansions of both yield surfaces.

Eqn. 2.1 which is somewhat similar to Eqn. 4.1 represents the concept of dividing the total strain increments into elastic and plastic parts for the work hardening model. However, the plastic strain increments,  $\{d\epsilon_{ij}^p\}$ , are not further sub-divided into plastic collapse and plastic expansive parts as in the case of the strain softening model. For example, the plastic strain increment taking place due to the stress change from P to D in Figure 5.2c, is represented as  $\{d\epsilon_{ij}^p\}$  alone by using the work hardening model while the same plastic strain increment is calculated as the sum of two components, i.e.,  $\{d\epsilon_{ij}^{col}\} + \{d\epsilon_{ij}^{exp}\}$  when using the strain softening model. For proportional loading, such as the stress path 1 of Figure 5.1,  $\{d\epsilon_{ij}^p\}$  becomes zero while both  $\{d\epsilon_{ij}^{col}\}$  and  $\{d\epsilon_{ij}^{exp}\}$  have non-zero values. It is clear that  $\{d\epsilon_{ij}^p\}$  of Eqn. 2.1 does not have the same meaning as  $\{d\epsilon_{ij}^{exp}\}$  of Eqn. 4.1.

When the stress changes take place along any one of the stress paths shown in Figure 5.1, the work hardening model without a cap predicts only elastic strains. On the other





hand, the work hardening model with a cap is able to predict plastic collapse strains in addition to the elastic increments of strain for the same stress paths.

A summary of requirements for calculating different parts of total strain increments, by using the work hardening model with a cap, is now provided.

a) When a stress path remains within the current conical yield surface (indicated as the shaded area in Figure 5.2a) the total strain increments are calculated by

$$\left\{ d\epsilon_{ij} \right\} = \left\{ d\epsilon_{ij}^e \right\} + \left\{ d\epsilon_{ij}^{col} \right\} \quad \dots\dots \text{Eqn. 5.1}$$

Calculation of  $\left\{ d\epsilon_{ij}^{col} \right\}$  is given by Eqn. 4.8, and the proportional loading path is included in its zone of application. Of course,  $df$  has to be bigger than zero for  $\left\{ d\epsilon_{ij}^{col} \right\}$  to be calculated, otherwise it must be zero.

b) If the stress increment is along a stress path directed outward from the conical yield surface, as in Figure 5.2c, and 5.2d, the total strain increments are calculated by

$$\left\{ d\epsilon_{ij} \right\} = \left\{ d\epsilon_{ij}^e \right\} + \left\{ d\epsilon_{ij}^p \right\} \quad \dots\dots \text{Eqn. 5.2}$$

which is identical to Eqn. 2.1.

c) When the state of stress follows the path from P to D as shown in Figure 5.2c, the plastic collapse strains are not calculated separately but  $\left\{ d\epsilon_{ij}^p \right\}$  of Eqn. 2.1 represents the



sum of all parts of plastic strain increments. Care has to be taken for this type of stress path. Although  $\{d\epsilon_{ij}^{col}\}$  is not calculated, the value of  $f_{col}$  has to be updated. In other words, the cap yield surface has to be moved to a new location passing through point D.

#### 5.4 JUSTIFICATION FOR WORK HARDENING MODEL WITH A CAP

As presented earlier in section 4.1, a cap improves the capabilities of the work hardening model and the calculation of plastic strains which may take place due to stress increments along certain paths remaining within the conical yield surface becomes possible. This point has been emphasized enough already.

Comparisons of observed stress strain curves with those predicted by the work hardening model with a cap are presented in Section 5.5. to illustrate the possible improvements that can be obtained in prediction of laboratory test results.

The significance of a cap yield surface in the analysis of a geotechnical engineering problem may be predicted, provided that the stress paths followed by the soil elements comprising the structure are known. If the majority of the elements undergo proportional loading while the remaining elements experience a very small amount of plastic expansive straining, the yield cap will have a dominant role in the prediction of behavior. Without a cap, the work hardening model predicts mostly elastic strains for such problems.





There are important soil structures where stress paths generally follow proportional loading, for example earth dams as indicated by Eisenstein and Law (1979).

For the justification to be complete, the following question is to be answered: why is there a need for a work hardening model with a cap while there already exists a more sophisticated model which has a cap and can take the strain softening into account? There are a number of reasons for this effort as discussed next.

1. Not all soils under all circumstances exhibit strain softening. Key conditions for strain softening to take place are presented in Chapter 4. Therefore there may not be a need for more sophistication and the work hardening model with a cap may be just as good.
2. For a problem where strain softening does not occur, an unnecessarily refined analysis using the strain softening model will be too costly.
3. The calculations required to obtain the parameters for the softening model are more involved.
4. The development of a finite element program for a strain softening model is more difficult.
5. One way of determining the significance of modelling the strain softening behavior of soil in analysis of soil structures, is to compare the predictions of two finite element programs developed for constitutive laws with different capabilities for modelling strain softening alone but otherwise exactly the same. It is believed





that the Lade's strain softening model and the work hardening model with a cap can be used for such a comparison.

6. Finally, the importance of using a cap yield criterion in the analysis of boundary value problems can be investigated by examining the differences of predictions made by two finite element programs developed for models such as Lade's work hardening model with and without a cap yield surface.

### 5.5 PREDICTIONS OF STRESS-STRAIN BEHAVIOR

The measured behavior of two different soils tested along various stress paths are presented next with the predictions of the work hardening model with a cap.

The first set of test results, using Ottawa sand was provided by the organizing committee of the NSF/NSERC North American Workshop on "Plasticity Theories and Generalized Stress-Strain Modelling of Soils" held in McGill University, Montreal in May 1980. The parameters required in the present work for the calculation of the elastic and plastic collapse strains were obtained from conventional triaxial compression and hydrostatic compression test results. The stress-strain curve as predicted and the experimental results for the stress path along the hydrostatic stress axis are plotted in Figure 5.4. The results show that there is a significant improvement in predictions.

The second experimental data is taken from the published work of Lade and Duncan (1976), in which the



results of tests on loose Monterey No.0 sand were provided for a stress path representing proportional loading. Those measured results and the predictions made using the cap model are presented in Figure 5.5. The value of Poisson's ratio used in this calculation is 0.26. Again, a comparison suggests that by adding a cap yield criterion, some improvement can be achieved over the work hardening model without a cap.

The results of experiments on loose Monterey No.0 sand tested along a stress path with increasing deviator stress and constant confining pressure after previous loading to a higher stress level were also given by Lade and Duncan (1976). These test results and the predictions made using the present model for the soil behavior along this stress path, are shown on Figure 5.6. Although a slight improvement is achieved, especially in the predictions of volumetric strains, there seems to be more room for further improvement in modelling soil behavior for this kind of stress path and stress history. It should be noted that the stress path from point A to point B involves reloading because the soil element was subjected to an earlier higher stress level before point A was reached. Therefore only elastic strains are predicted for the section between point A and point P when the loading follows the path from A to B. The stress-strain curves in Figure 5.6 show that the largest difference between predicted and measured curves is at point P. This difference does not change to a noticeable degree



under subsequent loading. It appears that during large unloading-reloading cycles soils tend to "forget" the maximum stress level attained previously. This contradicts an assumption used in the development of Lade's work hardening and strain softening models. In reality, the current yield surface during unloading-reloading cycles may not stay at the level corresponding to the maximum stress level reached in its history, but may shrink or shift its position or even may take another shape.

## 5.6 CONCLUSIONS

In this Chapter a cap type yield criterion was incorporated into Lade's work hardening model. The improvement that can be obtained by using a cap yield criterion was demonstrated by comparing experimental results with predictions made by the models with and without such a cap. In all cases examined, the predictions made by adding a cap to the model showed a better agreement with the experimental data. The degree of success attained in modelling soil behavior was dependent on the stress path and stress history. For certain stress paths involving unloading-reloading, improvement was not significant. Cyclic loading requires more attention.

The work hardening model with a cap links the work hardening model without a cap and the strain softening model, and altogether they provide a selection of different models with improved capabilities.





Furthermore, the procedure proposed in Section 5.2 to combine two models may be used by other model developers. Plastic strain increments need not be divided into plastic collapse and plastic expansive parts for all stress paths. If such a division exists, then certain assumptions have to be made in dividing the total plastic strain increment into its parts. For a general stress increment, direct measurement of separate plastic collapse and plastic expansive strain increments is not possible.

Finally, the finite element procedures become easier for constitutive laws dealing with smaller number of stress-strain relationships within the model.





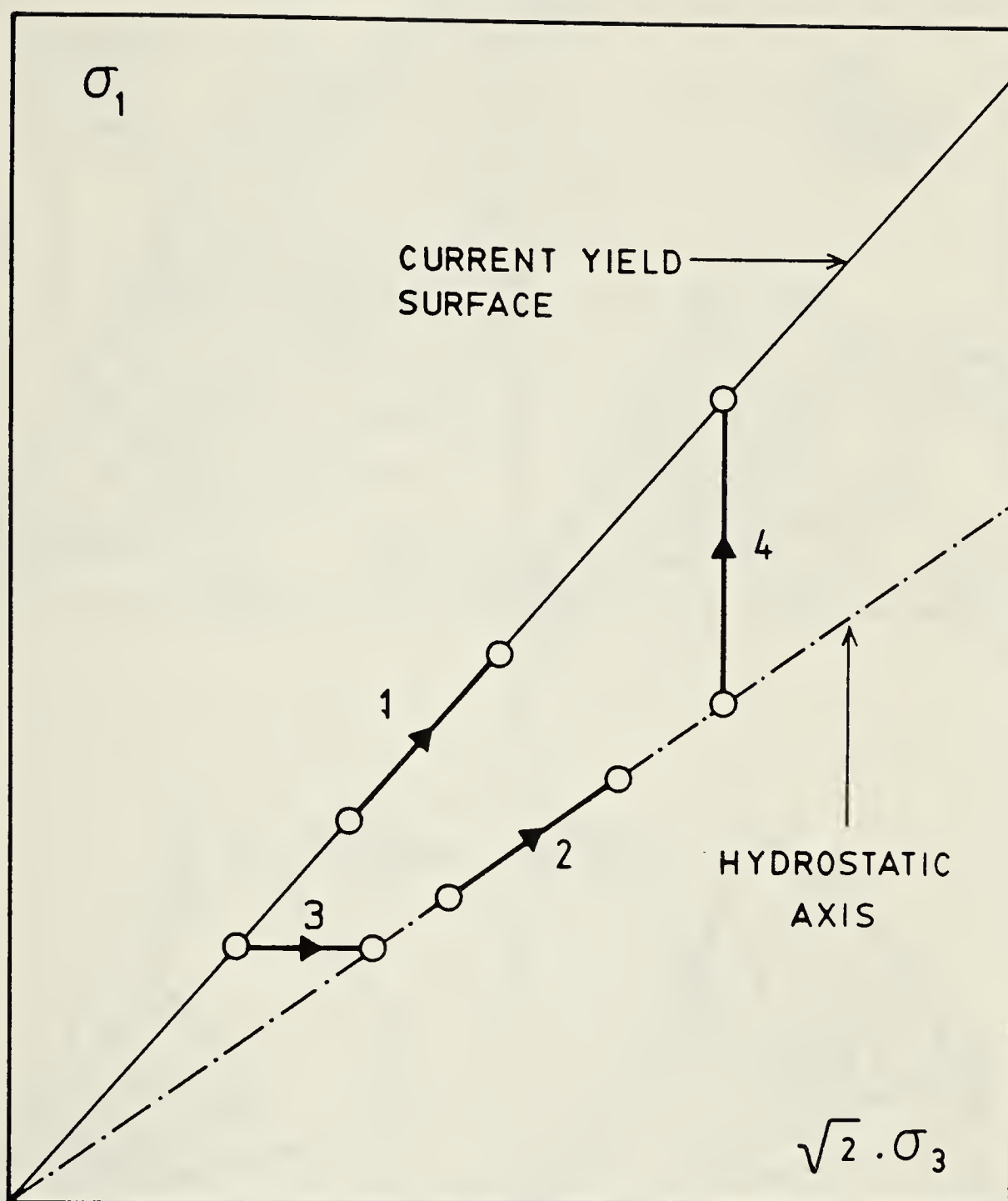


Figure 5.1 Example of stress paths where no plastic strain increments are predicted by the work hardening model without a cap.



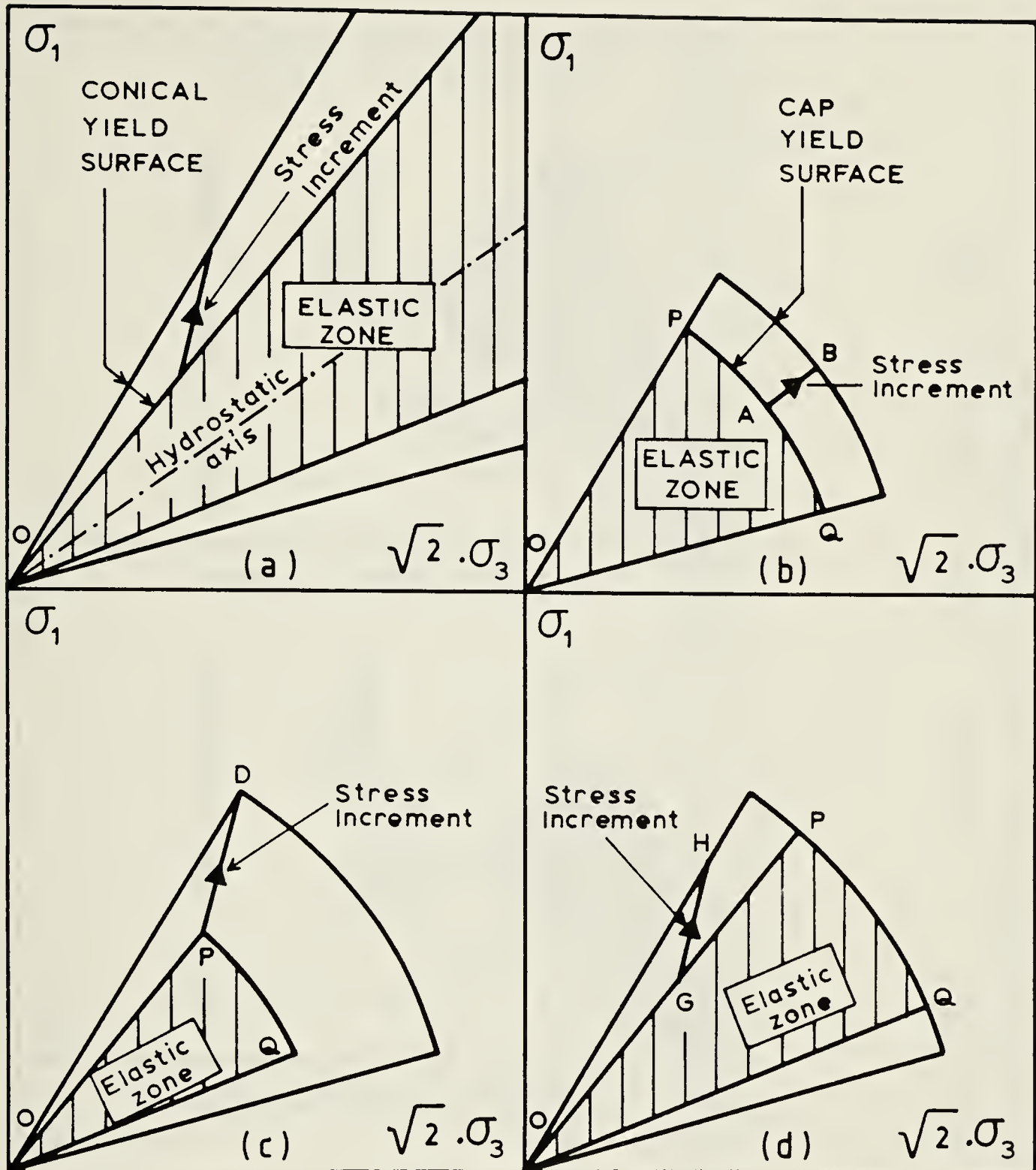


Figure 5.2 The effect of different stress paths on the expansion of yield surfaces for work hardening model (a) without a cap (b, c, d) with a cap.



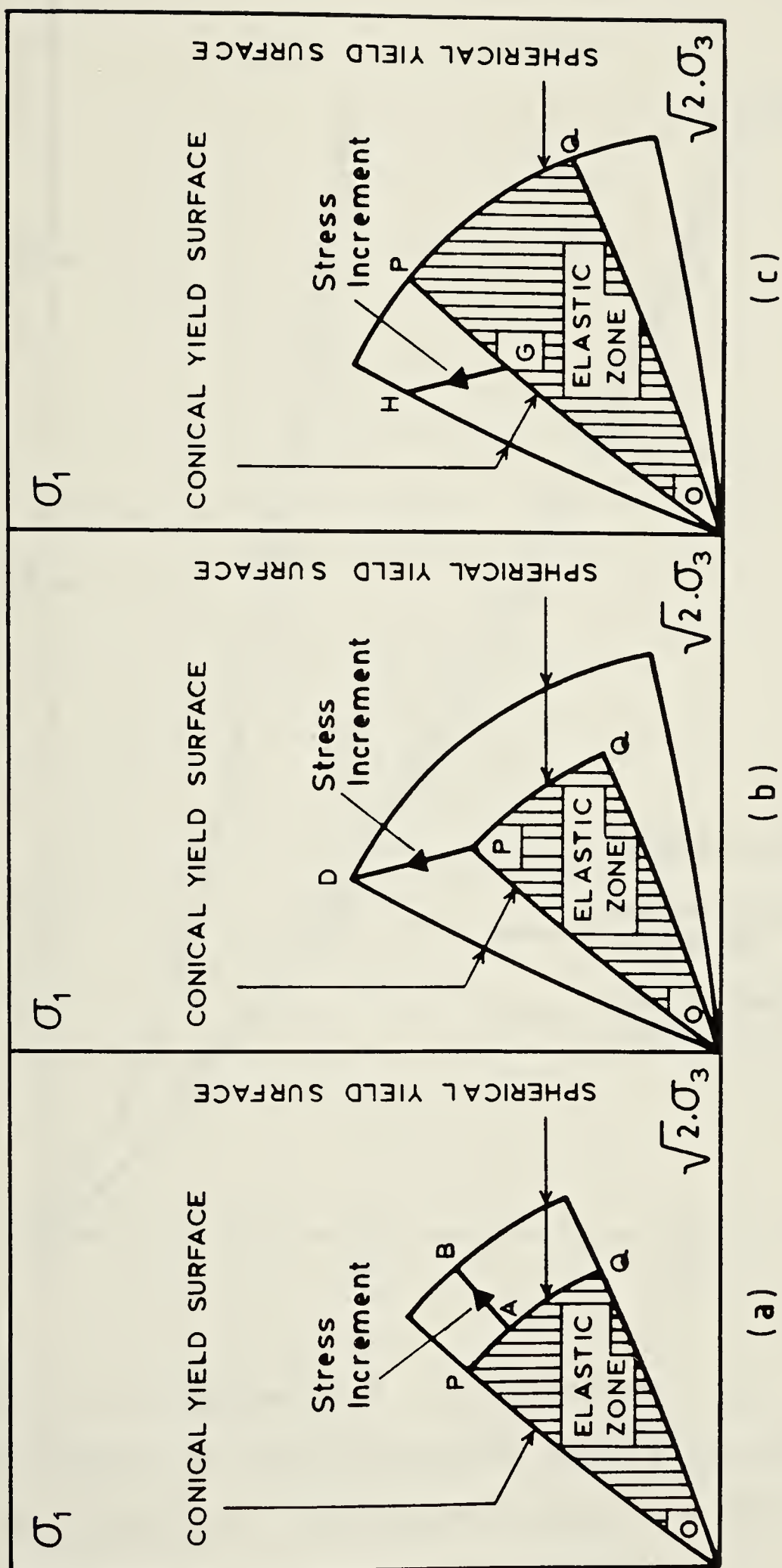


Figure 5.3 The effect of different stress paths on the expansion of yield surfaces for strain softening model.





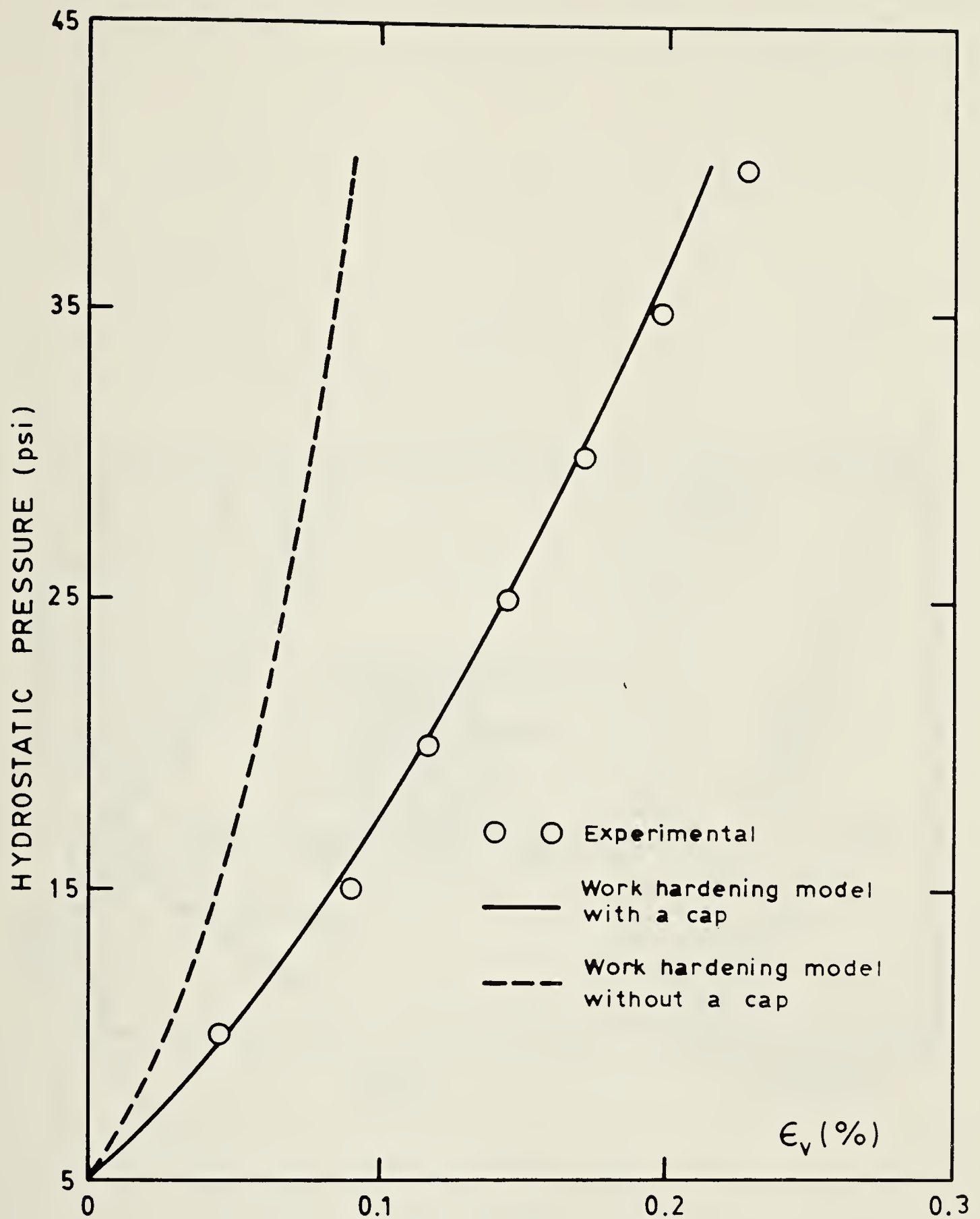


Figure 5.4 Hydrostatic compression of Ottawa sand. Predictions of work hardening model with and without a cap yield criterion. ( Experimental data from NSF/NSERC Workshop on Soil Plasticity, Montreal, May 1980)



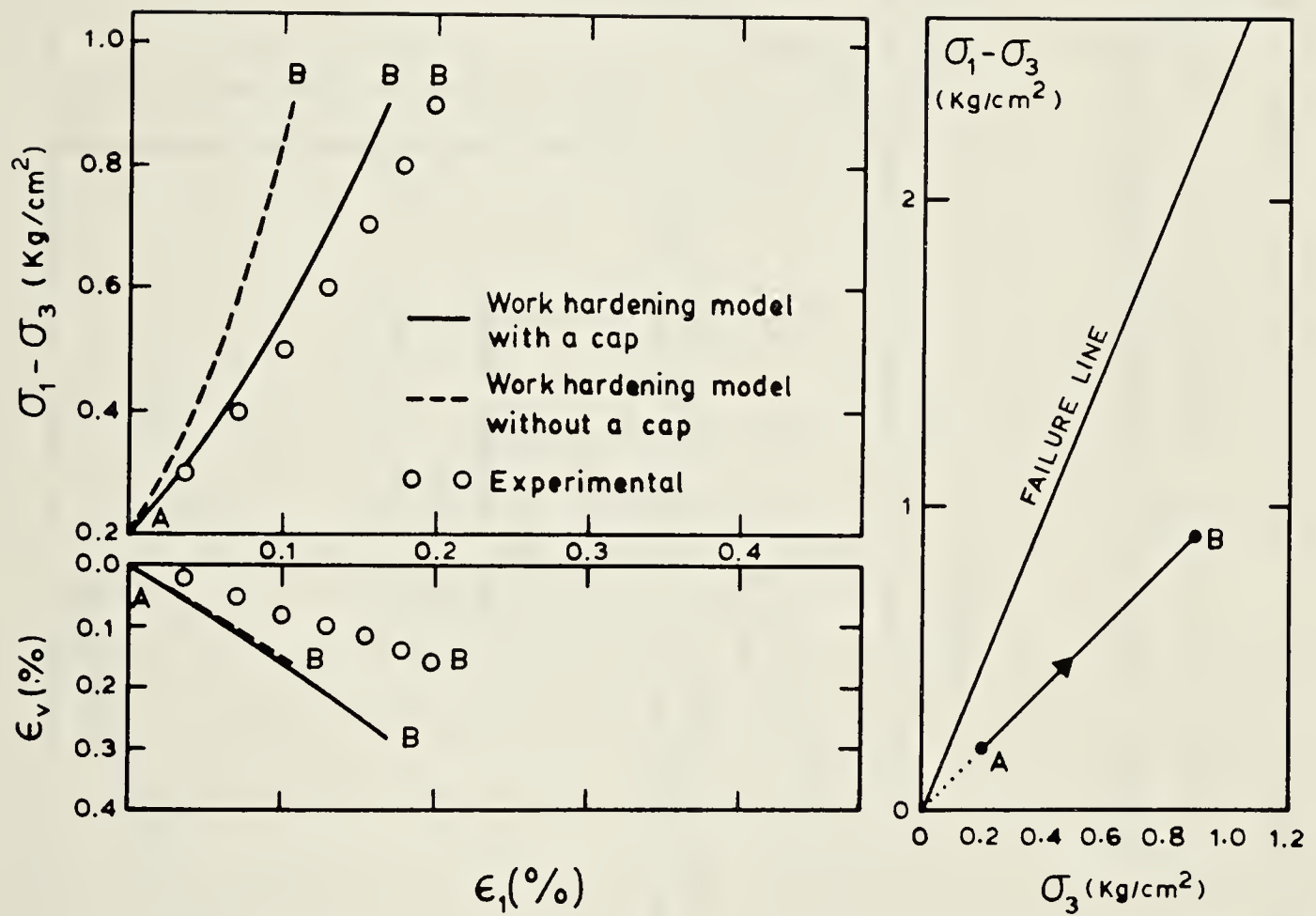


Figure 5.5 Proportional loading. Predictions of work hardening model with and without a cap. Loose Monterey No. 0 sand. Experimental data after Lade and Duncan (1976)



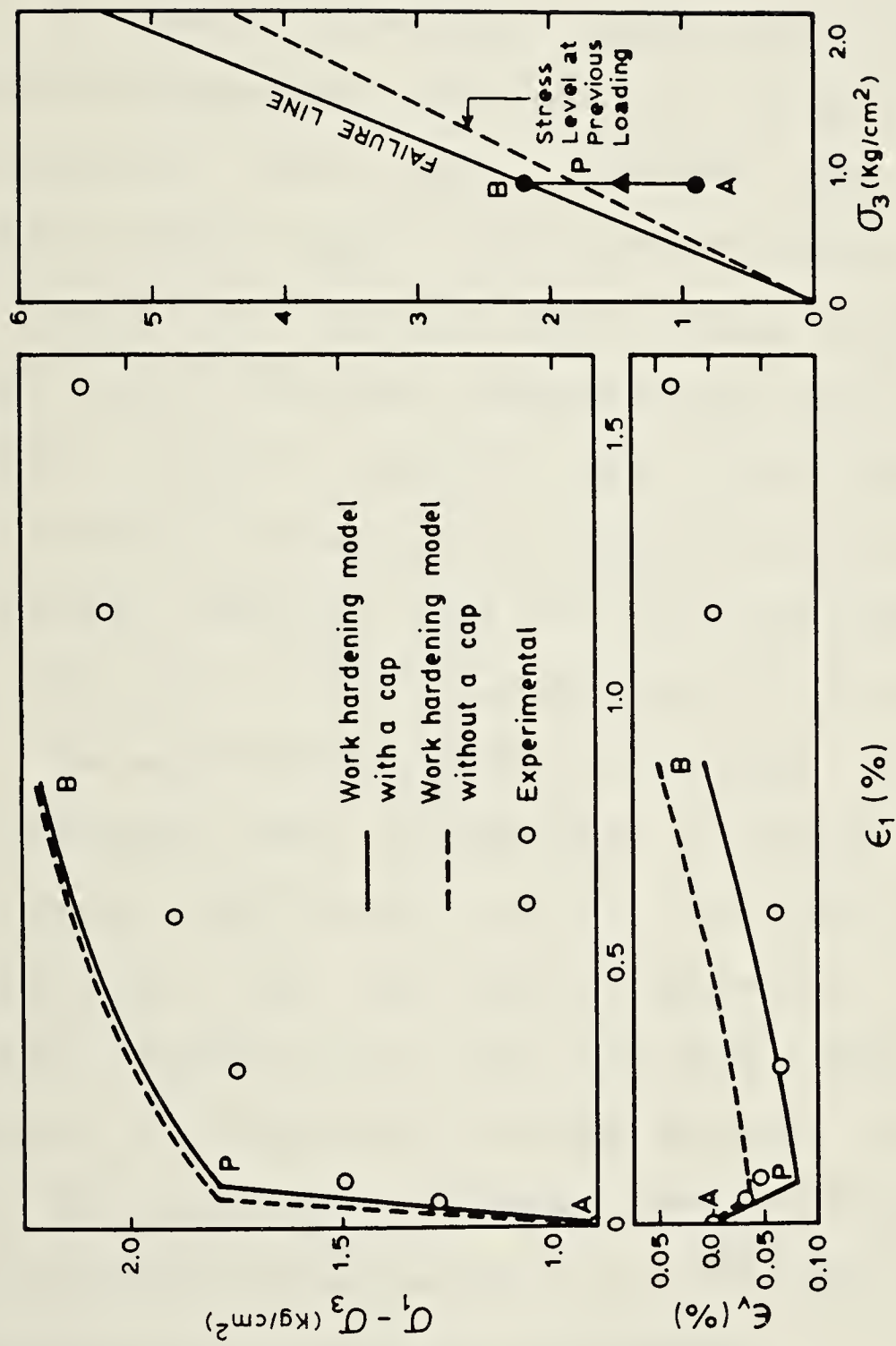


Figure 5.6 Stress path with increasing deviator stress and constant  $\sigma_3$  after previous loading to a higher stress level (Experimental data after Lade and Duncan, 1976)



## CHAPTER 6

### FINITE ELEMENT PROCEDURES FOR WORK HARDENING MODEL

#### 6.1 INTRODUCTION

In order to analyze plane strain problems, a finite element program was developed by using the displacement formulation. The main intention was to examine the capabilities of Lade's work hardening model (without a cap) to predict soil behavior under complex boundary conditions. Also, the difficulties related to the use of the model in a finite element analysis were investigated. Efficiency, simulation of construction stages or modeling soil structure interface behavior were not the prime concern; their study was left until after the usefulness of the model was proven.

The work hardening law of the model was used in its re-evaluated form as presented in Chapter 3. This led to a different constitutive matrix for the finite element formulation than the ones proposed by Ozawa and Duncan (1976a), Duncan et al (1977) and Wong (1978). Therefore, the results of the finite element analysis of the present work and the conclusions reached are different from the calculations and arguments of all the other studies, as will be discussed in the next two Chapters.

A linear elastic finite element program coded by Murray (1974) was used as a starting point. Major changes were made in order to assign initial stresses to elements, to solve a





system of algebraic linear simultaneous equations having an unsymmetric coefficient matrix, and to deal with material nonlinearity. Isoparametric elements were employed in this program.

## 6.2 SOLUTION METHOD FOR MATERIAL NONLINEARITY

Convergence problems encountered by others, such as Naylor (1975) and Wong (1978) were taken as a lesson in the present work for the selection of a solution method to handle the material nonlinearity. The solution technique chosen is called the tangent stiffness method. The basis of this procedure is the application of the load in small increments. A new stiffness matrix, reflecting the changing stress-strain relationship, is formed at each increment. Thus, the procedure approximates the nonlinear problem as a series of linear problems.

To improve the accuracy of the incremental procedure and to reduce the deviation from the true solution, an iterative technique was introduced for the tangent stiffness method. In Figure 6.1, the technique is illustrated for a single degree of freedom system. The starting point for the load increment,  $\Delta R$ , is represented by point A at which the stress,  $\sigma_A$ , is known. The tangent stiffness based on the state of stress at point A,  $K_1 = K(\sigma_A)$ , is calculated first. The solution using the stiffness  $K_1$  yields displacement increment  $\Delta \delta_1$ . From this a strain increment  $\Delta \epsilon_1$  is obtained. The stress increment  $\Delta \sigma_1$  corresponding to  $\Delta \epsilon_1$



is then evaluated by using the stress-strain relationship formed for the stress  $\sigma_A$  .

The procedure described so far constitutes the simple incremental tangent stiffness method. The iteration scheme introduced here to improve the approximation for the same load increment is as follows:

After the stress increment  $\Delta\sigma_1$  is calculated (as described above) a new stiffness  $K_2$  is formed as a function of the stress  $\sigma_A + \frac{1}{2}(\Delta\sigma_1)$  , and a new estimate for the displacement increment  $\Delta\delta_2$  is calculated by solving the system of equations for the same load increment. Then the corresponding strain increment  $\Delta\epsilon_2$  is obtained from  $\Delta\delta_2$  . Calculation of  $\Delta\sigma_2$  is based on the stress-strain relationship produced for the stress  $\sigma_A + \frac{1}{2}(\Delta\sigma_1)$  .

The iteration process can be repeated until the difference between two successive solutions is sufficiently small. In the present work the iterations were carried out once or twice.

### 6.3 DERIVATION OF CONSTITUTIVE MATRIX

The nonlinear material behavior is approximated by changes in stress-strain relationship during successive load increments. Therefore the constitutive matrix suitable for incremental finite element analysis has to be formulated such that the increments of stress can be calculated for given strain increments at known stress state of soil.



The following derivation is similar to the one given by Zienkiewicz (1971), with the exception that the necessary changes were introduced to take into account the non-associated flow rule used in the present study.

During an infinitesimal increment of stress, the strain increments taking place are assumed to be separable into elastic and plastic parts.

$$d \left\{ \epsilon \right\} = d \left\{ \epsilon^e \right\} + d \left\{ \epsilon^p \right\} \quad \dots\dots\dots \text{Eqn. 6.1}$$

The elastic strain increments are related to the stress increments by a symmetric matrix,  $[C^e]$ , as written explicitly in Eqn. 2.3. Plastic strain increments were given in Eqn. 2.7. Thus, Eqn. 6.1 can be written as

$$d \left\{ \epsilon \right\} = [C^e]^{-1} d \left\{ \sigma \right\} + \lambda \frac{\partial g}{\partial \left\{ \sigma \right\}} \quad \dots\dots\dots \text{Eqn. 6.2}$$

The yield function may be expressed for a work hardening material as

$$F \left( \left\{ \sigma \right\}, \left\{ \epsilon^p \right\} \right) = 0 \quad \dots\dots\dots \text{Eqn. 6.3}$$

When differentiated, Eqn. 6.3 gives







$$\left\{ \frac{\partial F}{\partial \{\sigma\}} \right\}^T d\{\sigma\} + \left\{ \frac{\partial F}{\partial \{\epsilon^p\}} \right\}^T d\{\epsilon^p\} = 0 \quad \dots\dots\dots \text{Eqn. 6.4}$$

or

$$\left\{ \frac{\partial F}{\partial \{\sigma\}} \right\}^T d\{\sigma\} + A \lambda = 0 \quad \dots\dots\dots \text{Eqn. 6.5}$$

in which a substitution is made for

$$A = \frac{1}{\lambda} \left\{ \frac{\partial F}{\partial \{\epsilon^p\}} \right\}^T d\{\epsilon^p\} \quad \dots\dots\dots \text{Eqn. 6.6}$$

Eqn. 6.2 and Eqn. 6.5 is now written in matrix form as given next.

$$\begin{bmatrix} d\epsilon_x \\ d\epsilon_y \\ \vdots \\ \vdots \\ \vdots \\ 0 \end{bmatrix} = \begin{bmatrix} & & & \frac{\partial g}{\partial \sigma_x} \\ & & & \frac{\partial g}{\partial \sigma_y} \\ & & & \vdots \\ & & & \vdots \\ & & & \vdots \\ \frac{\partial F}{\partial \sigma_x} & \frac{\partial F}{\partial \sigma_y} & \dots\dots & A \end{bmatrix} \begin{bmatrix} d\sigma_x \\ d\sigma_y \\ \vdots \\ \vdots \\ \vdots \\ \lambda \end{bmatrix} \quad \text{Eqn. 6.7}$$



By inverting the square matrix of Eqn. 6.7, an expression is obtained to determine the stress increments in terms of specified strain increments.

$$d\{\sigma\} = [C^{ep}]d\{\epsilon\} \quad \text{..... Eqn. 6.8}$$

where  $[C^{ep}]$  is the elasto-plastic constitutive matrix and is formed by using Eqn. 6.9. (see the next page.)



$$[C^p] = [C^e] + [C^e] \left\{ \frac{\partial g}{\partial \{\sigma\}} \right\} \left\{ A - \left\{ \frac{\partial F}{\partial \{\sigma\}} \right\}^T [C^e] \left\{ \frac{\partial g}{\partial \{\sigma\}} \right\} \right\}^{-1} \left\{ \frac{\partial F}{\partial \{\sigma\}} \right\}^T [C^e]$$

Eqn. 6.9



The elasto-plastic constitutive matrix  $[C^{ep}]$  replaces the elastic matrix  $[C^e]$  in incremental analysis when plastic as well as elastic straining takes place. It should be noted that  $[C^{ep}]$  is no longer a symmetric matrix because the partial derivatives of the plastic potential and the yield functions are not the same in Lade's work hardening model.

#### 6.4 VERIFICATION OF FINITE ELEMENT PROGRAM

In geotechnical engineering practice today, the trend to test the correctness of newly developed finite element programs for nonlinear stress-strain relationships is to compare the calculated values with laboratory test results. Here an alternative and more accurate procedure is offered. Rather than using experimental results, predictions made by the model (such as the ones given in Chapter 3) are employed for testing the results of the finite element program. The advantage of using the predictions is to separate the capabilities of the model from the correctness and the accuracy of the finite element program. This approach can be used effectively for boundary value problems where the state of stress and strain are uniform. Three test cases chosen for the verification of the finite element program of the present study follow.





## TEST CASE I: ANALYSES OF PLANE STRAIN TESTS

Plane strain test results shown in Figure 6.2 and Figure 6.3 for loose and dense Monterey No. 0 sand are used to illustrate the verification procedure. The related stress-strain parameters as derived by Lade are listed in Table 6.1. By using the constitutive model in a simple stress analysis, it is possible to predict the plane strain behavior of soil without resorting to finite element calculations. For a given constant cell pressure and an increment of axial stress from a known state of stress, the increment of intermediate principal stress can be calculated in an iterative procedure which satisfies the plane strain condition as defined by  $\Delta \epsilon_2 = 0$ . The predictions made by such an analysis are shown on Figure 6.2 and Figure 6.3. It should be noted that the comparisons of predictions with experimental results give simply an indication of the capabilities of the model. For the analysis of the same problems using the finite element method only one element is required because the state of stress and strain are assumed to be uniform. Calculated stress-strain and volume change values by finite element analysis are also plotted in Figure 6.2 and Figure 6.3. The agreement between these results and the predictions of simple stress analysis is excellent while they both deviate from the experimental curves. For example, as shown in Figure 6.3, the measured axial strain at deviator stress  $6.0 \text{ kg/cm}^2$  is 1.25 %. For the same deviator stress, the simple stress analysis and the finite element



method give axial strains approximately 5.0 % which is four times larger than the experimental value. This comparison clearly indicates that finite element programs should not be tested against experimental results, but the predictions made by simple stress analyses should be used for this purpose.

#### TEST CASE II: $K_0$ -LOADING CONDITION

$K_0$  - loading condition is satisfied when a soil element is subjected to vertical load increments with no deformations allowed in the horizontal directions. The behavior of soil under these boundary conditions has significant importance in geotechnical engineering because the accumulation of sediments is assumed to take place under similar conditions. Analyses of the behavior of soil deposits under subsequent changes in boundary conditions require the knowledge of in-situ stress state prior to these changes such as an excavation or foundation loading etc. Soil behavior under  $K_0$ -loading conditions has been studied extensively in the past. Although field measurements of the stress state of soil deposits have yet to be perfected, the results of laboratory studies starting with the comprehensive investigation by Bishop (1953) and subsequently by Brooker and Ireland (1965) indicated that the following expression proposed by Jaky for initial loading is valid for all practical purposes.





$$K_o = 1 - \sin \phi' \quad \dots\dots\dots \text{Eqn. 6.10}$$

where  $K_o$  denotes the coefficient of earth pressure at rest

$$K_o = \frac{\sigma_{\text{horz.}}}{\sigma_{\text{vert.}}}$$

and  $\phi'$  denotes the angle of shearing resistance in terms of effective stress.

As a second test for the correctness and accuracy of the finite element program, soil behavior under  $K_o$ -loading conditions is examined. While the vertical stress on a soil element is increased, the no horizontal strain increment condition can be met if the following equation is satisfied.

$$d\epsilon_h^p + d\epsilon_h^e = 0 \quad \dots\dots\dots \text{Eqn. 6.11}$$

where  $d\epsilon_h^e$  and  $d\epsilon_h^p$  refer to horizontal elastic and plastic strain increments respectively. Again, without using the finite element program, the behavior of an infinitesimal soil element under  $K_o$ -loading condition is predicted first. Starting from a very small hydrostatic state of stress, the vertical stress is increased in steps. For each step the horizontal stress increment which would satisfy the condition given by Eqn. 6.11 is searched. The predictions made by this analysis for both loose and dense sand are shown in Figure 6.5 and Figure 6.6. For the same boundary





conditions, the results of finite element calculations are also plotted on the same Figures. It appears that for this stress path too, the finite element program gives accurate results.

There are no experiments to support the predictions shown in these Figures, but the measured  $\phi'$  values for loose and dense sands are given 34.8 and 45 degrees respectively by Wong (1978). Using Eqn. 6.10, the coefficient of earth pressure at rest are calculated as  $K_0=0.43$  for loose sand and  $K_0=0.29$  for dense sand. These numbers are significantly different than the predicted values which are  $K_0=0.28$  for loose sand and  $K_0=0.24$  for dense sand.

Predictions might be improved by using the work hardening model with a cap since the measured stresses in  $K_0$ -loading conditions, such as given by Andrawes and El-Sohby (1973) indicate a stress path causing the cap yield surface to expand.

### TEST CASE III: PREDICTIONS OF PASSIVE EARTH PRESSURE BEHAVIOR

It was assumed that three soil samples representative of soil at different depths behind a retaining wall were subjected to passive earth pressure tests individually. Figure 6.6 shows the hypothetical retaining wall, the sampling locations and the initial state of stress for each element. The soil type chosen for this case is dense



Monterey No. 0 sand and its stress-strain parameters are given in Table 7.2. The behavior of these samples under plane strain boundary conditions were predicted by a stress analysis in which  $\sigma_{\text{horz.}}$  increased in small steps while  $\sigma_{\text{vert.}}$  was kept constant. The predictions of this stress analysis are shown in Figure 6.7. Calculated values by the finite element analysis are plotted on the same Figure. The agreement once again is excellent between the simple stress analysis and the finite element calculations. A discussion on these results in terms of their engineering significance will be given in Chapter 7 after the experimental results on passive earth pressure studies are reviewed.

## 6.5 CONCLUSIONS

In this Chapter the finite element procedures employed in the computer program were presented and a new approach was proposed for testing finite element programs. As demonstrated by three test cases, the finite element analyses give the same results as the predictions made by using the model and simple stress analysis. More complex studies by finite element analysis are expected to give a good indication of overall capabilities of the model to predict the behavior of soil structures.



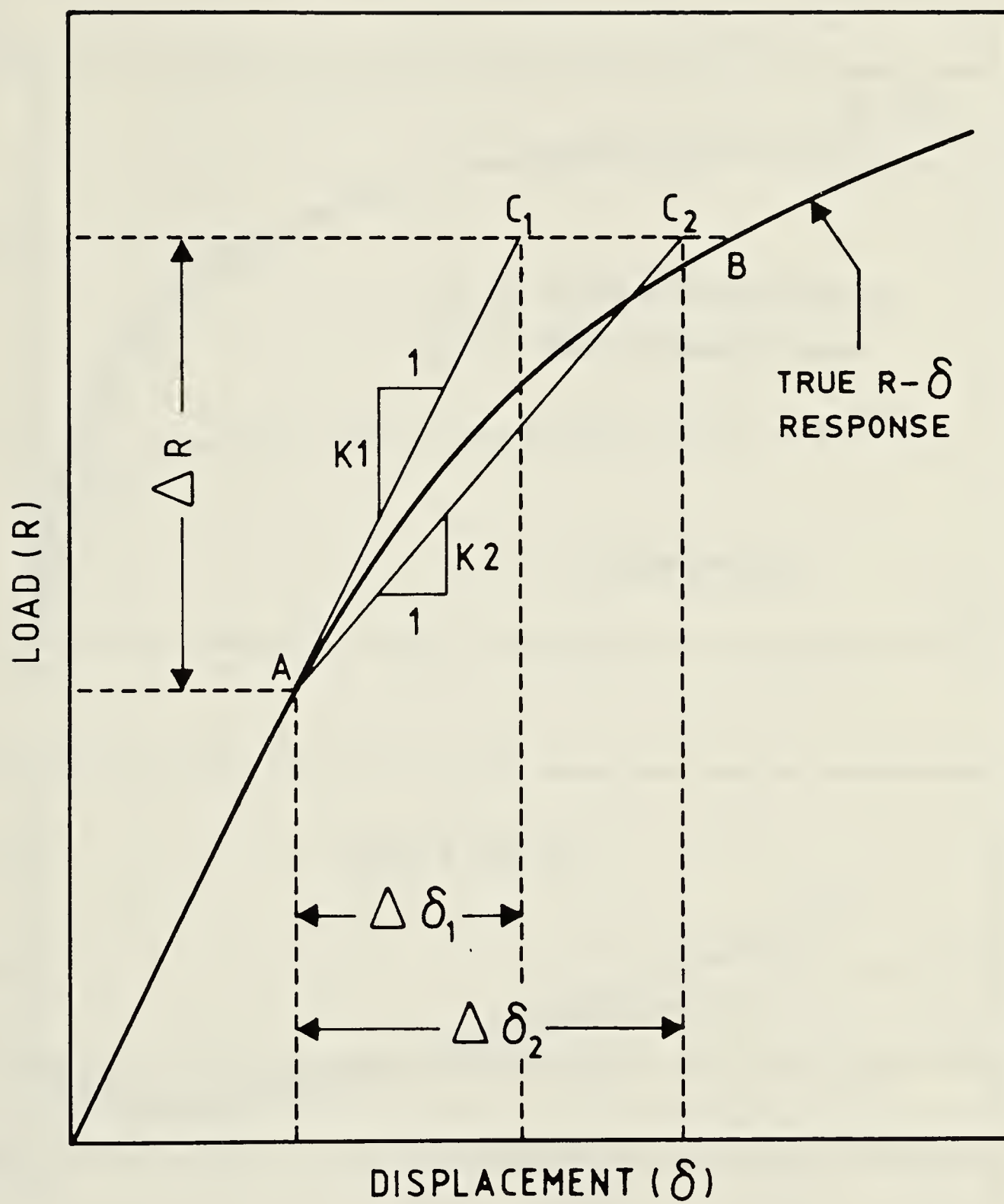


Figure 6.1 Single degree of freedom representation of incremental-iterative procedure.



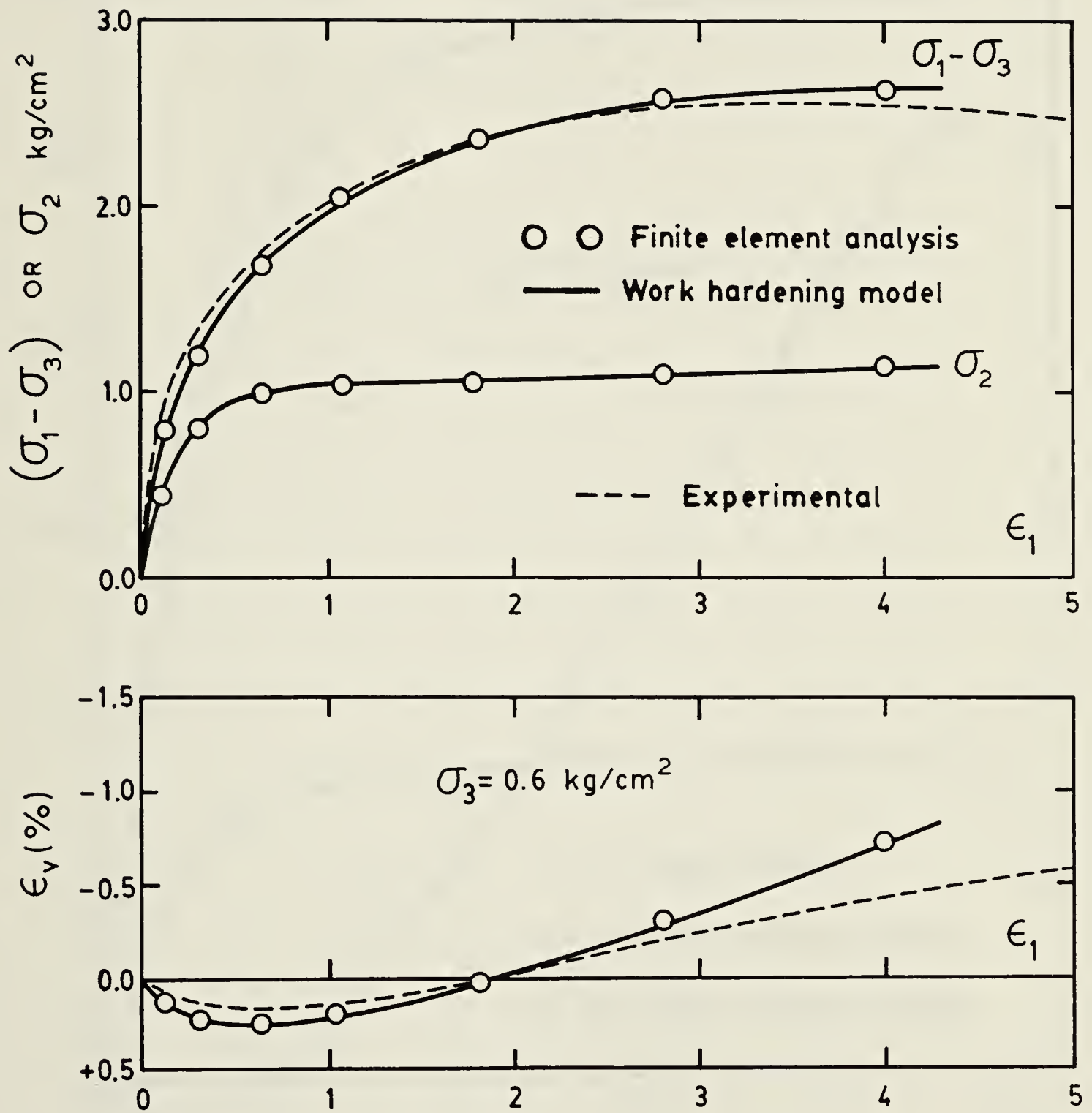


Figure 6.2 Results of plane strain analysis and experimental data for loose Monterey No 0 sand. (Experimental data after Lade, 1972)





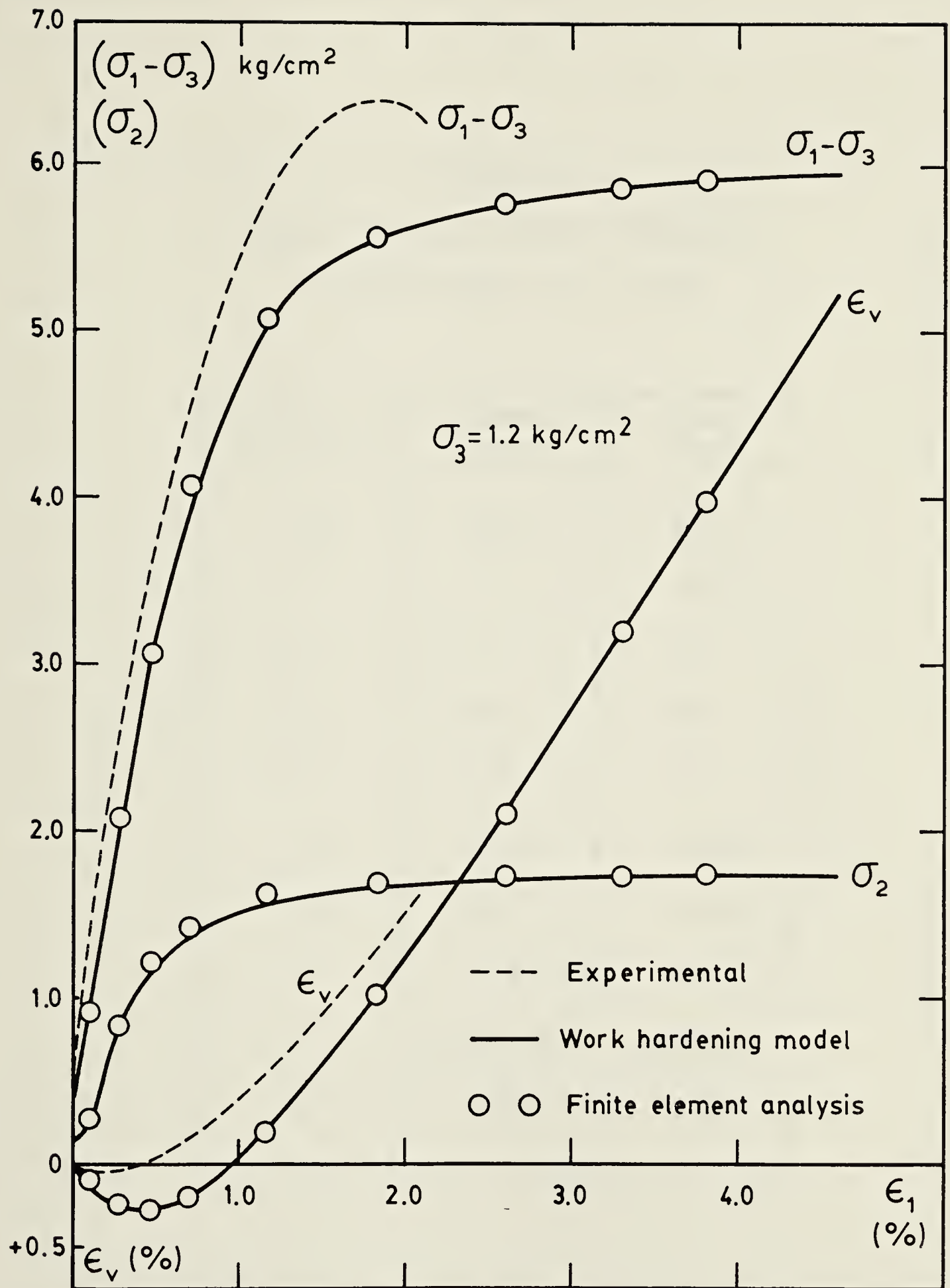


Figure 6.3 Plane strain analysis and experimental data for dense Monterey No 0 sand. (Experimental data after Lade, 1972)



TABLE 6.1  
LADE'S STRESS-STRAIN PARAMETERS  
FOR MONTEREY No. 0 SAND

Parameter	Dense Sand	Loose Sand
$K_{ur}$	2300	1600
$n$	0.8	0.86
$v$	0	0
$K_1$	103	58
$f_t$	40	33
$A_1$	0.44	0.39
$A_2$	15.12	16.48
$l$	1.32	1.17
$M$	0.000255	0.00068
$r_f$	0.957	0.970



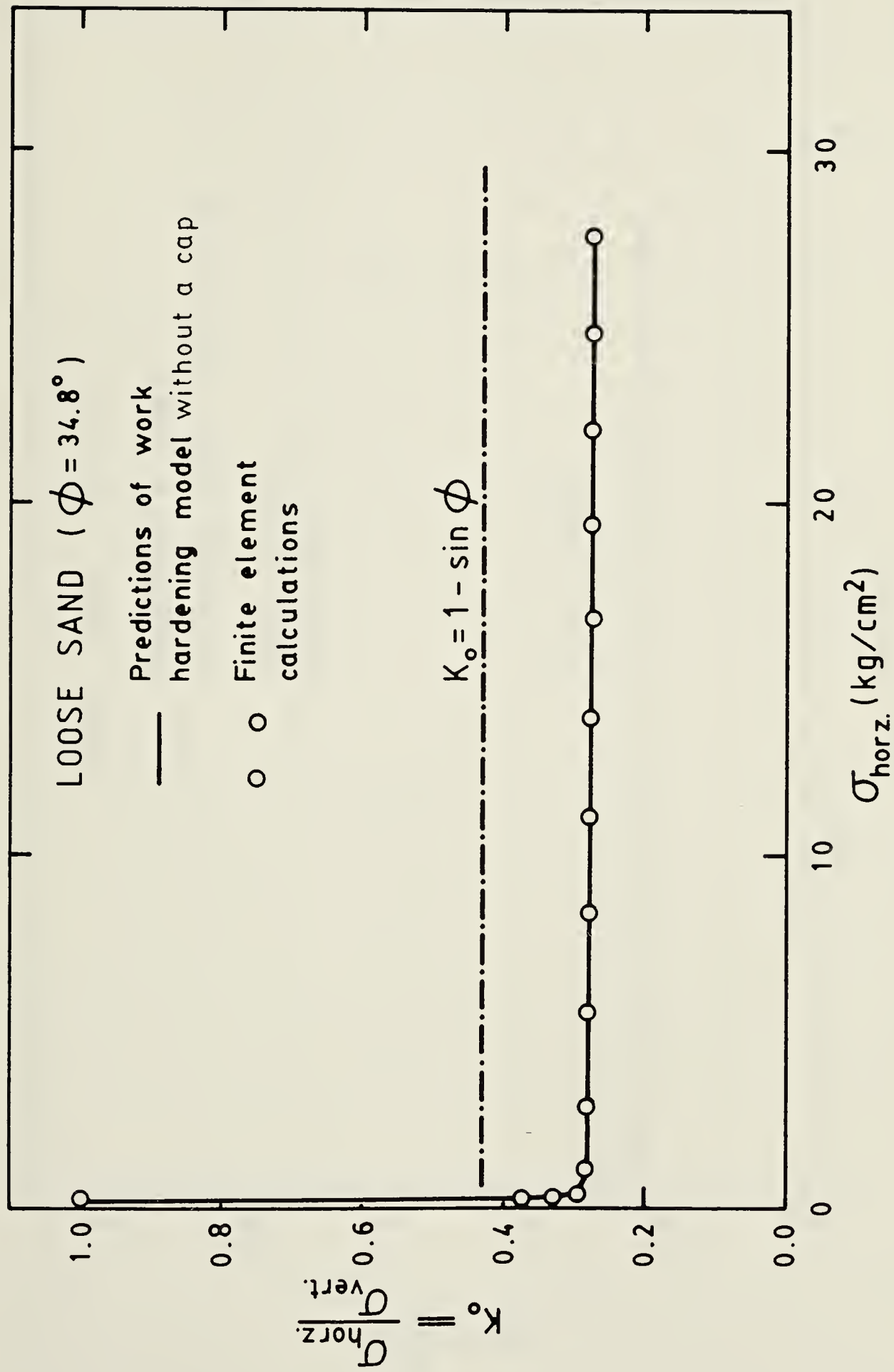


Figure 6.4 Predictions of stress state under  $K_o$ -Loading condition for loose Monterey No. 0 sand.





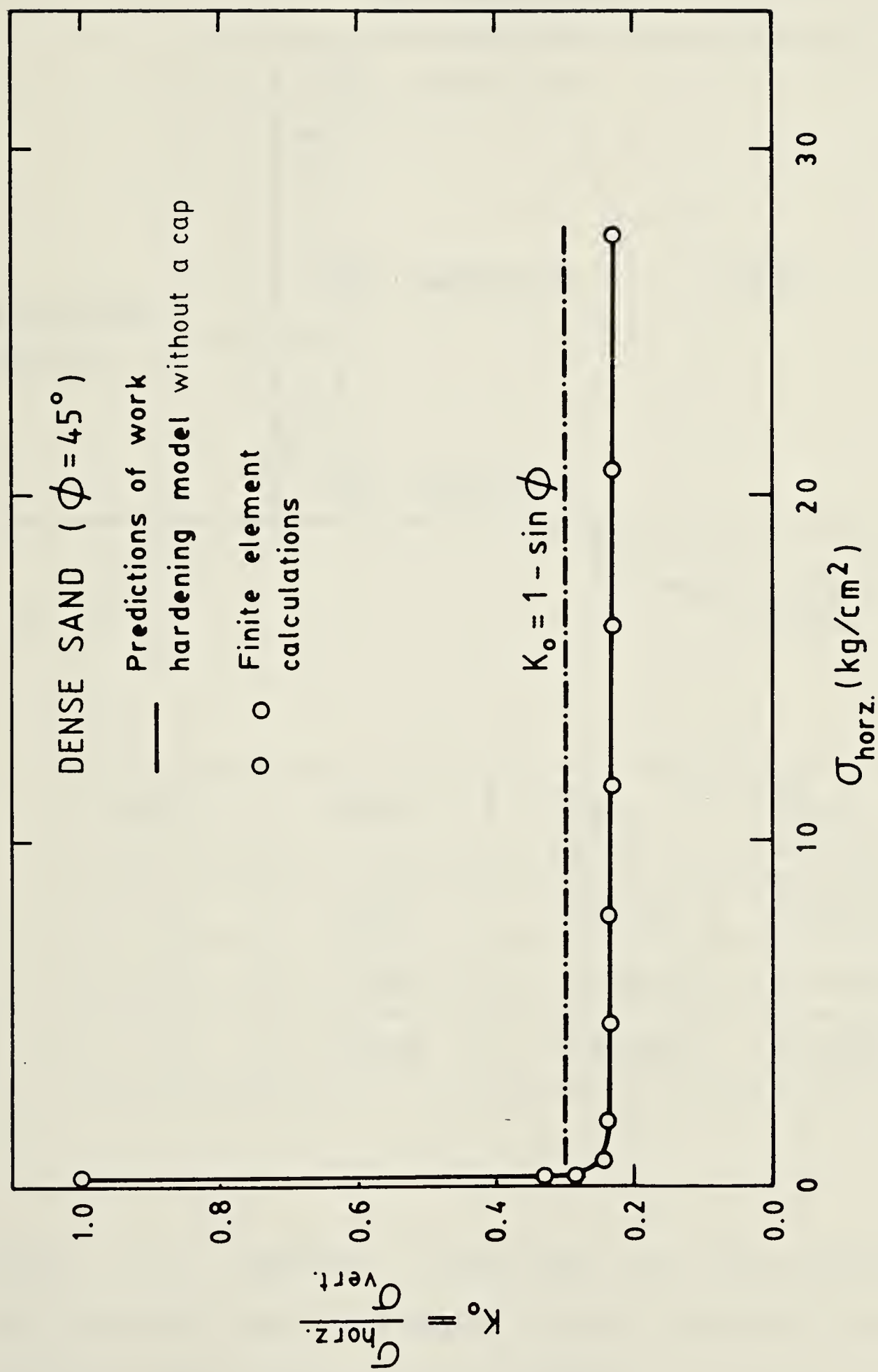
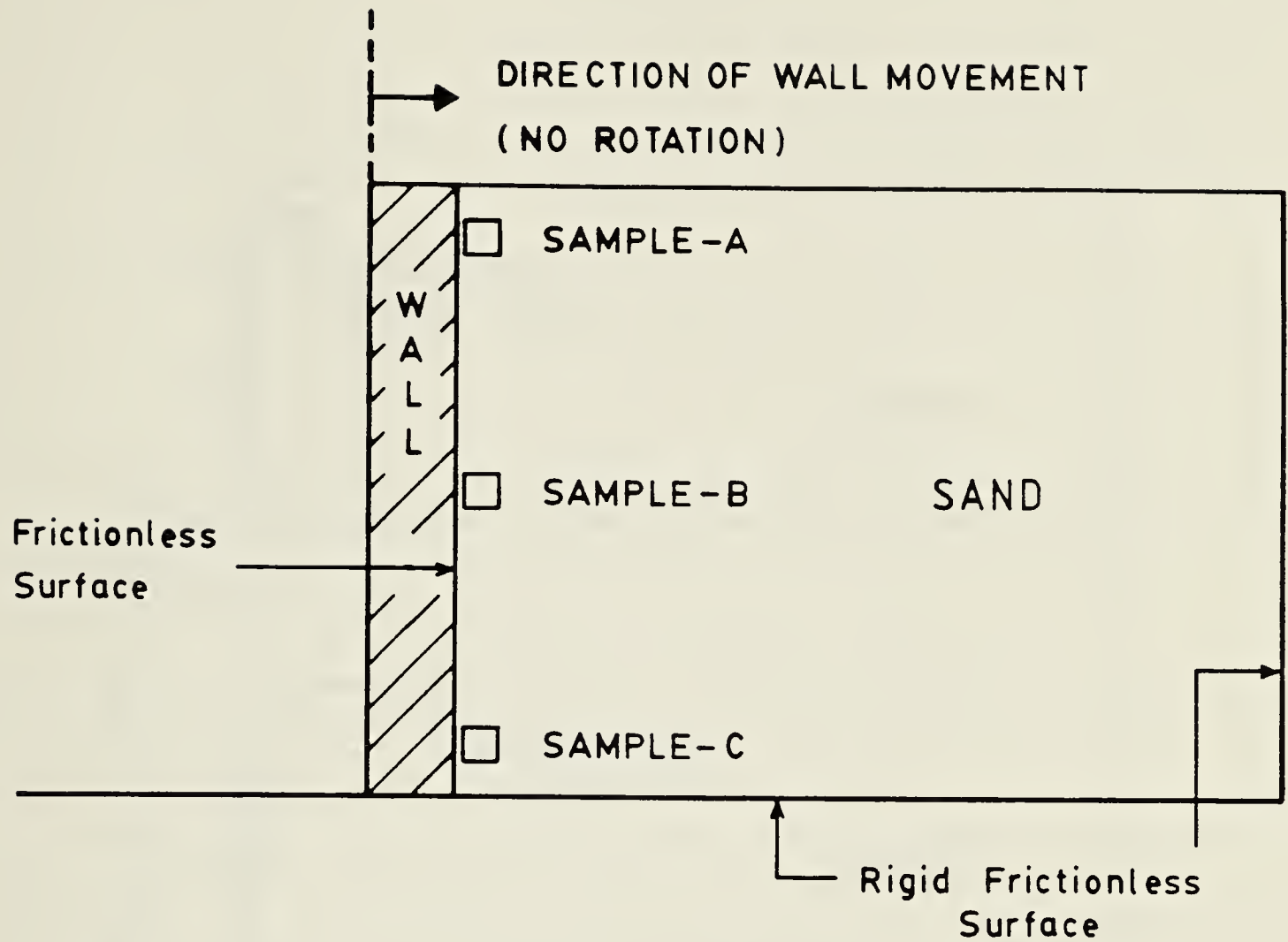


Figure 6.5 Predictions of stress state under  $K_o$ -Loading condition for dense Monterey No. 0 sand.





SAMPLE	DEPTH m	$\sigma_{\text{vert.}}$ kg/cm <sup>2</sup>	$\sigma_{\text{horz.}}$ kg/cm <sup>2</sup>
A	0.1524	0.025832	0.006975
B	1.5240	0.258320	0.069750
C	15.2400	2.583200	0.697500

Figure 6.6 Boundary conditions for the hypothetical retaining wall and the assumed initial state of stress at different depths before wall movement.



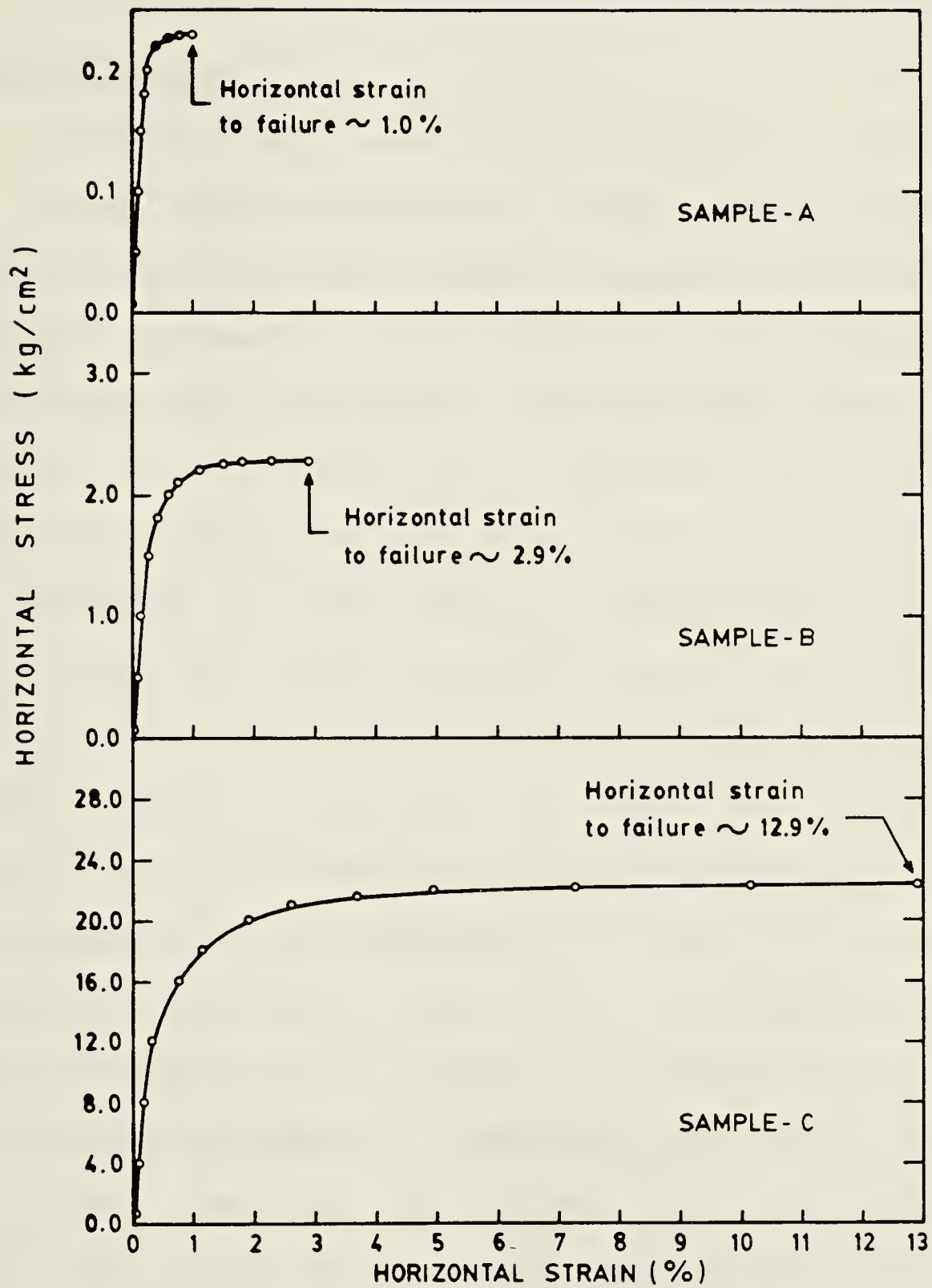


Figure 6.7 Predictions of passive earth pressure for dense Monterey No. 0 sand and finite element calculations.



## CHAPTER 7

### FINITE ELEMENT ANALYSIS OF PASSIVE EARTH PRESSURE

#### 7.1 INTRODUCTION

In recent years, several "non-classical" stress-strain laws have been proposed to model soil behavior more realistically. The predictions of some of these models show remarkable agreement with laboratory test results. Their capabilities were discussed in the NSF/NSERC North American Workshop on "Plasticity Theories and Generalized Stress-Strain Modelling of Soils," Montreal, May 1980. In this workshop it also became evident that the number of applications of "non-classical" models in engineering practice has been very little so far. From the practicing engineer's point of view, the goal of developing a constitutive law is not fully accomplished unless it can be used successfully and efficiently in the analysis of soil structures. Obviously there is a considerable amount of effort to develop finite element programs today. However, considering the number of researchers working on the subject and a rather long time lag between the development of a model and its first time engineering application, substantial amount of difficulties should be anticipated for the newcomers to this field. Previous to the present study, there have been two attempts, one by Ozawa (1974) and the other by Wong (1978), to use Lade's work hardening model in





a finite element analysis. Reference will be made quite frequently to their work in this Chapter. The work presented in the following aims essentially at finding an answer to one question which is "Does Lade's model work in complex boundary value problems?". The answer to this question has not been affirmative so far. Strain softening behavior or modelling the plastic collapse strains is not considered in the finite element analysis of the present study. Only the work hardening model without a cap yield surface is used as the stress-strain relationship for soils.

The passive earth pressure problem has been chosen as the field of application to test the capabilities of Lade's work hardening model. The reason for this choice is the availability of numerous experimental results of model earth pressure tests in the literature. The subject has been studied extensively in the past and with the help of advanced measurement techniques for stresses and strains, substantial amount of knowledge has accumulated about the behavior of earth retaining structures. Thus, the scope of this Chapter is to find the experimental facts from literature and compare them with the results of the finite element analysis. No attempt is made here to present a comprehensive review of earth pressure theories and current design methods for earth retaining structures. They can be found in textbooks as well as proceedings of several international and specialty conferences on the subject.

To proceed systematically, this Chapter is divided into



several major sections. In Section 7.2, a brief literature review reflecting the highlights of the experimental studies on passive earth pressure problems is presented and the factors which affect the behavior of earth retaining structures are identified. The purpose is to evaluate, at least qualitatively, the results of finite element studies presented here and to investigate the level of agreement between predicted and expected behavior. In order to make direct comparisons between predictions and experimental results in evaluating Lade's work hardening constitutive law, the model studies by Wong (1978) are used as a case history in present work. The details of this experimental work are given in Section 7.3. Unfortunately, not many case histories presented in the literature also provide sufficient data on soil properties to derive the parameters required for "non-classical" stress-strain laws. The matter has to be brought to the attention of publishers in geotechnical engineering field. Wong's finite element analyses of the wall behavior is summarized in Section 7.4. In Section 7.5 the predictions made by the finite element analysis of present study are compared with Wong's experimental and analytical results. This comparison provides enough evidence for the usefulness of Lade's work hardening model and its superiority to the other stress-strain laws used by Wong (1978) to predict passive earth pressure test results. The final Section is devoted to the interpretation of results found in this Chapter.





## 7.2 EXPERIMENTAL INVESTIGATION OF PASSIVE EARTH PRESSURE PROBLEM (LITERATURE SURVEY)

One of the earliest experimental studies on passive earth pressure problems was reported by Terzaghi (1934) who observed the importance of various modes of wall movement and the existence of differences between the behavior of dense and of loose backfill. In a series of tests using dry sand a rigid wall was rotated about its toe in both an active and passive sense. Based on the measurements of thrust acting on the wall, an average earth pressure was obtained as a function of wall rotation. Figure 7.1 shows the relation between wall movement and mobilized coefficient of earth pressure as provided by Terzaghi (1954). The important point to be observed in this Figure is that the magnitude of earth pressure is a function of the mode of wall movement, amount of wall movement and soil properties.

Based on experiments, Franzius (1924), Tschebotarioff and Johnson (1953) indicated the importance of wall friction (roughness of the surface) and the boundary conditions in testing apparatus. Tschebotarioff (1951) reported how dredging or backfilling may affect the earth pressure distribution along a flexible bulkhead. His work demonstrates the significance of the construction procedures and the flexibility of the retaining structure in pressure distribution. Work by Brinch Hansen (1953) and Narain et al. (1969) are all part of the effort to increase our understanding of passive earth pressure problem.





In a comprehensive series of tests in model scale, Rowe and Peaker (1965) investigated in detail the mobilization of normal and shear stresses acting on a wall which can be translated in a preset direction with the wall inclined to the horizontal at any desired angle. Measurements showed that passive earth pressure values vary with the orientation of the wall and the direction it is pushed against the soil. In these tests the mobilized wall friction and the coefficient of passive earth pressure  $K_p$  values did not always reach their peak values simultaneously. For dense sand, there was a significant drop in  $K_p$  after a peak was reached. The amount of movement required to reach maximum  $K_p$  was in the order of 15-25% of wall height for loose sand and 4-10% for dense sand. It is most likely that the magnitude of these movements is not acceptable in practice. Then, the analysis of passive earth pressure becomes a deformation problem. The authors have concluded that "a correct solution of earth pressure calculation must await the establishment of the stress-strain...laws for soils subjected to any stress path"

One of the most significant investigation in the subject comes from Cambridge University. James and Bransby (1970) reported observations of normal and shear stress distribution along a rotating wall as well as the strains within the sand mass. Shear strain contours, which were found by using an X-ray technique, for different degrees of wall rotation provided valuable information about the actual



behavior of sand mass. Based on this experimental fact, they then evaluated the validity of the assumptions made in current methods of earth pressure calculations. Some of the shear strain contours of their work are reproduced here in Figure 7.2 for an easy reference to be used later in this Chapter. Figure 7.3 shows the rupture planes as observed by James and Bransby (1970) on radiographs exposed at three stages of a passive pressure test in dense sand. It is clear that the failed zone of material becomes larger with the increase in wall rotation in a fashion shown in this Figure. In his Rankine lecture, Roscoe (1970) summarized the results of passive earth pressure tests on model walls tested at the Cambridge University. Comparisons of the wall behavior for different modes of wall movement indicate that when the wall rotates about its toe the required angle of rotation for peak resistance is about 8 degrees. If the same wall is rotated about the top, the peak is attained at only 1.4 degrees of wall rotation. For pure horizontal translation the displacement needed for maximum resistance is equivalent to 2 degrees of rotation.

There have been many more experimental studies carried out in the past. The details of all these are not included in this review. Nevertheless, it is believed that the essential points of passive earth pressure problem in ideal conditions are established sufficiently for our purposes. What is missing in the experimental work presented here is the measurement of intermediate principal stresses.



For large scale problems one has to be careful about size effects. Extrapolation of findings of small scale model tests may not be applicable directly to large scale problems. There are other factors such as in-situ state of stress, construction sequences, temperature changes, creep effect, seepage conditions and stresses caused by compaction which may affect drastically the behavior of real soil structures.

The most useful experimental work to the present study was carried out by Wong (1978), and forms the basis of comparison for the results of a finite element analysis which is presented in Section 7.5. For this purpose the related part of Wong's work is presented next.

### 7.3 EXPERIMENTAL WORK BY WONG

In a series of passive pressure tests carried out by Wong (1978), an instrumented wall was rotated about its toe into a bed of sand as illustrated in Figure 7.4. Measurements were taken for normal and shear forces on four panels of the wall at various stages of rotation. The outcrops of the slip planes on the surface were mapped at the end of each test. Tests were conducted by using dense ( $D_r=90\%$ ) and medium dense ( $D_r=65\%$ ) Monterey No.0 sand which is a uniform, medium sand composed mainly of quartz and feldspar. Sand particles are subangular to subrounded. Gradation curves for the Monterey No.0 sand used in passive pressure tests by Wong and that used by Lade (1972) in





triaxial and plane strain tests are shown in Figure 7.5. Sands used in both occasions are not only from the same source, but as it can be seen in that Figure, almost have the same grain size distribution. A summary of the characteristics of these sands as provided by Wong (1978) is given in Table 7.1.

Separate from the others two more passive pressure tests were carried out by Wong using sand which contained thin layers of dyed-red sand. These tests were used to identify the location and shapes of slip planes. Figure 7.6 illustrates the observed slip planes for  $D_r=90\%$  at the end of a test after a 10 degree wall rotation. What is shown in this Figure is the sum of all slip planes developed progressively from top to bottom for increasing wall rotation. For example, if the tests were carried out only up to 5 degrees rather than 10 degrees of rotation, the lower slip planes would not yet have developed.

Figure 7.7 and Figure 7.8 show average normal and shear stresses on the wall as well as the coefficient of passive earth pressure,  $K_p$ , for two different densities of sand. The distribution of these stresses along the wall are given in Figure 7.9 and Figure 7.10. The mobilization of stresses follow a pattern which can be summarized as follows. Stresses acting on the top panel of the wall reach to a maximum first. With increasing wall rotation, failure spreads along the wall downward, and larger portions of the soil mass away from the wall are affected. The movement





below the mid height of the wall is not sufficient to develop a failure state in the soil. As shown in Figure 7.9 and Figure 7.10, normal stresses on the third and fourth panels do not show any sign of reaching a peak even at 8 degrees of wall rotation.

The requirements for strain softening to take place are discussed in Chapter 5. In laboratory tests, for example see Figure 7.15, dense sands under low confining pressures show significant softening response. These conditions are satisfied for Wong's earth pressure tests when dense sand is used. Opposite to anticipations though, the strain softening does not seem to play a significant role on the measured normal stresses acting on the wall panels as shown in Figure 7.10. One would expect a larger drop in stresses beyond the peak stress level. Any explanation for this interesting observation will not be attempted here, but it is left to researchers who would like to work on the subject.

In any analysis based on rigid-plastic soil model, it is implied that an infinitesimal movement along a failure surface is sufficient to develop the full shear strength. Consequently, failure is reached simultaneously at every point within the deforming part of a soil mass. In most analysis, the same assumptions are also made for the soil-wall interface behavior. No attention is paid to the magnitude of deformations. A suitable factor of safety is expected to prevent excessive movements. For the analysis of a retaining structure subject to passive earth pressure, it



is conventional to draw a rupture surface that passes through the toe of the wall and extends to the free ground surface. In textbooks, most of the discussion goes around the shape of this assumed rupture surface. The observations by Wong (1978) as well as the experiments by James and Bransby (1970) contradict the basic assumptions of limit equilibrium method of analysis for this mode of wall movement. In reality, rupture surfaces do not start from the toe of a wall rotating about its base. Even at large deformations, the failure zone extends only from the surface to somewhere around the middle of the wall. This is a good example of a case where part of the soil mass is in a state of failure even at early stages of the test while the remaining parts are still loading. It appears then a realistic analysis of the passive earth pressure problem requires both the deformation properties and failure conditions of soils to be represented reasonably well. Based on these circumstances, the choice of the passive earth pressure problem for the evaluation of Lade's model seems to be a proper one.

#### 7.4 ANALYTICAL WORK BY WONG

In the analytical part of his work, Wong (1978) made predictions for the behavior of a model wall by using four constitutive models which were considered to have potential practical value. They are:

- 1) The nonlinear elastic hyperbolic model





- 2) The Mohr-Coulomb simple elasto-plastic model
- 3) The stress-dilatancy model
- 4) Lade's work hardening model

A summary of Wong's predictions in relation to all four models is reproduced in Figure 7.11 and Figure 7.12 in order to compare with the predictions of present study. As demonstrated in these Figures, the wall behavior is predicted quite well by the simple elasto-plastic model. Therefore, a brief presentation of the characteristics of simple elasto-plastic model, as used in Wong's analysis, is considered necessary. The model employs the Mohr-Coulomb yield criterion without any work hardening. Deformations are elastic up to failure and elasto-plastic thereafter. The flow rule used is non-associated. Hence, the cost of running a finite element analysis is very similar to that of Lade's model. The secant modulus at 70% of the maximum deviatoric stress is used as the elastic modulus. The friction angle at peak strength as well as the elastic modulus are obtained from conventional triaxial compression test data. It should be emphasized here that the finite element analysis of the experimental wall is a plane strain problem and the stress-strain behavior of soils in conventional triaxial tests is significantly different than the soil behavior under plane strain test conditions.

The details of the nonlinear elastic hyperbolic model and the stress-dilatancy model will not be given here. These and the soil parameters used for each model can be found in





Wong (1978).

## 7.5 PREDICTIONS BY THE FINITE ELEMENT ANALYSIS OF PRESENT STUDY

### A-PRELIMINARIES

Before a proper analysis of model wall behavior was attempted with a sufficient number of elements, the finite element program of the present study was used to predict the coefficient of earth pressure versus horizontal strain relationship similar to the one given in Figure 7.1. This is done by using a single element. The selected mode of wall movement considered here is a pure translation rather than a rotation. A vertical wall with frictionless surface is advanced horizontally to induce Rankine states of failure in soil. Using Lade's work hardening model, the predictions of the strains developed for the stress conditions ranging from  $K_0$  at rest to failure, in both active and passive sense, are calculated. The results are shown in Figure 7.13. The relative orders of magnitude of earth pressure and strain values are in accordance with experimental results given in the literature. Roscoe and Burland (1968) presented similar predictions for wet clays to illustrate and emphasize the practical significance of the Cambridge model. However, Morgenstern and Eisenstein (1970) have indicated that these relations have not been used in practice as yet. It should be noted that the relation between  $K_p$  and horizontal strain



is a function of the state of stress before the wall movement is initiated. In other words, the passive pressure coefficient  $K_p$  versus horizontal strain  $\epsilon_{\text{horz.}}$  relation varies with depth. As shown in Figure 6.7, horizontal strains to failure increase with increasing depth. It is well known that the strains required for soil samples to reach failure increase with increasing confining pressures in triaxial tests as shown in Figure 4.8 and Figure 4.9. It appears that, this characteristics of soil behavior is also applicable for stress paths following stress states in passive earth pressure conditions. However, the curves given in Figure 7.13 and the  $K_p$  versus  $\epsilon_{\text{horz.}}$  relationship offered by Roscoe and Burland (1968) are calculated for highly idealized boundary conditions. Even under these hypothetical conditions they only correspond to soil behavior at one point in the whole soil mass. Therefore, they should not be expected to be useful in great detail to practicing engineers. Lambe and Whitman (1969) use triaxial test data for the same problem to estimate the magnitude of strains. In order to find out possible consequences of using triaxial data for the analysis of passive earth pressure problems, the following calculations are carried out by using Lade's work hardening model. It is assumed that three soil samples are obtained from locations shown in Figure 6.6. It is also assumed that  $K_0$  conditions prevail in these soil elements, and this provides the initial state of stress before the loading commences. During subsequent loading vertical stress



is kept constant but all around horizontal normal stresses are increased until failure occurred. These calculations are carried out for the same soil used for the passive pressure calculations which are shown in Figure 6.7. The results of such calculations are given in Figure 7.14. A comparison of Figure 6.7 with Figure 7.14 indicates that horizontal strains required to reach failure are about 50-100% more for plane strain calculations than triaxial results. Before the failure state is reached, the stress-strain curves of triaxial tests have steeper slopes. The implication of this is that the use of triaxial data, ( $\sigma_{\text{vert}} = \text{const.}$  and  $\sigma_{\text{horz.}}$  increasing to failure), in the analysis of passive earth pressure problems gives deformation results which are on the unsafe side.

## B-ANALYSES OF THE WALL IN PRESENT STUDY

In the present study two analyses were performed to predict the experimental results of passive earth pressure tests by Wong (1978). The predictions were made for both dense and medium dense sands.

### I- Analysis of Wall Behavior for Dense Sand

#### a-Soil Parameters

The representative soil parameters for the analysis of wall behavior are obtained from the triaxial test data which are provided by Wong (1978). The procedures followed to





calculate soil parameters are the same as described by Lade and Duncan (1975). Their values are listed in Table 7.2. Because Wong employed a different method of evaluation than Lade and Duncan(1975), (compare the parameters in Table 7.1 and Table 7.2), the parameters of the present study are not exactly the same as the ones used by Wong (1978). Using the data given in Table 7.2, plane strain behavior of a soil element is predicted and compared with experimental results to demonstrate that the parameters used in the analyses of present study are appropriate. This comparison is shown in Figure 7.15.





### b-Boundary Conditions

The finite element mesh and the boundary conditions for the analysis of the rigid wall are shown in Figure 7.16. For each load increment, the horizontal displacements of the nodes along the rotating wall and soil interface are specified. The measurements of shear stresses given in Figure 7.9 are used to calculate the equivalent shear forces to be applied to the nodes. Thus, the wall is no longer needed in the analysis of this problem.

### c- Results of Analysis

Results of the analysis involving dense sand are shown in Figure 7.17 and Figure 7.18. In these figures the average normal stress as well as its distribution along the wall are plotted against the angle of wall rotation. The experimental results and the predictions made by Wong are also plotted on the same figures for the purpose of comparison. Additional curves for the average values of coefficients of passive earth pressure are given in Figure 7.17. If the variation of  $K_p$  on each panel is calculated separately, the following numbers would be obtained according to the present study.

#### $K_p$ values on each panel:

(Note: The numbers in parentheses indicate the experimental values.)

At 0.5 degree wall rotation:

PANEL 1 = 13 (13)

PANEL 2 = 12 (11)

PANEL 3 = 5 (4.6)

PANEL 4 = 0.9 (1.0)



At 1.0 degree wall rotation:

PANEL 1 = 15 (15)

PANEL 2 = 15 (14)

PANEL 3 = 9 (7.4)

PANEL 4 = 1.9 (1.2)

As the angle of wall rotation increases,  $K_p$  values increase as well, but not at the same rate for all panels.

The growth of highly stressed zones is shown in Figure 7.19.

## II- Analysis of Wall Behavior for Medium Dense Sand

### a- Soil Parameters

The soil parameters used for medium dense sand in the analysis of the wall are different than the ones provided by Wong (1978). The reasons for not using Wong's parameters are discussed next.

1-Wong used a different method of evaluation for the soil parameters than Lade and Duncan (1975).

2-Wong's description of the state of medium dense sand in the soil bin indicates that the density of each layer varied within its depth. Dense and loose sublayers were present within each layer.

3-There was another difficulty in obtaining a homogeneous soil deposit in medium dense sand. This is related to the striations as photographed by Wong.

4-Measurements on the experimental wall by Wong showed that the coefficient of earth pressure at rest  $K_0$  was 0.35 at zero wall rotation. This value of coefficient of



earth pressure corresponds to a maximum stress level  $K_1=64$  rather than 68.4 which is derived from interpolated triaxial curves by Wong (1978).

Due to the uncertainties about the state of soil in medium dense sand, the following approach is taken to evaluate soil parameters. First  $K_1$  is chosen 64. Then the stress-strain curves corresponding to  $K_1$  are obtained by interpolating between the triaxial test data for dense and loose sands. After that the procedures given in Appendix A are followed to determine the soil parameters. The results are listed in Table 7.2.

#### b- Boundary Conditions

The finite element mesh for the analysis of the wall in medium dense sand is the same as for dense sand as shown in Figure 7.16. Boundary conditions along the wall are simulated by specifying horizontal displacements and the shear forces which are obtained from experimental results given in Figure 7.10.

#### c- Results of the Analysis

Figure 7.20 and Figure 7.21 show the average normal stress and its distribution along the wall respectively. The experimental results and the predictions of Wong are given on the same figures. The average value of the coefficient of passive earth pressure is illustrated in Figure 7.20. The breakdown of  $K_p$  into each panel is given next.





### K<sub>p</sub> values on each panel:

(Note: The numbers in parentheses indicate the experimental values.)

At 0.5 degree wall rotation:

PANEL 1 = 7.3 (7.3)	PANEL 2 = 5.8 (4.2)
PANEL 3 = 3 (3)	PANEL 4 = 0.7 (0.45)

At 1.0 degree wall rotation:

PANEL 1 = 8.5 (8.7)	PANEL 2 = 7.5 (5.9)
PANEL 3 = 4.6 (4.4)	PANEL 4 = 1.4 (0.6)

Growth of highly stressed zones for medium dense sand is shown in Figure 7.22. Contours of cumulative shear strain and volumetric strains are given in Figure 7.23.

## 7.6 INTERPRETATION OF FINITE ELEMENT PREDICTIONS

In this Section particular details of the finite element predictions are examined in the following order.

I) The significance of the results presented in previous sections are discussed on the bases of comparisons between:

- a) the experimental results and the results of present study,
- b) the calculations of Wong and the predictions of present study.

II) Several important factors which have possible effects on the results are elaborated.

III) Finally, in the light of evidence presented above, the theoretical and practical value of



Lade's model is discussed.

1) Comparative studies of average normal stresses on the instrumented wall, as shown in Figure 7.17 and Figure 7.20, indicate that the predictions of the present study at all stages of tests are within reasonable limits of the experimental data for both dense and medium dense sands. The analysis of the present study gave average stress values which were not different from the experimental results by more than 15-20% for any specified angle of wall rotation. For similar conditions Wong's calculations gave average normal stresses reaching up to 1.7 to 1.9 times the experimental values. Beyond approximately 2.3 degrees of wall rotation Wong was not able to continue his finite element analysis for numerical reasons. Calculations of the present study were not continued any further than 2.2 degrees and 3.7 degrees for dense and medium dense sands respectively, because the trend had already been established.

On the other hand, if the angle of wall rotation is to be predicted for a specified average normal stress, the following examples will be more relevant. For dense sand, at a normal stress of 500 psf ( $=0.245\text{kg/sq.cm}$ ), the experimental results are 3.16 times larger than the calculations of Wong and 1.67 times larger than the predictions of the present study. For medium dense sand at a normal stress of 300 psf ( $=0.148\text{kg/sq.cm}$ ), the experimental results are 4.01 times larger than Wong's calculations and



1.6 times larger than the predictions of present study. These numbers can be taken as an indication of:

- 1) The finite element analysis of the present study gave much better predictions than Wong's calculations.
- 2) The predictions of the present study are reasonably good for both low and high stress levels.
- 3) Although the results of the present study are very reasonable, they are still on the unsafe side of the experimental results.

When attention is turned to the distribution of normal stresses along the wall a better understanding of the details of the problem, such as the development of contact pressures, can be obtained. Experimental results indicate that the soil elements at shallow depths behind the wall reach the maximum stress level first. As the angle of rotation increases, the failure grows deeper. For example, as shown in Figure 7.18 and Figure 7.21 the soil elements next to the top two panels reach to the maximum stress level first while the soil against lower two panels is still loading. This phenomenon has been modelled well by Lade's stress-strain law as the results of the present study show. Yet it is not possible to observe this feature in Wong's calculations. For example, in his calculations the soil next to Panel 1 in both dense and medium dense sands does not seem to be getting closer to failure state. Differences between the predictions of the present study and that of





Wong are most likely due to different procedures in using the hardening law of the model in these analyses (see Chapter 3).

Figure 7.19 and Figure 7.22 show the expansion of highly stressed zones in soil mass as predicted by the present study. It appears that highly stressed zones in dense sand spread out more than that of medium dense sand for the same degree of wall rotation. For example at 2 degrees of rotation, the region of dense sand stressed above  $f_p > 0.98 K_1$  is about 2 to 3 times more than the corresponding area for medium dense sand. It should be noted that the gradual growth of the zone of failure is well represented in this analysis. Failure has not been reached in all soil elements (see for example Figure 7.19) along the wall face, but only the sand within one third of the wall height from the surface has experienced failure.

Figure 7.23 shows predictions of present study for the cumulative maximum shear and volumetric strains at the end of 2 degrees of wall rotation. When compared with curves measured by James and Bransby (1970), (see Figure 7.2), the shear strain contours given in Figure 7.23 indicate that the strains within the soil mass are predicted very well by Lade's model for complex loading conditions.

The finite element analysis of the wall by Wong employs several stress-strain laws. The level of success of each model is shown in Figure 7.11 and Figure 7.12. If these results are compared with the predictions of the present





study which are given in Figure 7.18 and Figure 7.21, one can conclude that, Lade's model gives much better results than the hyperbolic stress-strain law and the stress-dilatancy model. Comparisons between the simple elasto-plastic model and Lade's model indicate that the predictions related to the top three panels are in favor of Lade's model.

II) Factors which have possible effects on the finite element results are discussed next. These are related to:

- a) Accuracy of experimental results
- b) Influence of soil parameters
- c) Approximations related to the finite element analysis.

#### a) Accuracy of experimental data

As will be quoted next from Wong (1978), there were several difficulties related to the experimental work.

"Good uniformity of sand density was obtained except in the areas adjacent to the wall...

Although the measured densities appeared to be uniform throughout the bin, the density of each thin layer varied within its depth. The loose and dense sublayers were more pronounced in loose samples than in dense samples...

Each layer deposited in the medium dense samples ( $D_r=65\%$ ) was about 0.3in. thick, and those in the dense ( $D_r=90\%$ ) samples were about 0.07in. thick. Striations were



readily identifiable within the medium dense sample,..."

In addition to the difficulties involved in achieving a uniform sand deposit, there was another problem related to the rigidity of the testing apparatus. This will be quoted again from Wong (1978).

"It was found that the bottom of the wall tended to move away from the sand during rotation; the amount, however, was very small. When the tank was filled with dense Monterey No.0 sand, the movement was less than 0.03in..."

Although it is quite possible to model such a wall movement in the finite element analysis, this was not attempted in the present study. Yet its importance may not be ignored. If this movement was not allowed in experiments, the bottom panel of the wall would have carried larger load than what is shown in Figure 7.18 and Figure 7.21. This would allow the predictions of the present study to be closer to the experimental results.

#### b) Influence of soil parameters

The parameters used for soil have major influence on the outcome of the finite element analysis. It should be noted that the selection of the parameters for Lade's model is not based on the past experience; they have to be obtained from conventional triaxial test data by following the steps given in Appendix A. In soil testing repeatability of tests within 10% error is considered to be normal. If the triaxial compression test data given in Figure A.1 in



Appendix A is examined, one can observe that measured maximum stress level  $K_1$  for three tests with different confining pressures vary from  $K_1=78.67$  for  $\sigma_3=0.6$  kg/sq.cm to  $K_1=88.9$  for  $\sigma_3=0.3$  kg/sq.cm. For confining pressure 1.2 kg/sq.cm,  $K_1$  is 80.95. The parameter  $K_1$  used in the present analysis is the average of all three  $K_1$  values which is 83.6. If  $K_1$  obtained from triaxial test with  $\sigma_3=0.3$ kg/sq.cm. was excluded, a lower value would be used for  $K_1$  and that would bring predictions of present study closer to experimental results.

c) Approximations related to the finite element analysis

It is most likely that a finer mesh would further increase the flexibility of soil mass in the finite element analysis. Especially, where the gradient of stress change is large, an increased number of elements would improve the predictions. Such a point in the analysis of the wall is around the toe.

Finally, the procedure used for the nonlinear analysis may have an effect on the results. It is well known that the tangent stiffness method gives results which are stiffer than the correct solution.

It is believed that these factors listed above have some influence on the predictions of present study. The investigation of their relative importance requires more effort. Subject to the problems mentioned above, conclusions will be drawn next for the value of Lade's work hardening







model.

### III) Evaluation of the model

The main objective of the work presented in this Chapter is to investigate the degree of agreement between the predictions made by Lade's model and the experimental results for complex problems. Comparisons indicate a very good agreement in general between the observed stress distribution on the wall and the measured values. Predictions of zones of high stress level and their growth as a function of wall rotation agree well with the measured values. Predictions at working load range as well as at high stress levels are rather impressive. It seems that the success in predictions is due to the abilities of the model to predict the path dependent soil behavior and the failure conditions reasonably well. These results show that a unified analysis of deformations and stability can successfully be carried out. To conduct a reliable analysis though, the soil model used has to be a capable one. Comparisons of predictions made by the model used here and the other models selected by Wong show clearly that Lade's model gives better results than simple elasto-plastic, nonlinear elastic and stress-dilatancy models. In this conclusion it is assumed that Wong's calculations for these models are correct.



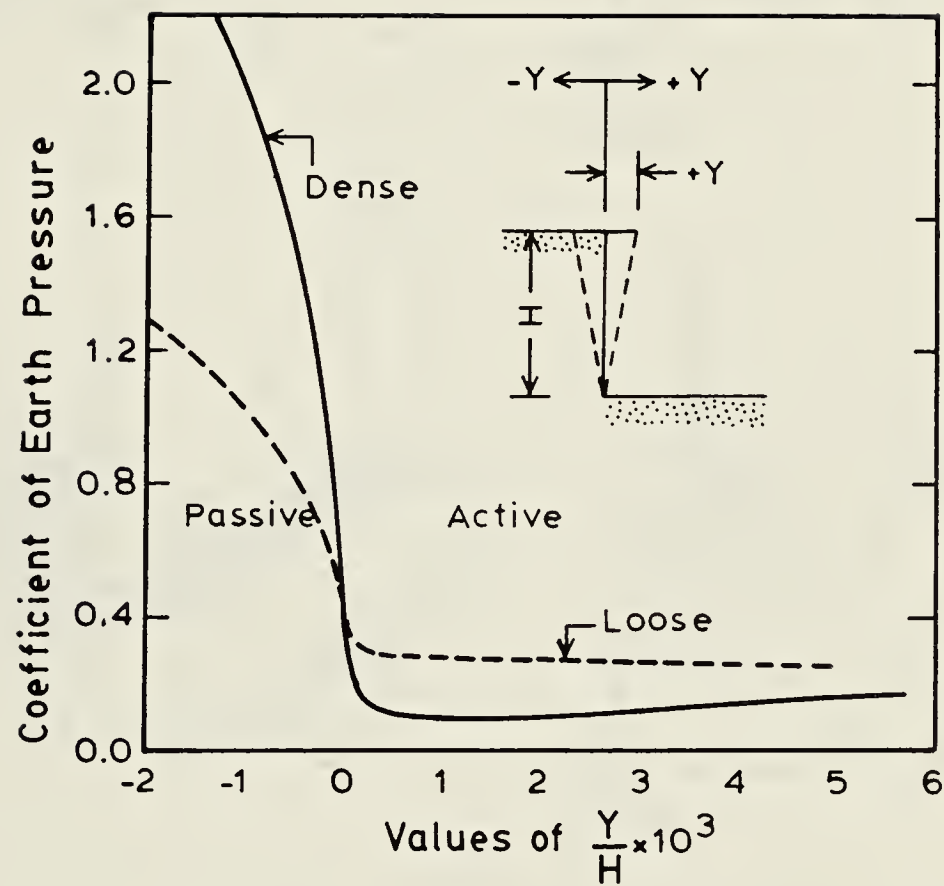
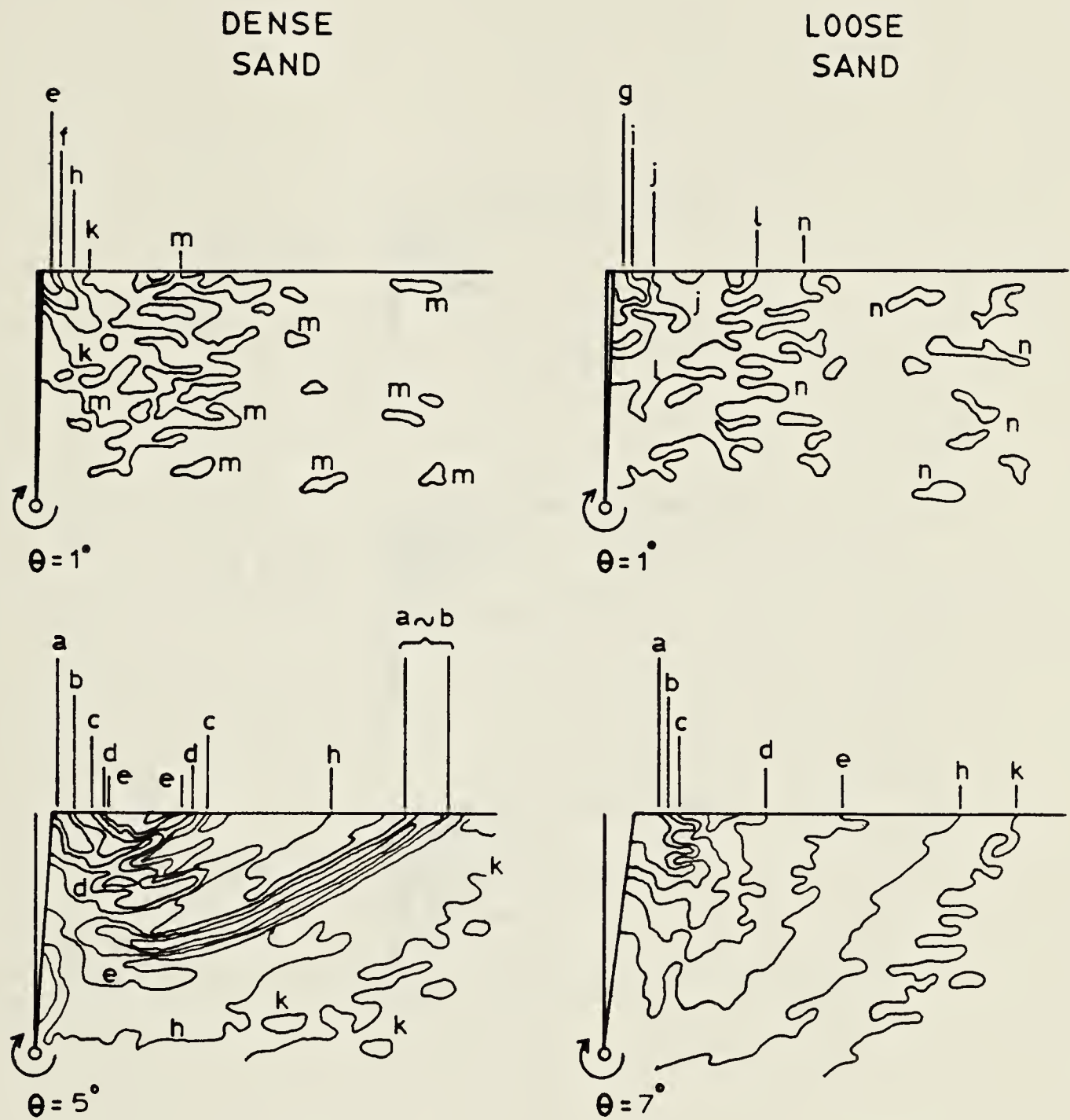


Figure 7.1. Relation between wall rotation and earth pressure for different densities (After Terzaghi, 1954).

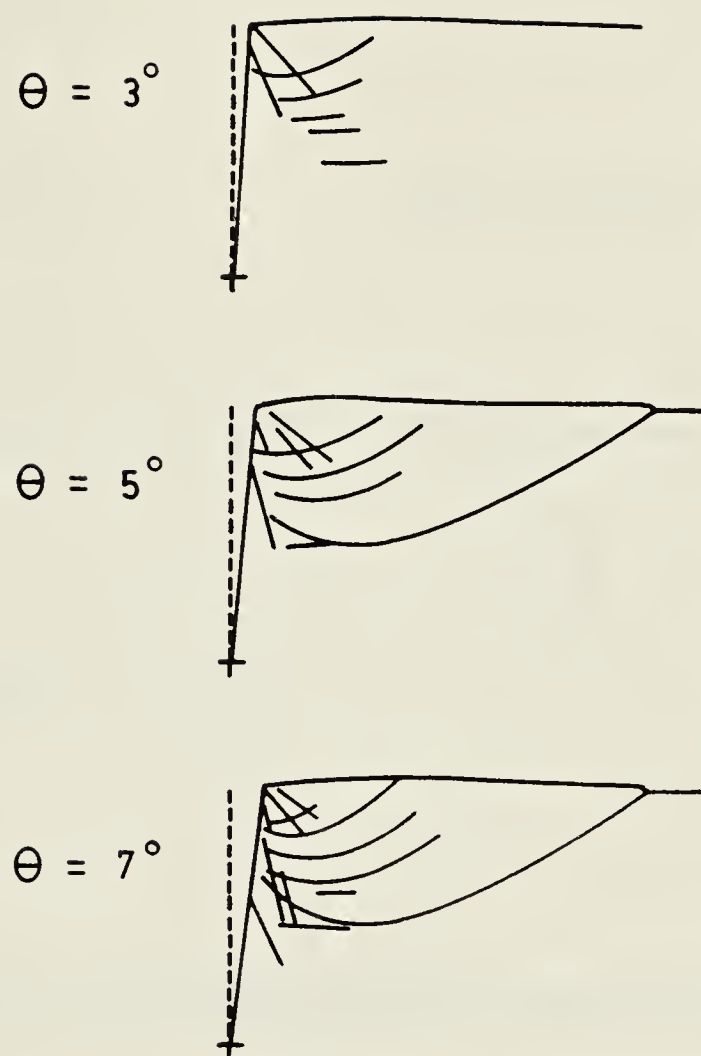




Symbol	Strain	Symbol	Strain	Symbol	Strain
a	0.30	f	0.075	k	0.025
b	0.25	g	0.06	l	0.02
c	0.20	h	0.05	m	0.015
d	0.15	i	0.04	n	0.01
e	0.10	j	0.03		

Figure 7.2. Shear strain contours for dense and loose sand (After James and Bransby, 1970).





$\theta$  : Angle of wall rotation about the toe

Figure 7.3. Rupture planes observed on radiographs exposed at three stages of wall rotation (After James and Bransby, 1970).





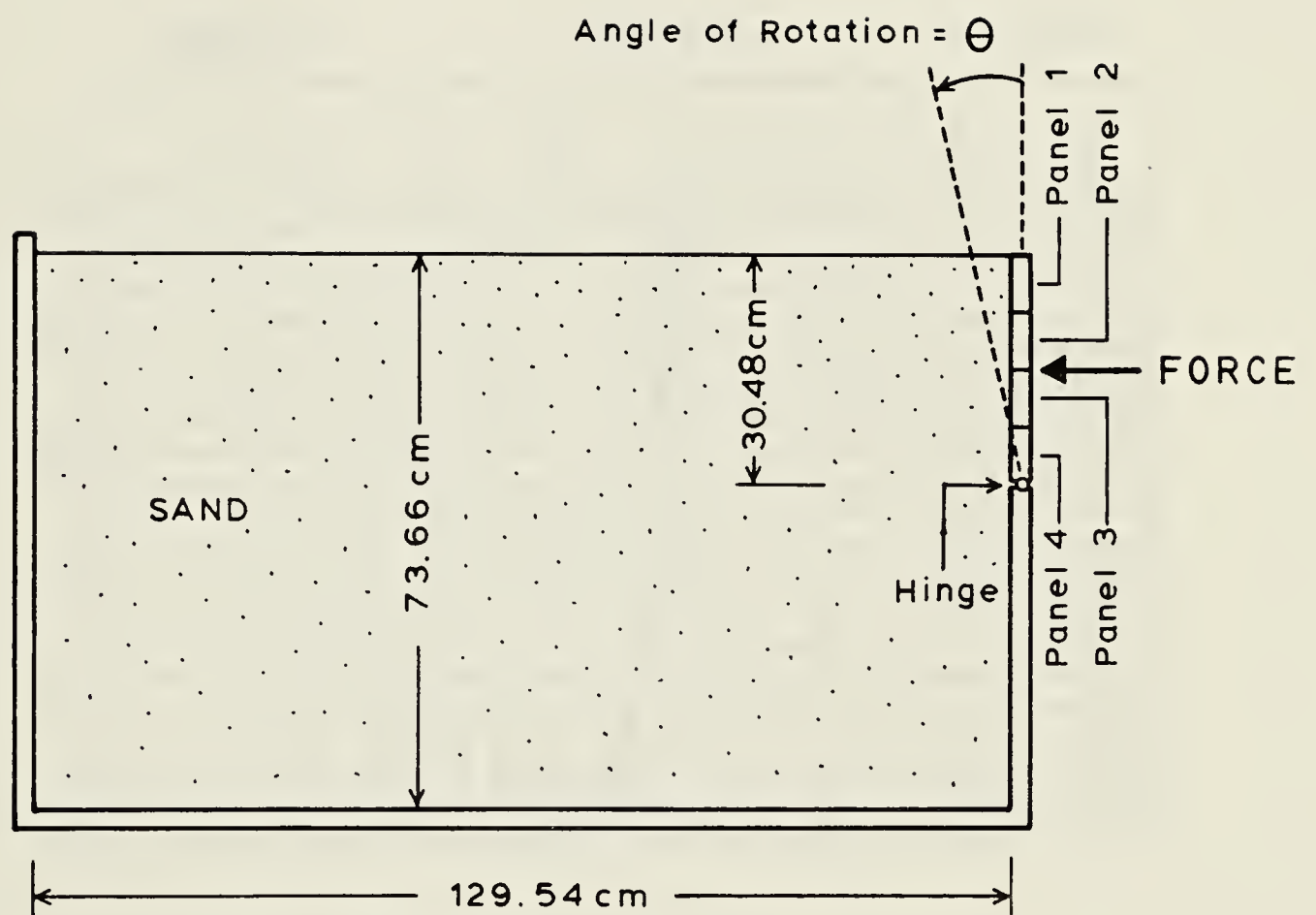


Figure 7.4. Instrumented wall for passive pressure tests (After Wong, 1978).



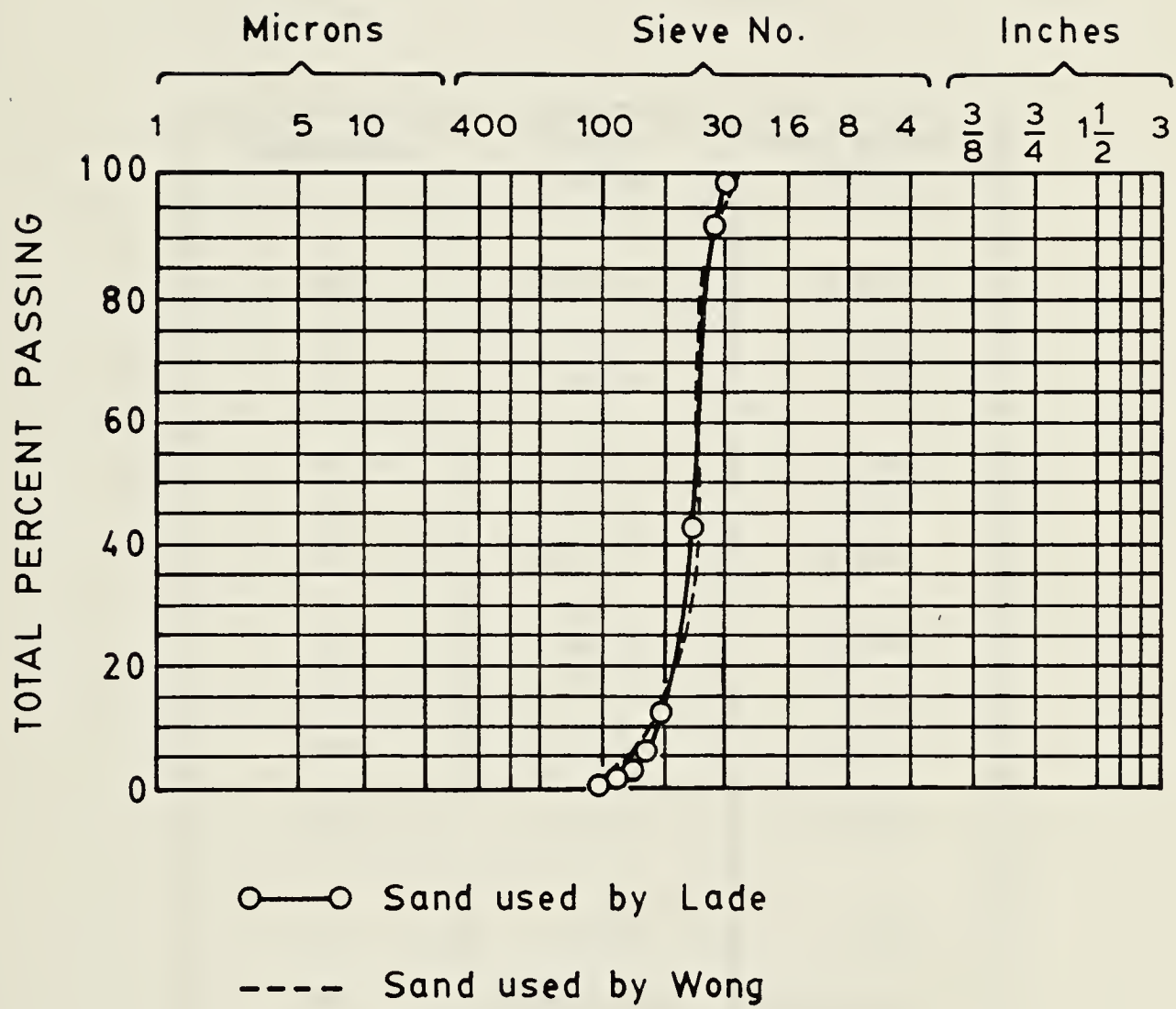


Figure 7.5. Gradation curves for Monterey No. 0 sand (After Wong, 1978).



TABLE 7.1  
STRESS-STRAIN PARAMETERS OBTAINED BY WONG (1978)  
FOR MONTEREY No.0 SAND.

Parameter	Dense Sand	Med.Dense Sand
$K_{ur}$	3720	2330
$n$	0.78	0.79
$v$	0.2	0.26
$K_1$	83.6	68.4
$f_t$	30.3	30.9
$A_1$	0.572	0.451
$A_2$	7.11	12.96
$l$	1.45	1.38
$M$	0.0000746	0.000196
$r_f$	0.97	0.99





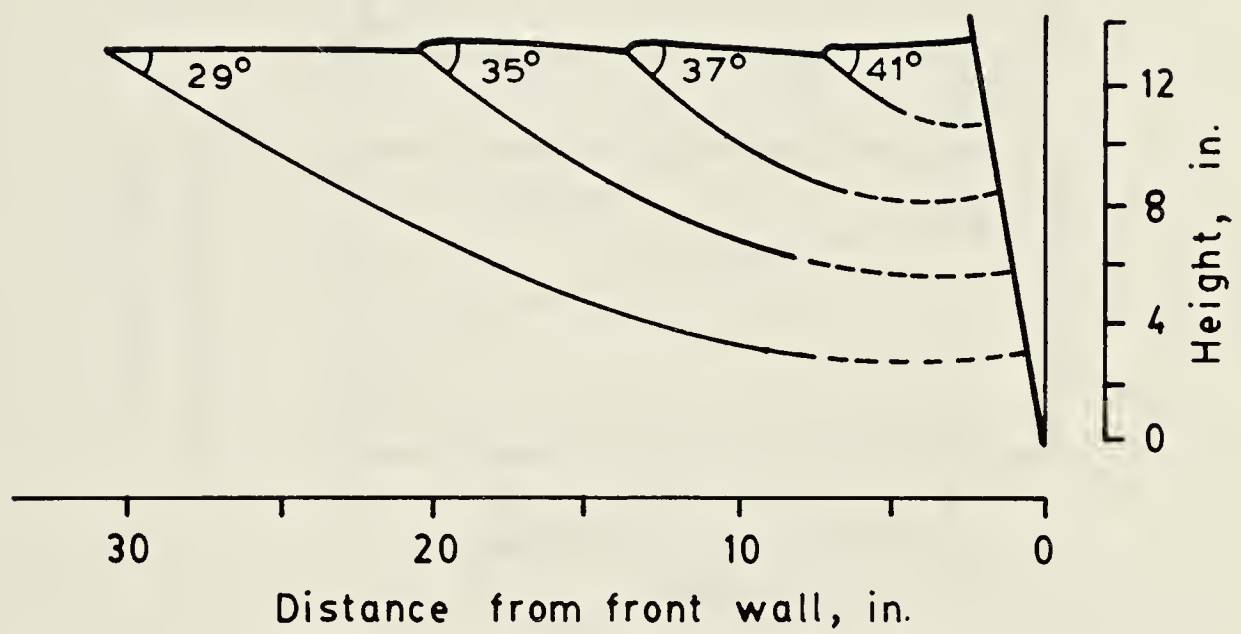


Figure 7.6. Observed rupture planes at 10 degree wall rotation (After Wong, 1978).



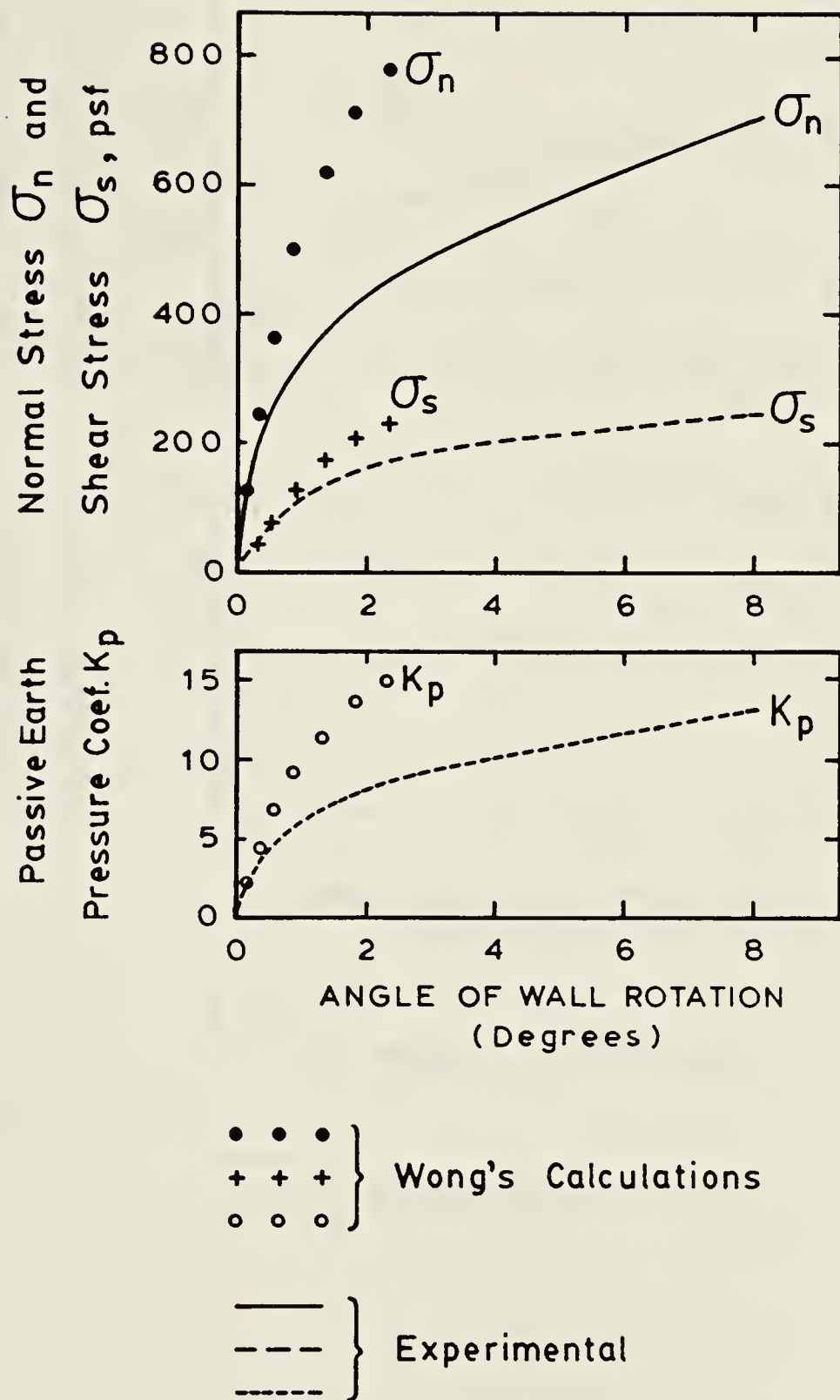


Figure 7.7 Experimental results for dense sand. Variations of average normal and shear stresses and passive earth pressure coefficient with the angle of wall rotation. (After Wong, 1978).



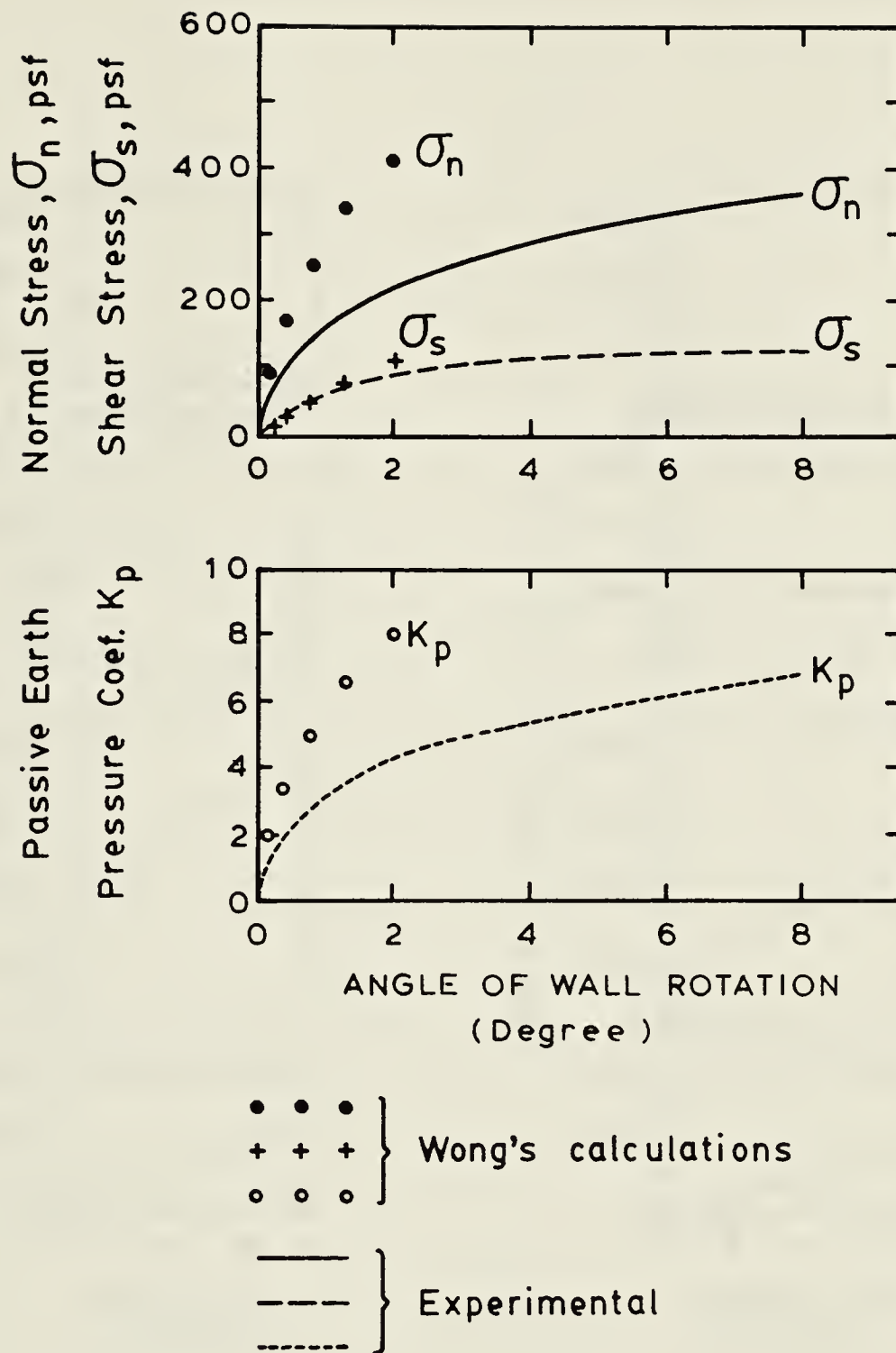


Figure 7.8 Experimental results for medium dense sand. Variations of average normal and shear stresses and passive earth pressure coefficient with the angle of wall rotation. (After Wong, 1978).



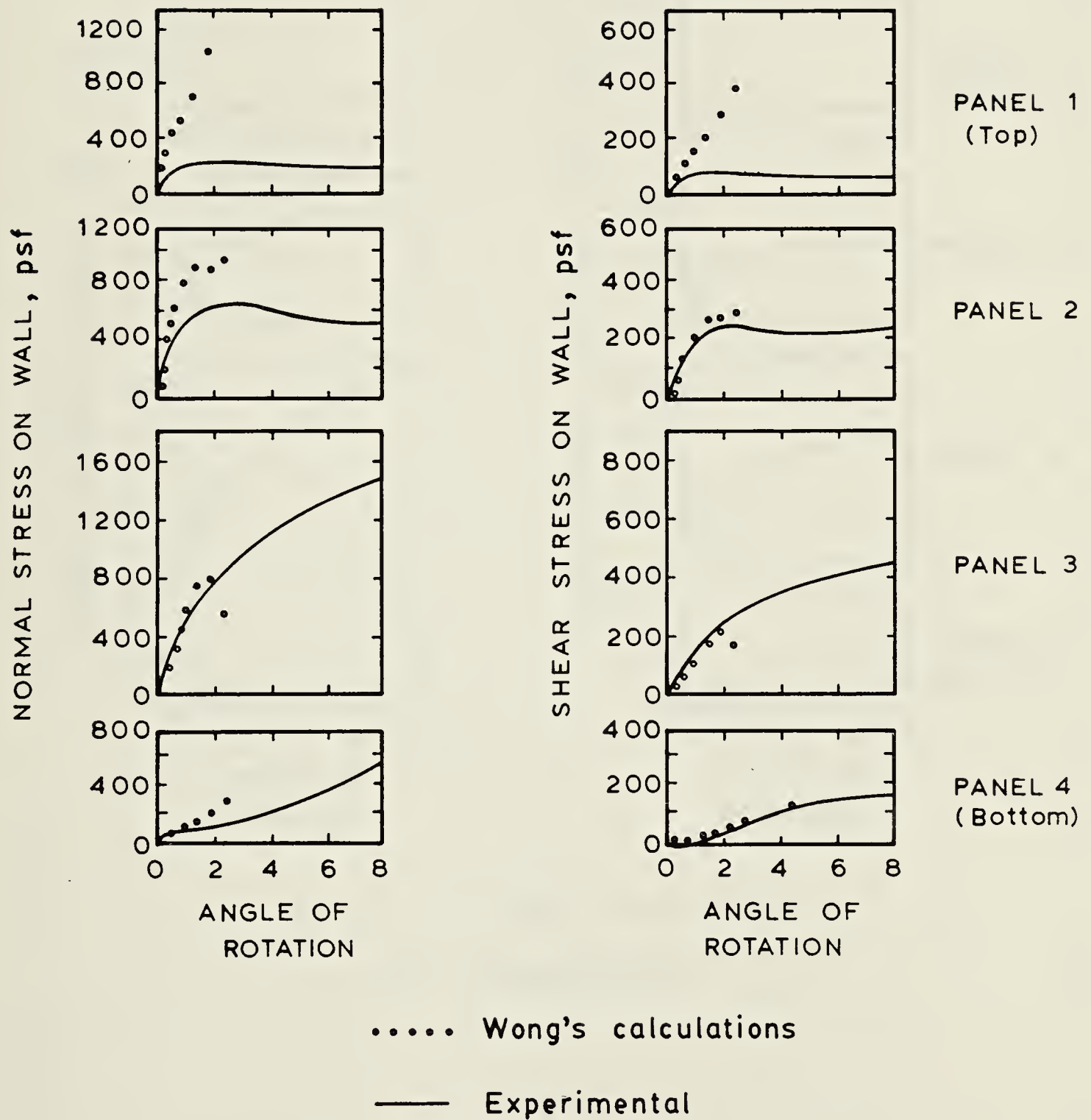


Figure 7.9 Experimental results for dense sand. Distribution of normal and shear stresses on four panels of the wall. (After Wong, 1978).





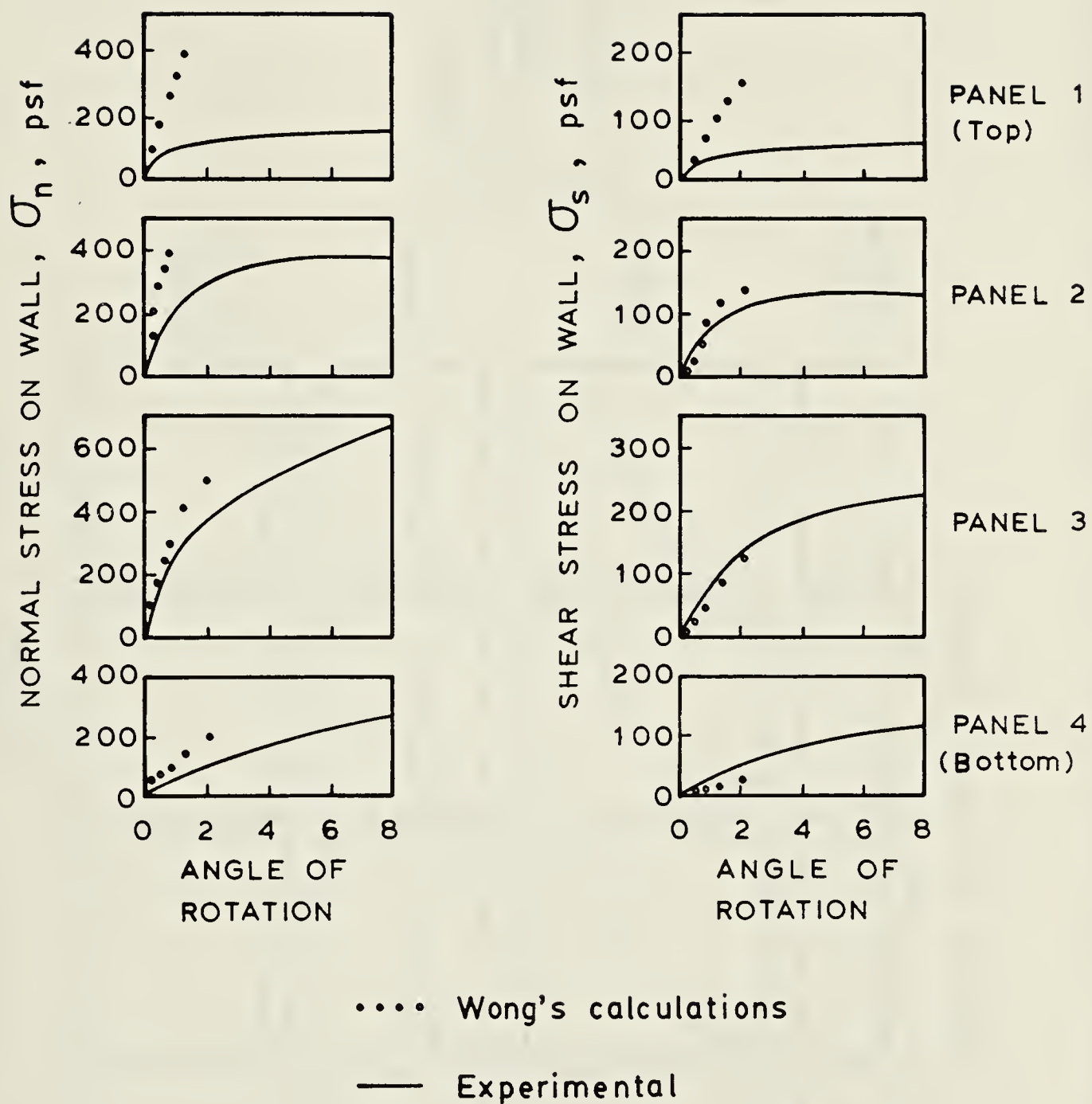


Figure 7.10 Experimental results for medium dense sand. Distribution of normal and shear stresses on four panels of the wall. (After Wong, 1978).



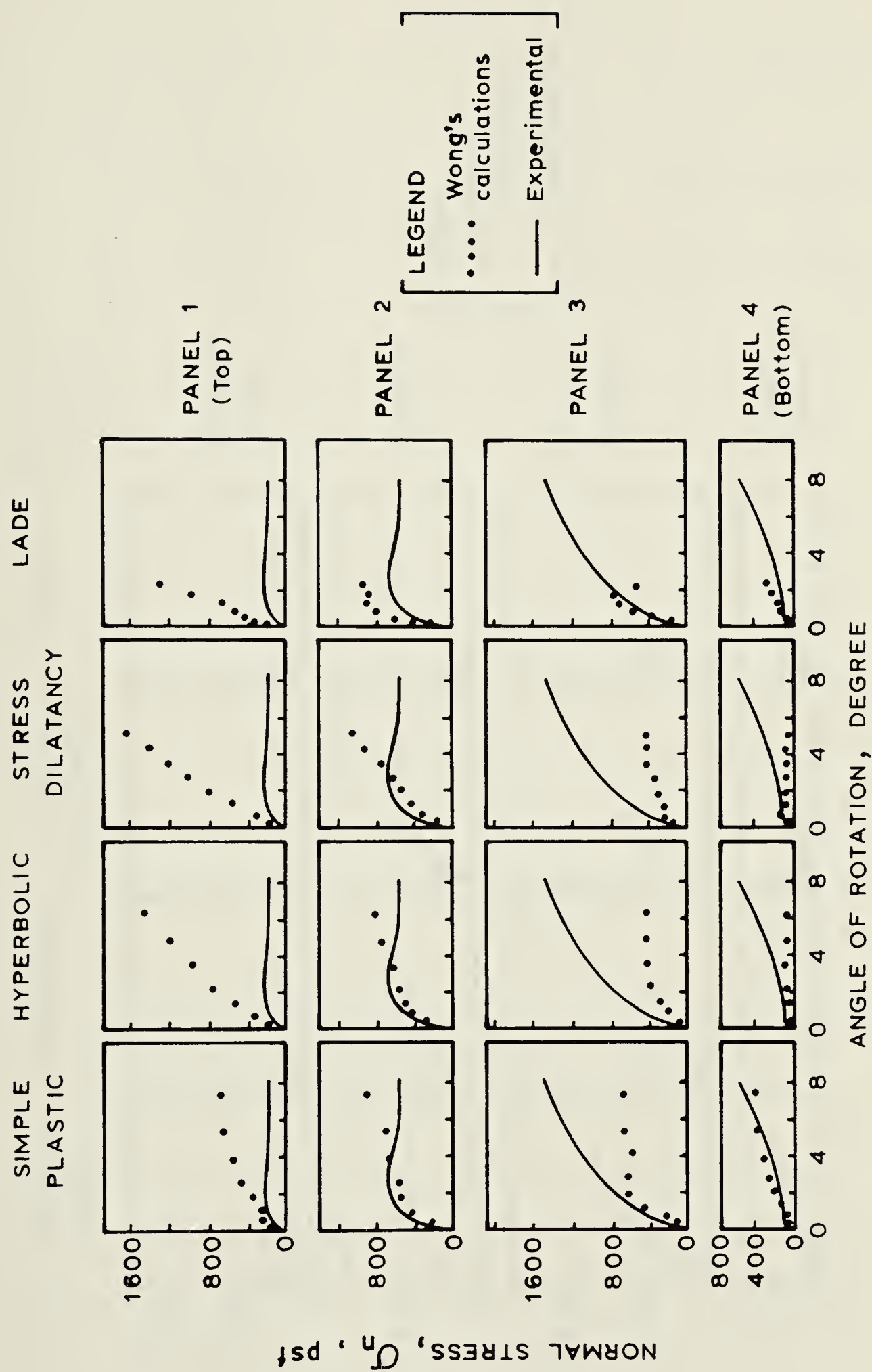


Figure 7.11 Summary of Wong's work for dense sand. (After Wong, 1978).



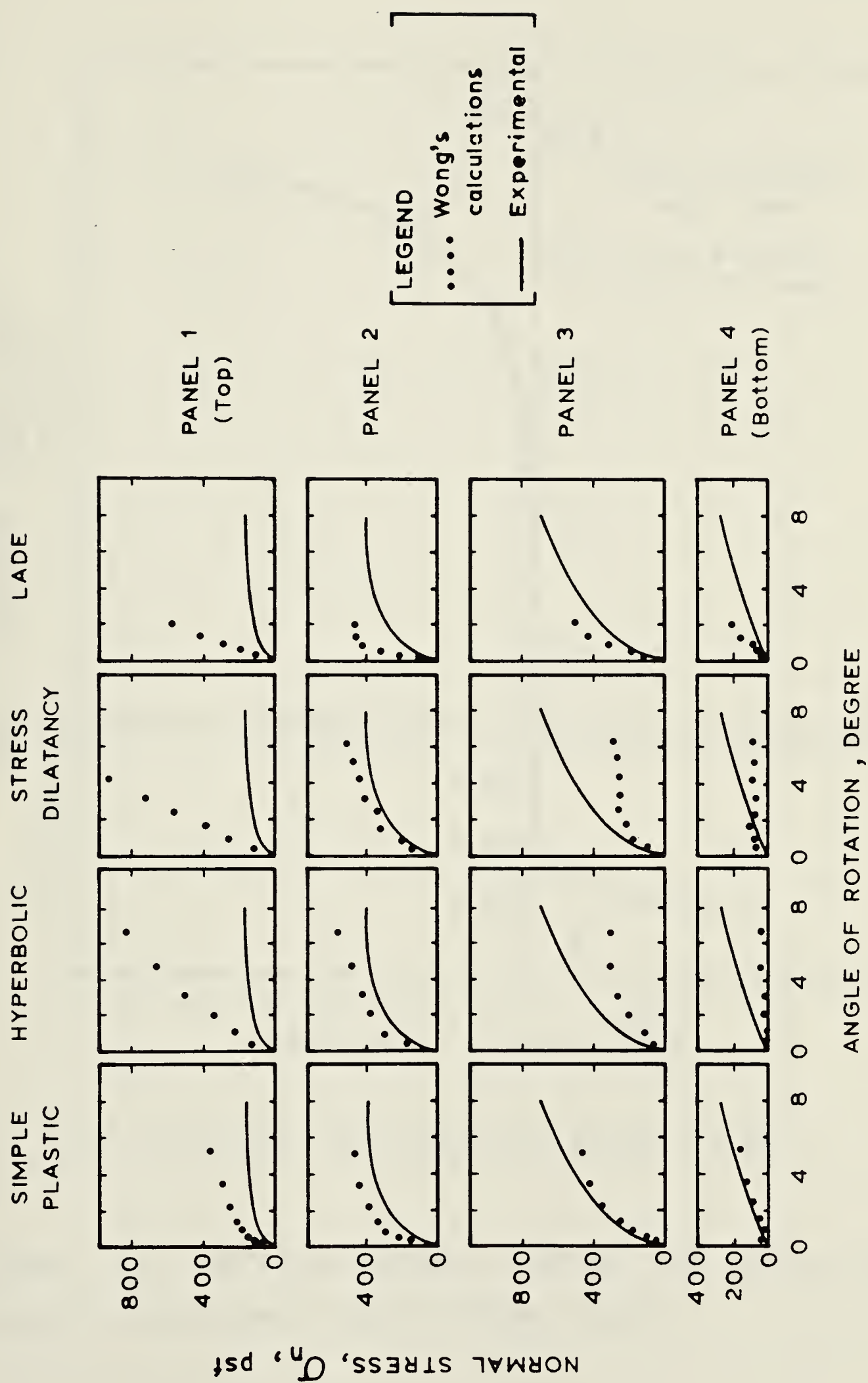
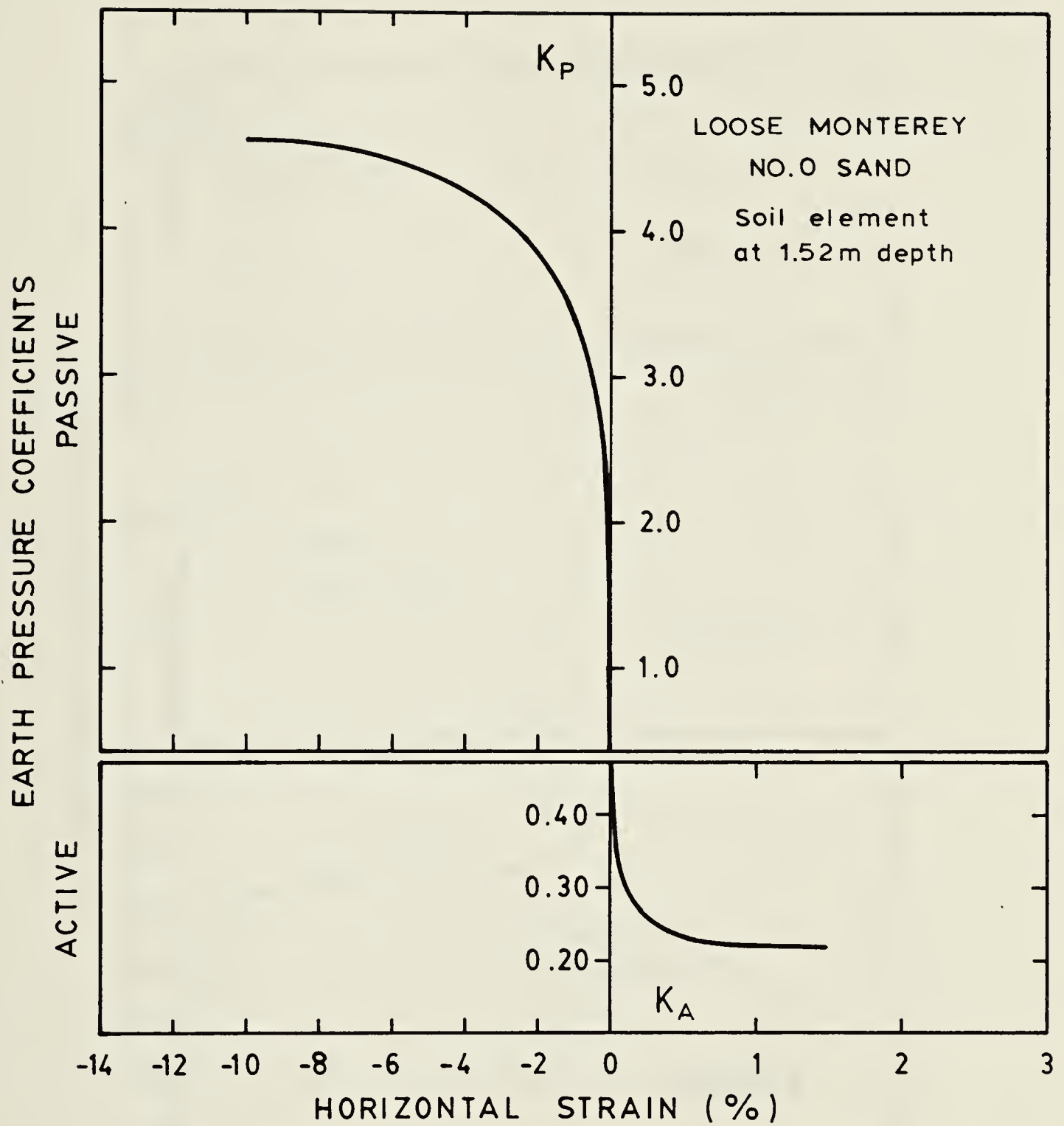


Figure 7.12 Summary of Wong's work for medium dense sand. (After Wong, 1978).







Soil parameters from Ozawa and Duncan (1976a)

Figure 7.13 Relation between active and passive earth pressure coefficient and horizontal strain.



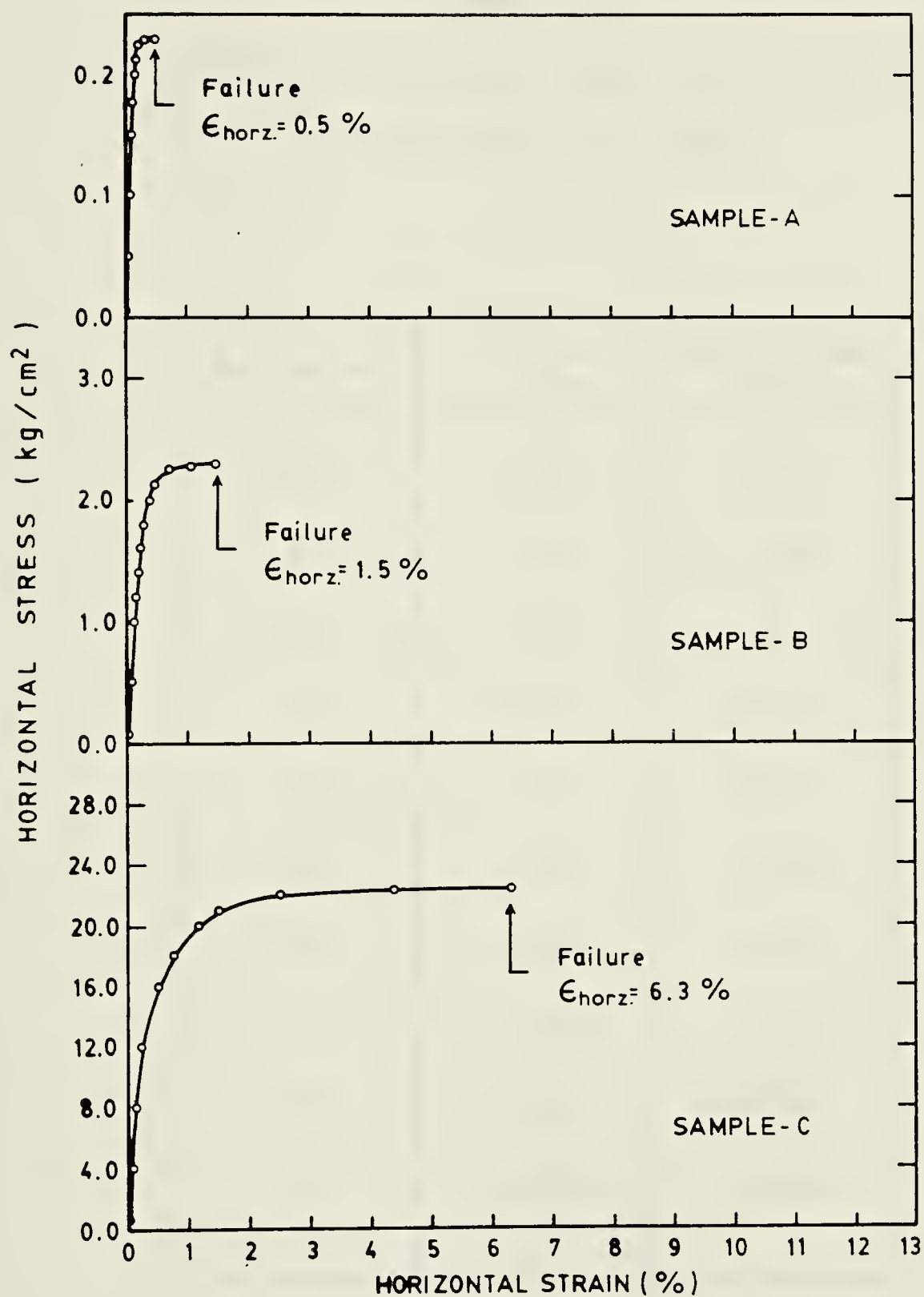


Figure 7.14 Predictions for  $\sigma_{\text{vert.}} = \text{const.}$  tests with  $\sigma_{\text{horz.}}$  increasing to failure.



TABLE 7.2  
STRESS-STRAIN PARAMETERS USED IN PRESENT STUDY  
FOR MONTEREY No.0 SAND

Parameter	Dense Sand	Med. Dense Sand
$K_{ur}$	2800	1693
$n$	0.8	0.85
$v$	0	0
$K_1$	83.6	64.0
$f_t$	38	33.9
$A_1$	0.45	0.397
$A_2$	14.85	16.28
$l$	1.686	1.19
$M$	0.00025	0.00062
$r_f$	0.973	0.968



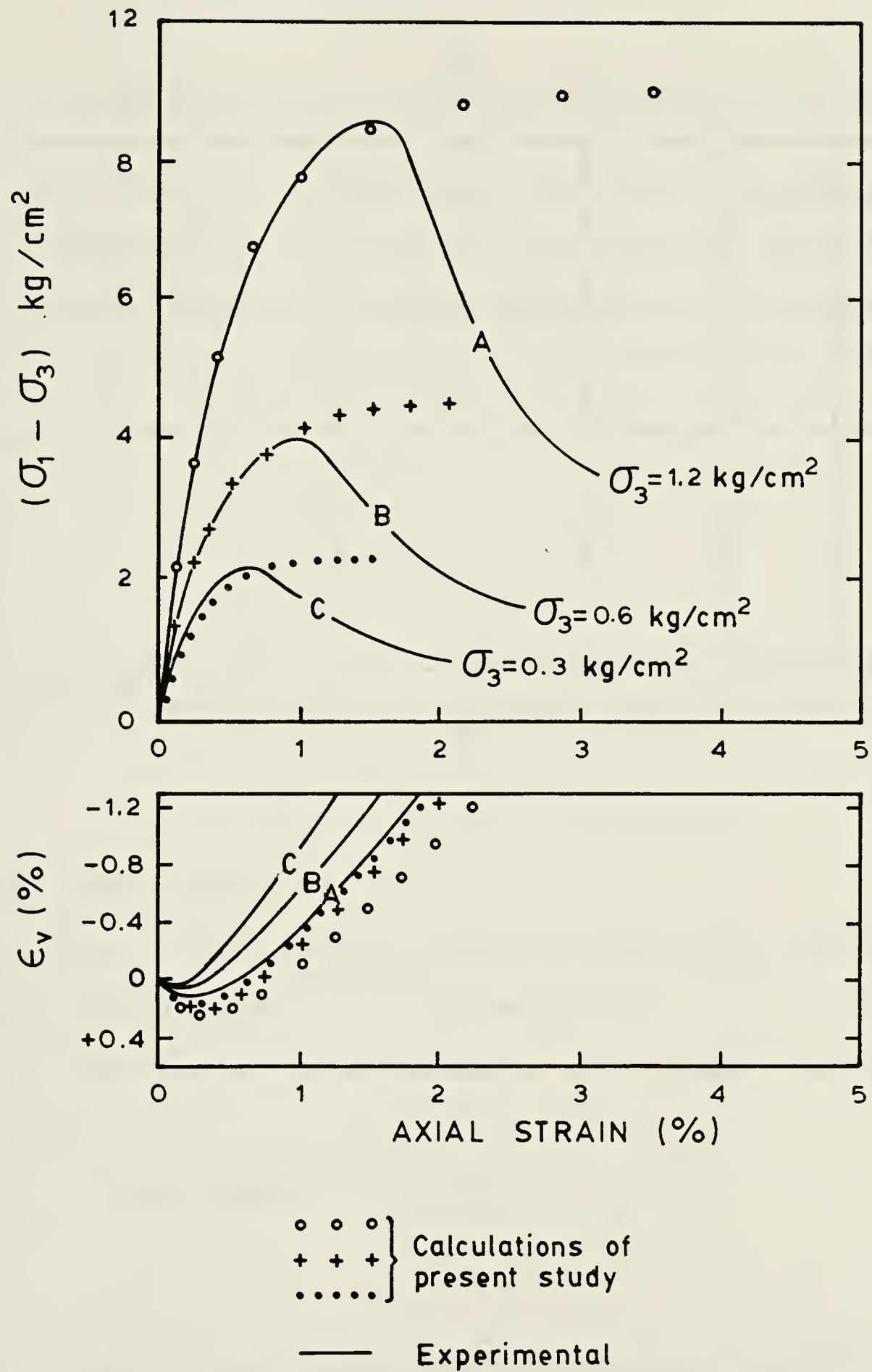
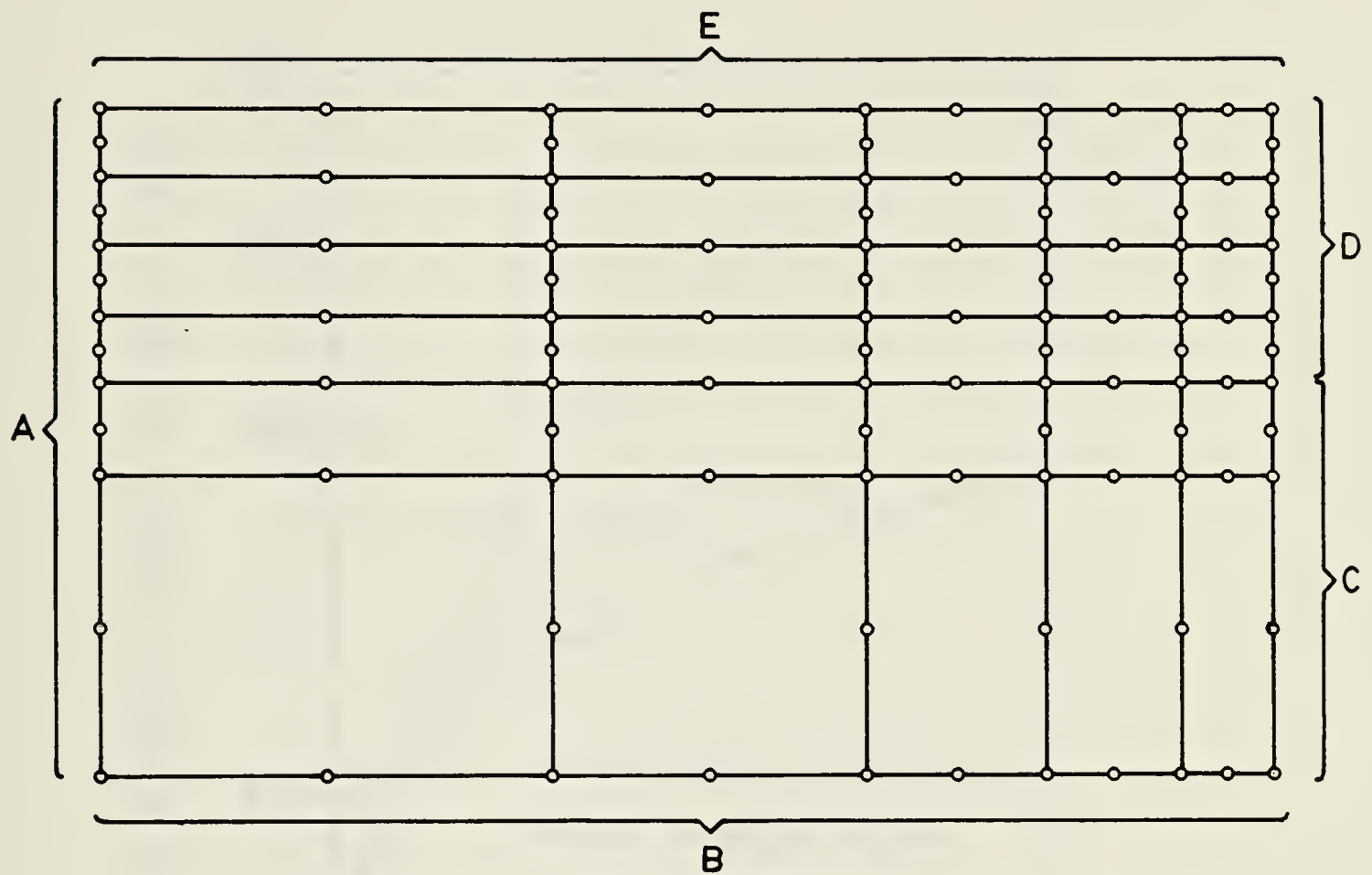


Figure 7.15 Experimental results and predictions of present study for dense Monterey No.0 sand in plane strain tests. (Experimental data after Lade, 1972)







BOUNDARY CONDITIONS:

Along A and C : only vertical displacements are allowed.

Along B : displacements are not permitted.

Along D : horizontal displacements and shear forces are specified.

Along E : Free to move.

Figure 7.16 Finite element mesh and boundary conditions for the analysis of rigid wall.



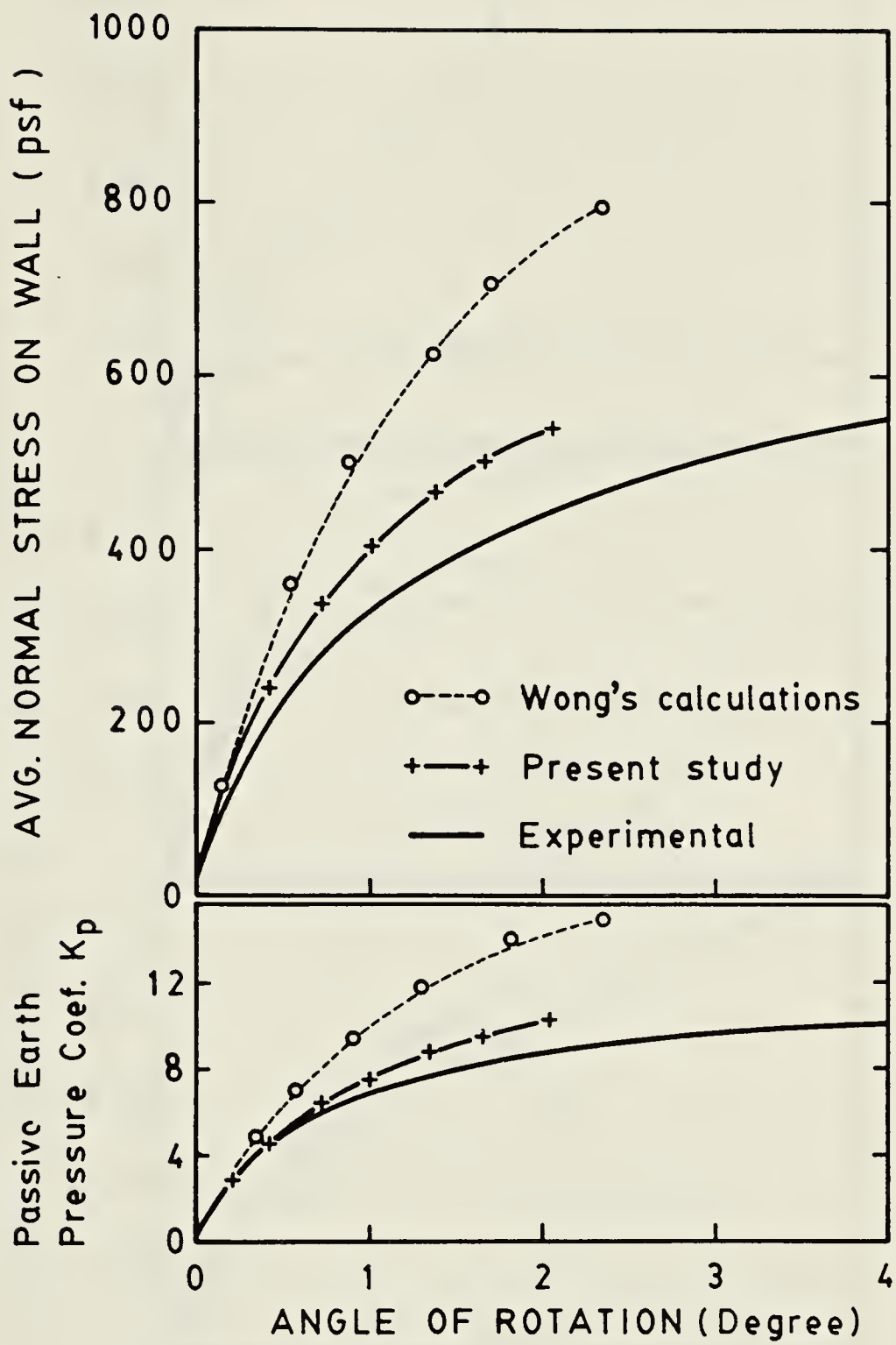


Figure 7.17 Variation of average normal stress with wall rotation for dense Monterey No.0 sand.



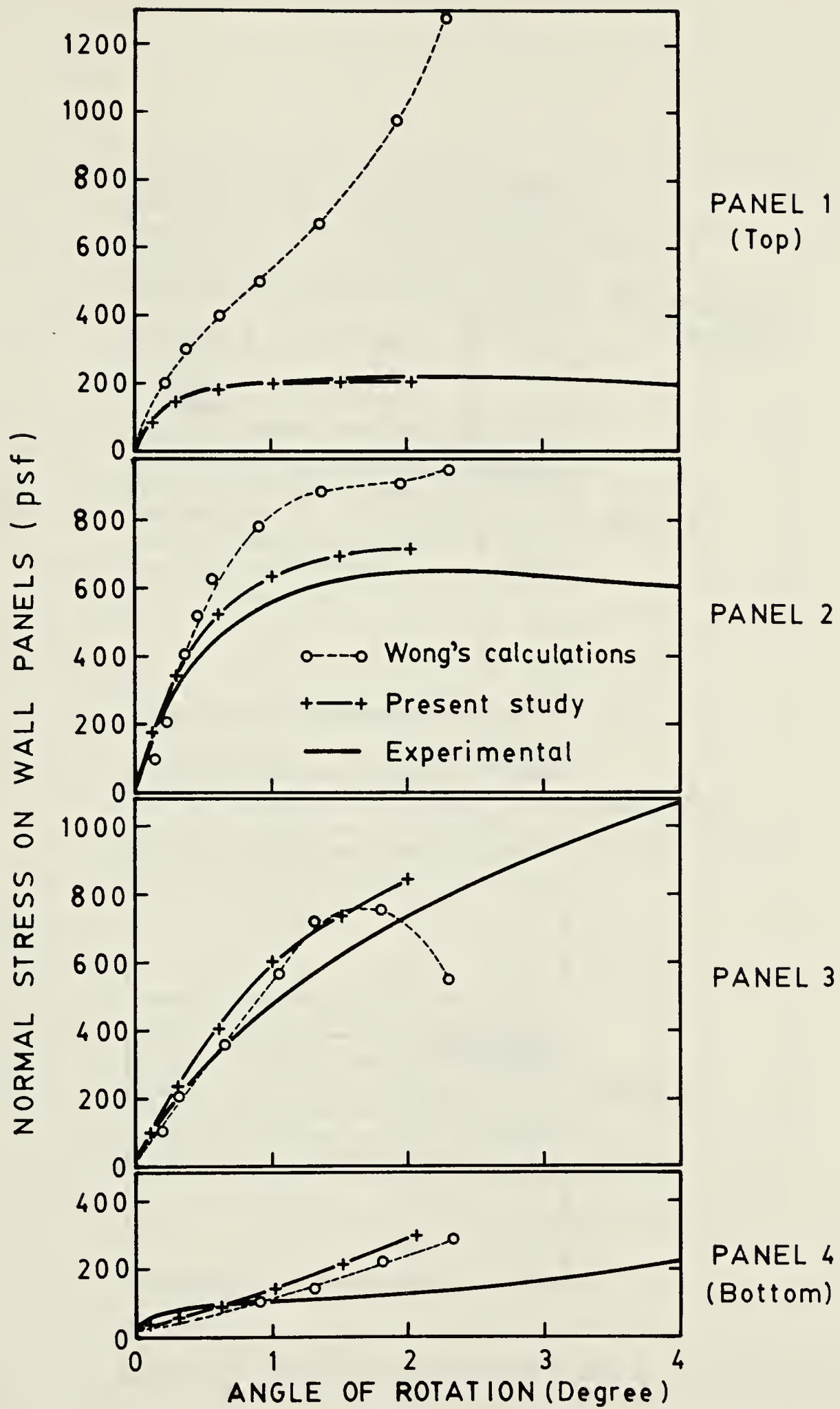


Figure 7.18 Distribution of normal stresses along the wall for dense Monterey No.0 sand.





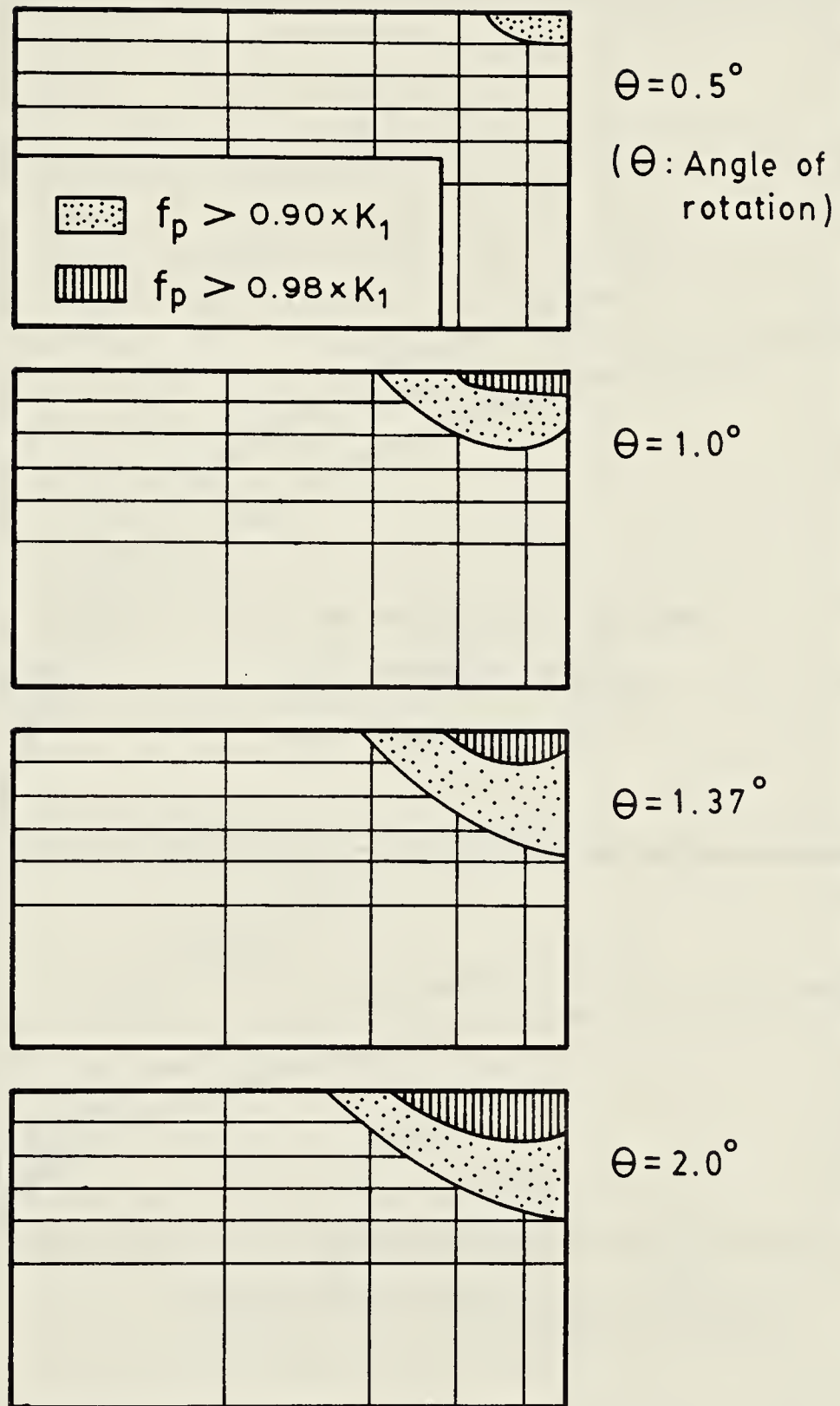


Figure 7.19 Zones of high stress level as a function of wall rotation for dense Monterey No. 0 sand.



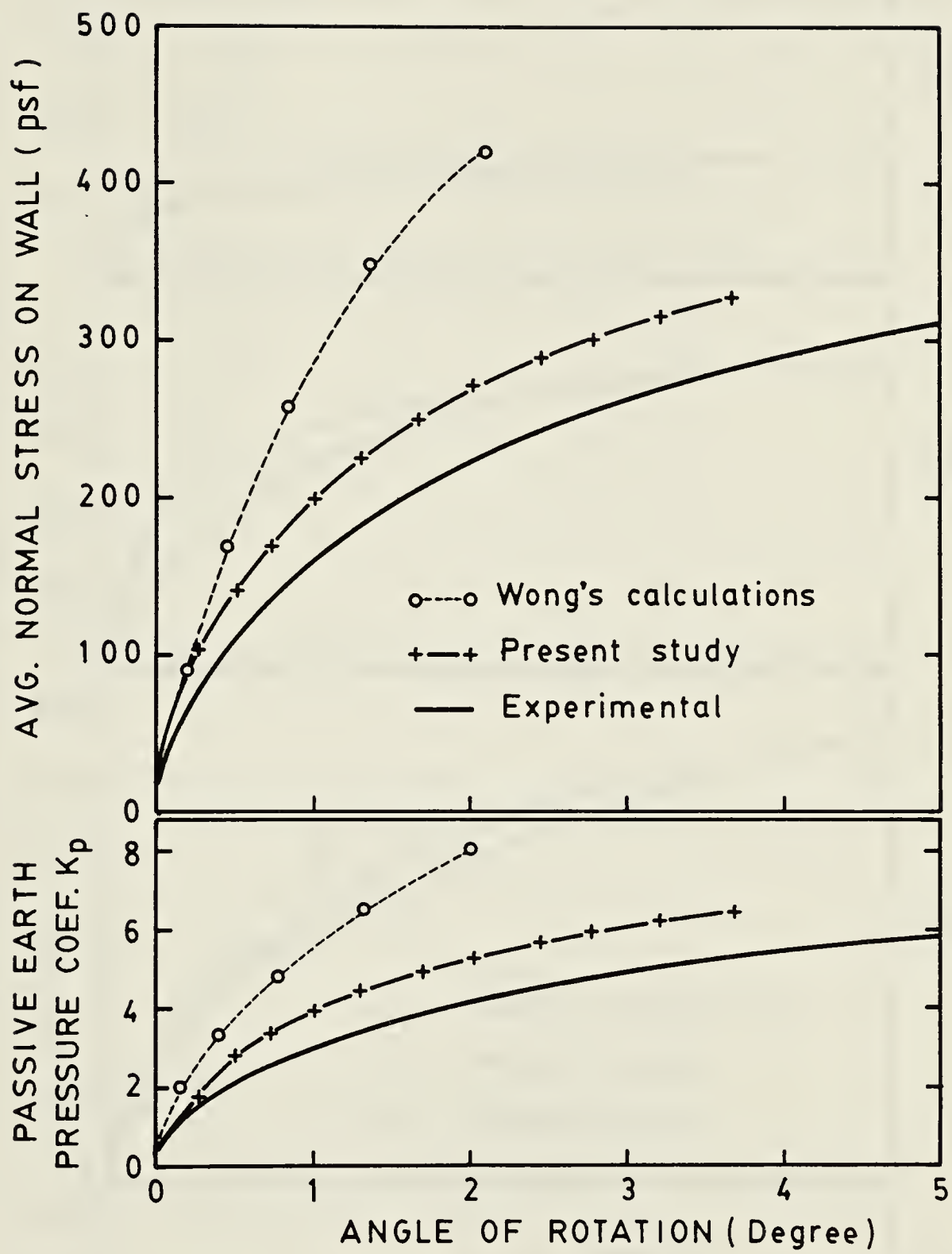


Figure 7.20 Variation of average normal stress with wall rotation for medium dense Monterey No.0 sand.



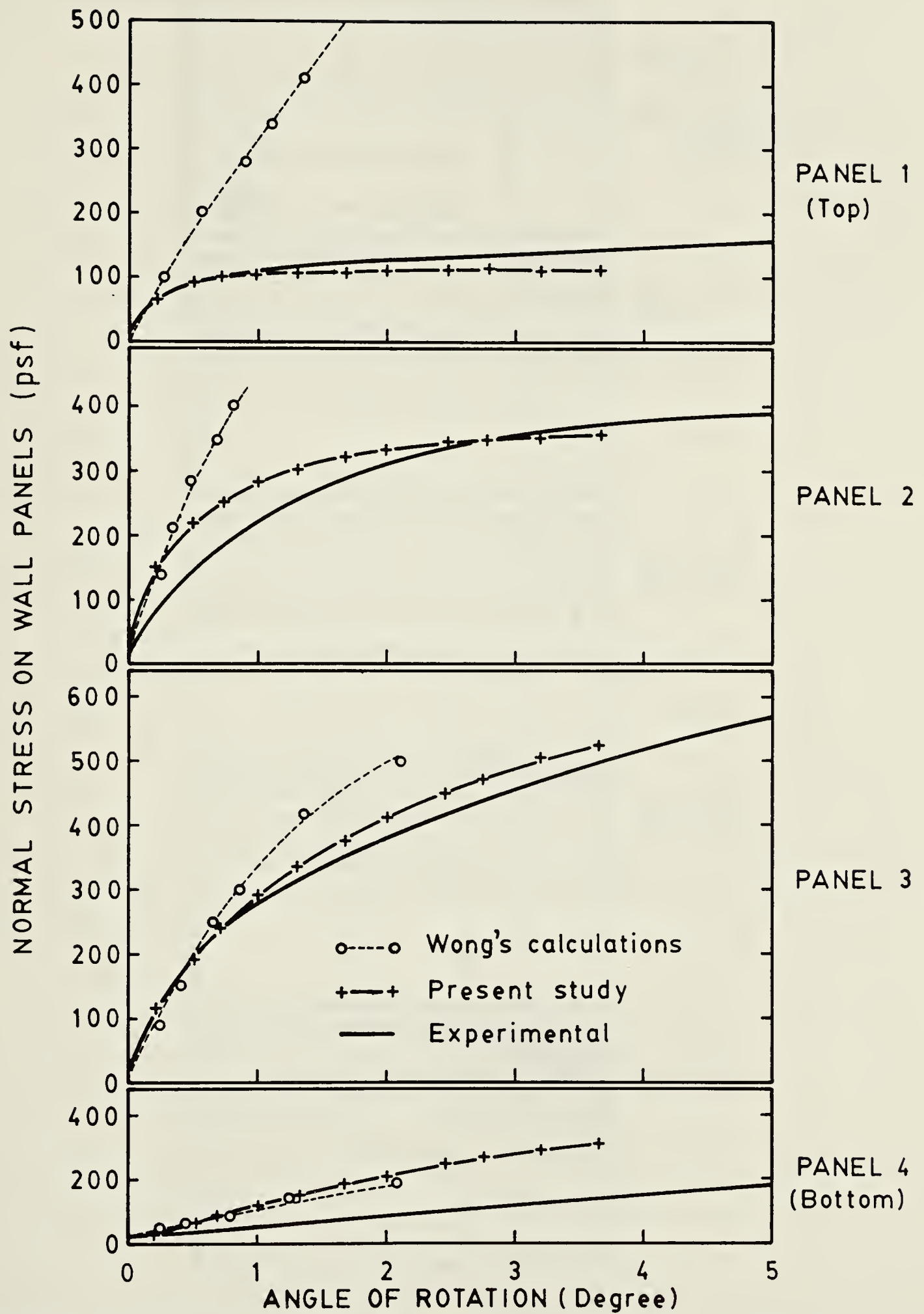


Figure 7.21 Distribution of normal stresses along the wall for medium dense Monterey No.0 sand.



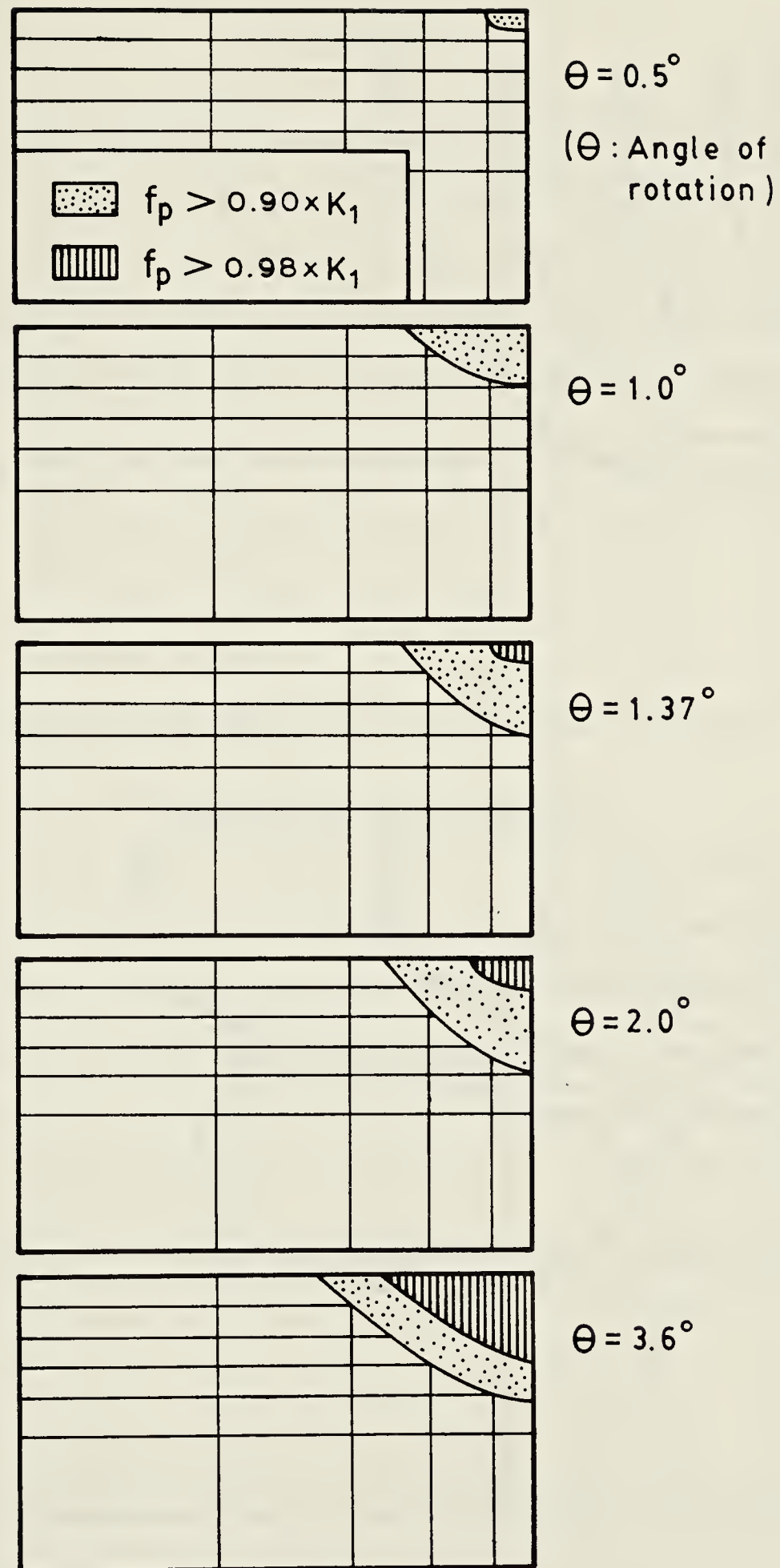


Figure 7.22 Zones of high stress level as a function of wall rotation for medium dense Monterey No. 0 sand.





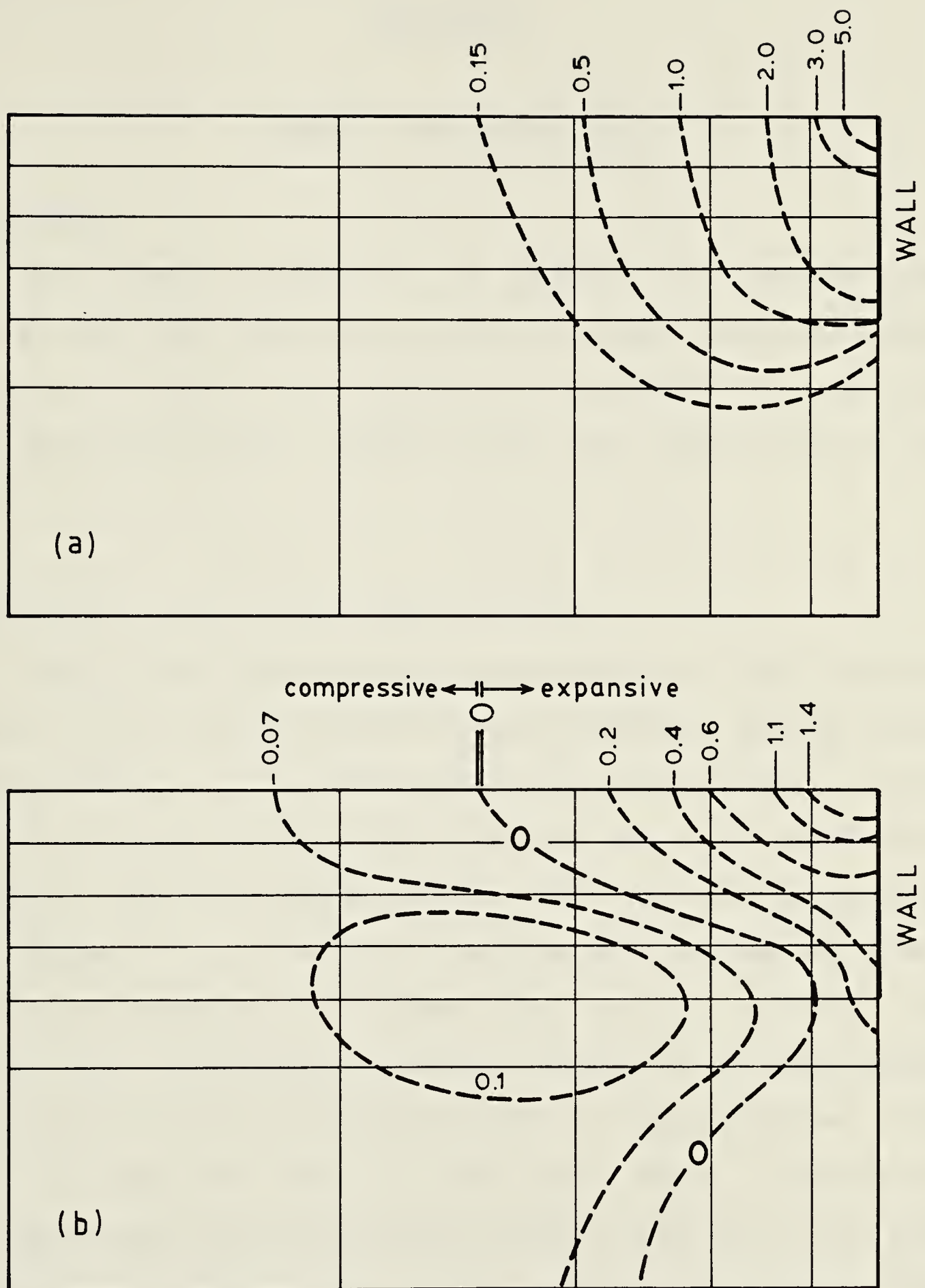


Figure 7.23 Contours of a) cumulative shear strains and b) volumetric strains at 2 degree wall rotation for medium dense Monterey No. 0 sand.



## CHAPTER 8

### SUMMARY AND CONCLUSIONS

#### 8.1 SUMMARY

The present study is an attempt to reassess the theoretical and practical value of Lade's work hardening constitutive law. It is, therefore, relevant to summarize the characteristics, capabilities and limitations of the model.

#### CHARACTERISTICS OF WORK HARDENING MODEL

Lade's first model which is evaluated in the present study, is an elasto-plastic work hardening stress-strain relationship. It is developed for cohesionless soils. Essential components of the model are the yield and failure criteria, flow rule and hardening law. The yield surface has the shape of a cone which expands with increasing stress levels and eventually reaches the failure surface. The effect of intermediate principal stress in the development of state of failure is accounted for. A non-associated flow rule is used for better modelling. Hence, the plastic potential and the yield surface are not identical. The work hardening law is based on an experimentally determined relationship between plastic work and stress level. Details of the formulation of the model can be found in Chapter 2 or in the original work by Lade (1972).



## CAPABILITIES OF WORK HARDENING MODEL

The stress-strain law is designed for modelling the most essential features of soil behavior such as nonlinearity, inelasticity, path dependancy and shear dilatancy. The effect of intermediate principal stress on soil behavior is included in the formulation. Coincidence of strain increment and stress increment axes at low stress levels with transition to coincidence of strain increment and stress axes at high stress levels is another significant feature of the model. The soil behavior under reorientation of principal stress axes can be predicted for stress paths with increasing stress levels. Comparisons between predictions of the model and the observations in true triaxial, plane strain, torsion shear and conventional triaxial apparatus (used in both compression and tension) have demonstrated that the stress-strain law gives good results for all stages of loading up to and including failure.

Once the capabilities of the model were understood and the level of success in predictions was established, the attention is focused on the limitations of the model.

## LIMITATIONS OF WORK HARDENING MODEL

As presented in Section 2.3 the limitations of the stress-strain law are:

1. Inability to model strain softening (conditions for strain softening to take place are given in Chapter 4).





2. Inexistence of a cap yield surface results in inadequate modelling for certain stress paths (see Chapter 5).
3. Yield and failure surfaces are conical rather than the shape of a bullet. A better fit to experimental results may be obtained with bullet shape surfaces (see Chapter 4).
4. Poisson's ratio is equal to zero. Due to this limitation the predictions for elastic strain increments do not correspond with experimental results very well.
5. If the stress level remains the same during reorientation of principal stress axes, soil behavior cannot be modelled accurately.
6. Under cyclic loading within the bounds of a given stress level, the predictions for strains are purely elastic. Experiments show that plastic strains take place for large stress reversals.

#### REMARKS ON PREVIOUS FINITE ELEMENT ANALYSES

Since the first development of the model, several modifications have been proposed to the original formulation. These are discussed in Chapter 3. For the analysis of boundary value problems, a finite element program was developed by Ozawa (1974). All previous modifications to the model, before the present study, were implemented into Ozawa's finite element program by Wong (1978). For the reasons discussed in Chapter 3, the results



of the finite element analysis presented by Ozawa (1974) and Wong (1978) are not correct. Therefore, their conclusions about the significance of Lade's work hardening model are not relevant.

## 8.2 CONCLUSIONS OF PRESENT STUDY

During the course of present work various conclusions have been reached in connection with:

1. The formulation of work hardening model
2. The hardening law of strain softening model
3. A possible improvement in work hardening model
4. Finite element analysis
5. Passive earth pressure problem.

These conclusions are presented next.

### FORMULATION OF WORK HARDENING MODEL

In order to find reasons for unsatisfactory results of the finite element analyses of the past, the original formulation of the model and the previous modifications are re-evaluated. It is found that the work hardening law is the source of difficulties of the past. It is emphasized here that the relationship between stress level and plastic work depends on the confining pressure for conventional triaxial compression tests. For a general three dimensional problem, a unique relation between stress level and plastic work does not exist. To make use of the  $f$  versus  $W_p$  relation obtained from triaxial tests in the analysis of a general 3-D



problem, a somewhat arbitrary assumption has to be made. This assumption simply suggests that, for a general stress change from a known stress level and  $\sigma_3$  value, the slope of the  $f$  versus  $w_p$  curve of a conventional triaxial test is to be used to relate the increment of stress level to the plastic work increment. In triaxial data, at the point where the slope of the  $f$  versus  $w_p$  curve is considered, the value of  $\sigma_3$  and  $f$  have to correspond to that of the soil element under general state of stress (see Chapter 3). Using that assumption, measured stress-strain behavior of cohesionless soils can be successfully predicted. At the same time, the problems that are created in the finite element analysis can be avoided.

It is also shown here that the modification suggested by Ozawa (1974) in relation to parameter  $a$  adversely affects the capabilities of the model for certain stress paths (see Chapter 3).

The use of modified plastic potential function which is proposed by Ozawa (1974) produces results identical to those obtained from Lade's original formulation. Therefore, it is unnecessary.

#### HARDENING LAW OF STRAIN SOFTENING MODEL

Hardening-softening law of Lade's strain softening model is based on a relationship between stress level and total plastic work. This relationship is not unique but is a function of the confining pressure for conventional triaxial





compression tests. In order to use such a relation for general stress changes and also to avoid problems in finite element analysis, an interpretation of the law is proposed (see Chapter 4).

#### POSSIBLE IMPROVEMENT IN WORK HARDENING MODEL

One of the limitations of the work hardening model is unsatisfactory modelling for certain stress paths as discussed in Chapter 5. To eliminate this limitation, a cap type yield surface is incorporated into Lade's work hardening model. The improvement that can be obtained in predictions is demonstrated by comparing experimental and calculated results.

#### FINITE ELEMENT ANALYSIS

Related to the finite element analysis, the conclusions reached in different sections of the present study follow.

1. It has already been emphasized that the proper use of the hardening law of Lade's work hardening model is essential for the results of finite element analysis to be reliable (see Chapter 3).
2. Constitutive laws dealing with several stress-strain relationships within the model may be formulated in a more suitable way for finite element programming (see Chapter 5).
3. A method to test the accuracy and the correctness of newly developed finite element programs is proposed in





Chapter 6. This is a better technique than what has been used in geotechnical practice.

#### PASSIVE EARTH PRESSURE PROBLEM

Preliminary calculations have shown that the passive earth pressure coefficient versus horizontal strain relation is a function of the state of stress at rest conditions. In other words, it depends strongly on the depth of soil element under consideration.

Also, the analysis of passive earth pressure problems should not be carried out on the basis of triaxial tests where soil samples are subjected to constant vertical stress and increasing horizontal stresses until failure occurs. The use of such triaxial test data gives deformation results which are on the unsafe side.

The finite element analysis of the instrumented wall has indicated that Lade's work hardening model can be used successfully for deformation analyses. Comparative studies of experimental and analytical results of passive earth pressure tests show that the model is capable of predicting the most important features of the wall behavior such as the distribution of contact pressure and the magnitude of deformations reasonably well.

When compared with other models such as the hyperbolic stress-strain law and the stress-dilatancy model, Lade's model gave much better results for the wall behavior.



### 8.3 CLOSING REMARKS

In the present study, the first time successful application of Lade's work hardening model to a complex problem has been achieved. Undoubtedly, the model works well at all stages of loading. Therefore, it has the potential to be very useful to engineering practice. It is hoped that the model will attract more attention in the future.



## BIBLIOGRAPHY

Aggour, M.S., and Brown, C.B., (1974). "The Prediction of Earth Pressure on Retaining Walls due to Compaction," *Geotechnique*, Vol. 24, No. 4, pp. 489-502.

Andrawes, K.Z., and El-Sohby, M.A., (1973). "Factors Affecting Coefficient of Earth Pressure  $K_p$ ," *Journal of the Soil Mechanics and Foundation Division, ASCE*, Vol. 99, No. SM7, Proc. Paper 9863, July, pp. 527-539.

Arthur, J.R.F., Dunstan, T., Al-Ani, Q.A.J.L., and Assadi, A. (1977). "Plastic Deformation and Failure in Granular Media," *Geotechnique* 27, No.1, pp. 53-74.

Aubry, D., and Des Croix, Ph., (1979). "Numerical Algorithm for an Elastoplastic Constitutive Equation with Two Yield Surfaces," *Proceedings of the 3rd International Conference on Numerical Methods in Geomechanics, Aachen, April, Vol. 1*, pp.283-288.

Bishop, A.W., (1958). "Test Requirements for Measuring the Coefficient of Earth Pressure at Rest," *Proceedings of the Brussels Conference on Earth Pressure Problems, Vol. 1*, pp. 2-14.





Bishop, A.W., (1971). "Shear Strength Parameters for Undisturbed and Remolded Soil Specimens," Stress-Strain Behavior of Soils, Proc. Roscoe Memorial Symp. Camb. G.T.Foulis, Henley-on-Thames.

Bjerrum, L., (1973). "Problems of Soil Mechanics and Construction on Soft Clays," Proc. 8th Int. Conf. Soil Mechs. Found. Eng., Moscow, Vol. 3, pp. 111-159.

Brooker, E.W., and Ireland, H.O., (1965). "Earth Pressures at Rest Related to Stress History," Canadian Geotechnical Journal, Vol. II, No.1, February, pp.1-15.

Cornforth, D.H., (1964). "Some Experiments on the Influence of Strain Conditions on the Strength of Sand," Geotechnique, Vol. 14, No. 2, June, pp. 143-167.

Davis, E.H., (1968). "Theories of Plasticity and Failure of Soil Masses," Soil Mechanics: Selected Topics (Ed. I.K. Lee), pp. 341-380, Butterworths London.

Davis, E.H., and Booker, J.R., (1973). "Some applications of classical plasticity theory for soil stability problems," Symposium on Plasticity and Soil Mechanics, pp. 24-41, Cambridge, U.K.

DiMaggio, F.L. and Sandler, I.S., (1971). "Material Models



for Soils," Journal of the Engineering Mechanics Division, ASCE, Vol. 97, No. EM3, June., pp. 935-950.

Drucker, D.C., Gibson, R.E. and Henkel, D.J., (1957). "Soil Mechanics and Work-Hardening Theories of Plasticity," Transactions, ASCE, Vol. 122, pp. 338-346.

Drucker, D.C., and Prager, W., (1952). "Soil Mechanics and Plastic Analysis of Limit Design," Quarterly of Applied Mathematics, Vol. 10, pp. 157-175.

Duncan, J.M. and Chang, C-Y., (1970). "Nonlinear Analysis of Stress and Strain in Soils," Journal of the Soil Mechanics and Foundation Division, ASCE, Vol. 96, No. SM5, Proc. Paper 7513, September.

Duncan, J.M., Ozawa, Y., Lade, P.V. and Booker, J.R., (1977). "An Elasto-Plastic Stress-Strain Relationship for Cohesionless Soil", Specialty Session No. 9, Ninth International Conference on Soil Mechanics and Foundation Engineering, Tokyo, Japan, pp.45-50.

Eisenstein, A. and Law, S.T.C., (1979). "The Role of Constitutive Laws in Analysis of Embankments", Proceedings of the 3rd International Conference on Numerical Methods in Geomechanics, Aachen, April, pp.1413-1430.



Franzius, O., (1924). "Experiments with Passive Earth Pressure," Bauingenieur, Helf 10, Berlin.

Green, G.A., (1972). "Strength and deformation of sand measured in an independent stress control cell," Proc. Roscoe Memorial Symp. pp. 285-323, Foulis.

Hansen, J.Brinch., (1953). "Earth Pressure Calculation," Danish Technical Press, Copenhagen.

Harr, M.E., (1966). Foundations of Theoretical Soil Mechanics. McGraw-Hill, New York.

Hill, R., (1950). "The Mathematical Theory of Plasticity," Oxford University Press, London, 1950.

Hoeg, K., (1973). "Finite element analysis of strain-softening clay," Proc. ASCE, J. of Soil Mechs. Found. Div., Vol. 98, SM1.

James, R.G. and Bransby, P.L., (1970). "Experimental and Theoretical Investigations of a Passive Earth Pressure Problem," Geotechnique, Vol. 20, No. 1, pp. 17-37

Khosla, V.K., and Wu, T.H., (1976). "Stress-Strain Behavior of Sands," Journal of the Geotechnical Engineering Division, ASCE, Vol. 102, No. GT4, Proc. Paper 12079, April, pp.





303-321.

Kondner, R.L., and Zelasco, J.S., (1963). "A Hyperbolic Stress-Strain Formulation for Sands," Proc. 2nd Pan American Conference Soil Mech. Found. Eng., Brazil, Vol.I., pp. 289-324.

Ladd, C.C., Foott, R., Ishihara, K., Schlosser, F. and Poulos, H.G., (1977). "Stress-Deformation and Strength Characteristics," State-of-the-Art Report for Session I, Proc., 9th Int. Conf. on Soil Mechs. and Found.Eng., Tokyo, Vol. 2, pp. 421-494.

Lade, P.V., (1972). "The Stress-Strain and Strength Characteristics of Cohesionless Soil," thesis presented to the University of California, at Berkeley, Calif., in partial fulfillment of the requirements for the degree of Doctor of Philosophy.

Lade, P.V., (1975). "Elasto-Plastic Stress-Strain Theory for Cohesionless Soil with Curved Yield Surface," Report No. UCLA-ENG-7594, School of Engineering and Applied Science, University of California, Los Angeles, Calif.

Lade, P.V., (1977). "Elasto-Plastic Stress-Strain Theory for Cohesionless Soil with Curved Yield Surface," Int. Journal of Solids and Structures, Pergamon Press, Inc. New York,





N.Y., Vol. 13, Nov. pp. 1019-1035.

Lade, P.V., (1978). "Prediction of Undrained Behavior of Sand," Journal of the Geotechnical Engineering Division, ASCE, Vol. 104, No. GT6, Proc. Paper 13834, June, pp. 721-735.

Lade, P.V., and Duncan, J.M., (1975). "Elastoplastic Stress-Strain Theory for Cohesionless Soils," Journal of the Geotechnical Engineering Division, ASCE, Vol. 101, No. GT10, Proc. Paper 11670, October, pp. 1037-1053.

Lade, P.V., and Duncan, J.M., (1976)., "Stress-Path Dependent Behavior of Cohesionless Soil", Journal of the Geotechnical Engineering Division, ASCE, Vol. 102, No. GT1, Proc. Paper 11841, January, pp. 51-68.

Lade, P.V., and Musante, H.M., (1976). "Three-Dimensional Behavior of Normally Consolidated Cohesive Soil," REPORT No. UCLA-ENG-7626, School of Engineering and Applied Science, University of California, Los Angeles, Calif.

Lade, P.V., and Musante, H.M., (1978). "Three-Dimensional Behavior of Remolded Clay," Journal of the Geotechnical Engineering Division, ASCE, Vol. 104, No. GT2, Proc. Paper 13551, February, pp. 193-209.



Lambe, T.W., (1973). "Up-to-date methods of investigating the strength and deformability of soils." Proc. 8th Int. Conf. Soil Mechs. Found. Eng., Moscow, Vol. 3, pp. 3-25.

Lambe, T.W., and Marr, W.A., (1979). "Stress Path Method: Second Edition," Journal of the Geotechnical Engineering Division, ASCE, Vol. 105, No. GT6, Proc. Paper 14655, June, pp. 727-738.

Lambrechts, J.R., and Leonards, G.A., (1978). "Effects of Stress History on Deformation of Sand," Journal of the Geotechnical Engineering Division, ASCE, Vol. 104, No. GT11, Proc. Paper 14170, Nov., pp. 1371-1387.

Lee, K.L., and Seed, H.B., (1967). "Drained Strength Characteristics of Sand," Journal of the Soil Mechanics and Foundation Division, ASCE, Vol. 93, No. SM6, Proc. Paper 5561, November, pp. 117-141.

Lo, K.Y. and Lee, C.F., (1973). "Stress Analysis and Slope Stability in Strain-Softening Materials," Geotechnique, Vol. 23, No.1

Medeiros, L., "Deep Excavations in Stiff Soils", thesis presented to the University of Alberta, at Edmonton, Alberta, in 1979, in partial fulfillment of the requirements for the degree of Doctor of Philosophy.



Mendelson, A., (1968). "Plasticity: Theory and Application," The McMillan Company, New York, 1968.

Morgenstern, N.R., (1975). "Stress-Strain Relations for Soil in Practice," Fifth American Conf. on Soil Mech. and Found. Engineering Vol. IV. pp. 1-41.

Morgenstern, N.R., and Eisenstein, Z., (1970). "Methods of estimating lateral loads and deformations." Proc. Conf. on Lateral Stresses and Design of Earth-Retaining Structures, ASCE, p 51-102.

Narain, J., Saran, S., and Nandakumaran, P., (1969). "Model Study of Passive Pressure in Sand," Journal of Soil Mechanics and Foundation Engineering Div., ASCE, 95, SM 4, pp. 969-983.

Naylor, D.J., (1975). "Non-linear Finite Element Models for Soils," Ph.D. Thesis, University of Wales, Swansea.

Oda, M., (1972). "Initial fabrics and their relations to mechanical properties of granular material," Soils and Foundations 12, No. 1, pp. 17-36. Japanese Society of Soil Mechanics and Foundation Engineering.

Ozawa, Y. and Duncan, J.M., (1976a). "Elasto-Plastic Finite Element Analyses of Sand Deformation", Proceedings of the





2nd International Conference on Numerical Methods in Geomechanics, Blacksburg, Virginia, June, pp.243-263.

Ozawa, Y. and Duncan, J.M., (1976b). "Correction to Elasto-Plastic Finite Element Analyses of Sand Deformations", Proceedings of the 2nd International Conference on Numerical Methods in Geomechanics, Blacksburg, Virginia, June, pp.III-1477, III-1479.

Palmer, A.C., and Rice, J.R., (1973). "The growth of slip surfaces in the progressive failure of overconsolidated clay, " Proc. Roy. Soc. Lond. A 332, pp. 527-548.

Poorooshasb, H.B., Holubec, I., and Sherbourne, A.N. "The yielding and flow of sand in triaxial compression," Canadian Geotechnical Journal 3, No. 4, 179.

Prevost, J.H. and Hoeg, K., (1975). "Soil mechanics and plasticity analysis of strain-softening," Geotechnique, Vol. 25, pp. 279-298.

Roscoe, K.H., (1970). "The Influence of Strains in Soil Mechanics," Tenth Rankine Lecture, Geotechnique, Vol. 20, No. 2, pp. 129-170.

Roscoe, K.H., and Burland, J.B., (1968). "On the Generalized Stress-Strain Behavior of 'Wet' Clay," Engineering



Plasticity, Edited by Heyman and Leckie, Cambridge University Press, pp. 535-609.

Roscoe, K.H., Schofield, A.N., and Wroth, C.P., (1958). "On the Yielding of Soils," *Geotechnique*, London, England, Vol. 8, No. 1, March, pp. 22-52.

Rowe, P.W., (1962). "The Stress-Dilatancy Relation for Static Equilibrium of an Assembly of Particles in Contact," *Proceeding of the Royal Society of London, Series A*, Vol. 269, pp. 500-527.

Rowe, P.W., (1963). "Stress-Dilatancy, Earth Pressure, & Slopes," *Journal of the Soil Mechanics and Foundation Division, ASCE*, Vol. 89, No. SM3, May, pp. 37-61.

Rowe, P.W., (1971). "Theoretical Meaning and Observed Values of Deformation for Soils," *Stress-Strain Behavior of Soils*, Proc. Roscoe Memorial Symp. Camb. G.T.Foulis, Henley-on-Thames.

Rowe, P.W. and Peaker, K., (1965). "Passive Earth Pressure Measurements." *Geotechnique*, 15, pp. 57-78.

Sandler, I.S., DiMaggio, F.L., and Baladi, G.Y., (1976). "Generalized Cap Model for Geological Materials," *Journal of the Geotechnical Engineering Division, ASCE*, Vol. 102,



No.GT7, Proc. Paper 12243, July, pp. 683-699.

Scott, R., and Ko, H.Y., (1969). "Stress-deformation and strength characteristics," Proc. 7th Int. Conf. Soil Mech. Found. Eng., Mexico, State-of-the-Art Volume, pp. 1-47.

Smith, I.M., (1973). "Numerical analysis of plasticity in soils," Symposium on Plasticity and Soil Mechanics, pp. 279-289, Cambridge, U.K.

Terzaghi, K., (1934). "Large Retaining Wall Tests. I. Pressure of Dry Sand." Engineering News Record, 112, pp. 136-140.

Terzaghi, K., (1954). "Anchored Bulkheads," Trans. Am. Soc. Civ. Engrs. 119, p. 1243.

Tschebotarioff, G.P., (1951). Soil Mechanics, Foundation and Earth Structures, New York, McGraw-Hill.

Tschebotarioff, G.P. and Johnson, E.G., (1953). "The Effects of Restraining Boundaries on the Passive Resistance of Sand," Princeton University.

Wong, K.S., (1978). "Elasto-Plastic Finite Element Analyses of Passive Earth Pressure Tests", thesis presented to the University of California, at Berkeley, Calif., in partial





fulfillment of the requirements for the degree of Doctor of Philosophy.

Wroth, C.P., (1972). "General Theories of Earth Pressures and Deformation," Proc. 5th European Conf. on Soil Mechanics and Foundation Engineering, Madrid, Vol. 2, pp. 33-52.

Wroth, C.P., (1973). "A brief review of the application of plasticity to soil mechanics," Symposium on Plasticity and Soil Mechanics, pp. 279-289, Cambridge, U.K.

Wroth, C.P., (1975). "In situ measurements of initial stresses and deformation characteristics," Proc. Conf. on In Situ Measurements of Soil Properties,

Wroth, C.P., (1976). "Review of Earth Pressure Theory and Earth Behavior," Geotechnical Lecture Series on Lateral Earth Pressure, Boston Society of Civil Engineers, pp. 1-51.

Wroth, C.P., (1979). "Correlations of Some Engineering Properties of Soils." Proc. of Second International Conf. on the Behavior of Off-Shore Structures, London, England. Vol. 1, pp. 121-132.

Wroth, C.P. and Wood, D.M., (1978) "The correlation of Index properties with some basic engineering properties of soils," Canadian Geotechnical Journal 15, 2, pp. 137-145.





Zienkiewicz, O.C., Humpheson, C., and Lewis, R.W., (1975). "Associated and Non-Associated Visco-Plasticity and Plasticity in Soil Mechanics," *Geotechnique*, Vol. 25, No. 4, Dec., pp. 671-689.

Zienkiewicz, O.C., (1971). *The Finite Element Method in Engineering Science*. London: McGraw-Hill Book Company.



## APPENDIX A

### DERIVATION OF SOIL PARAMETERS

The procedures to derive stress-strain parameters of Lade's work hardening model are presented here by using dense Monterey No.0 sand ( $e=0.577$ ). There are nine parameters in this model, and they can be obtained from drained conventional triaxial compression test data. A minimum of two and preferably three or more triaxial tests with different confining pressures are required. For the evaluation of elastic parameters, a minimum of two unloading-reloading branches are necessary. Figure A-1 shows three triaxial test data which are used to derive the parameters.

#### 1. DERIVATION OF PARAMETERS FOR ELASTIC STRAINS

The procedures described here for elastic parameters can also be found in Duncan and Chang (1970).

Unloading-reloading branches of the curves given in Figure A-1 are used first to calculate the elastic modulus,  $E_{ur}$ . In a log-log plot,  $E_{ur}$  versus  $\sigma_3$  relation is shown in Figure A-2. The slope of the straight line connecting the data points gives the value of parameter  $n$ . The modulus value at confining pressure equal to unity provides the magnitude of  $K_{ur}$ .



## 2. DERIVATION OF PARAMETERS RELATED TO PLASTIC STRAINS

There are six parameters for the calculation of plastic strain increments. Derivation of these parameters follows.

### a) PARAMETER $K_1$ IN FAILURE CRITERION

Stress level,  $f$ , corresponding to peak strength is calculated for each stress-strain curve shown in Figure A-1. The results are:

$$K_1 = 81.24 \quad \text{for} \quad \sigma_3 = 1.2 \text{ kg/sq.cm}$$

$$K_1 = 78.95 \quad \text{for} \quad \sigma_3 = 0.6 \text{ kg/sq.cm}$$

$$K_1 = 88.93 \quad \text{for} \quad \sigma_3 = 0.3 \text{ kg/sq.cm}$$

The mean value of  $K_1$  is used in the analysis of instrumented wall.

### b) PARAMETER A IN PLASTIC POTENTIAL

Parameter A is introduced in Eqn. 2.6 for the calculation of  $K_2$ . It is related to the direction of plastic strain increments. Steps to be followed for the calculation of A are given next.

- Calculate elastic strain increments (use Eqn. 2.3).
- Subtract elastic strain increments from total strain increments to find plastic strain increments.
- For each stress increment, calculate  $v_p$  which is defined next.

$$-v = \frac{\Delta \epsilon_3^p}{\Delta \epsilon_1^p} \quad \dots \text{Eqn. A.1}$$





-The next step requires the following calculations.

An explicit form for  $\nu_p$  is derived first by using Eqn.2.5 and Eqn. 2.7.

$$-\nu = \frac{\lambda \cdot K_2 \left( \frac{3}{K_2} \cdot I_1^2 - \sigma_1 \cdot \sigma_3 \right)}{\lambda \cdot K_2 \left( \frac{3}{K_2} \cdot I_1^2 - \sigma_3^2 \right)} \quad \dots \text{Eqn. A.2}$$

If Eqn. A.2 is rearranged, an expression can be obtained for  $K_2$ .

$$K_2 = \frac{3 \cdot I_1^2 (1 + \nu)}{\sigma_3 (\sigma_1 + \sigma_1 \cdot \sigma_3)} \quad \dots \text{Eqn. A.3}$$

All variables on the right hand side of Eqn. A.3 are known.

-Plot  $K_2$  versus  $f$  for each load increment. As shown in Figure A-3, the slope of  $K_2$  versus  $f$  relation gives the parameter  $A$ .

#### c) PARAMETERS RELATED TO WORK HARDENING LAW

Experimental results by Lade (1972) show that for a constant confining pressure, there is a unique relation between  $W_p$  and  $f$ . The values of  $W_p$  and  $f$  calculated from experimental data for dense Monterey No.0 sand are shown in Figure A.4. As a convenience in fitting curves, the stress level at which  $W_p$  is practically equal to zero is called threshold stress level,  $f_t$ . As shown in Figure A.4,  $f_t$  is chosen 38. The relation between  $W_p$  and  $(f - f_t)$  is approximated by hyperbolas, for which the following



expression is used.

$$(f - f_t) = \frac{W_p}{a + b \cdot W_p} \quad \dots \text{Eqn. A.4}$$

The values of  $a$  and  $b$  can be derived from a plot on transformed axes as shown in Figure. A.5. In this Figure,  $a$  is the intercept of a straight line with the vertical axis, and  $b$  is the slope of that straight line. As shown in Figure. 2.3, the reciprocal of  $b$  is equal to  $(f - f_t)_{ult}$ . In order to find the parameter  $r_f$ , Eqn. 2.11 is utilized: An average value of  $r_f$  is used in the finite element analysis of rotating wall (see Table 7.2).

The value of  $a$  increases with increasing confining pressures. This relation is given by Eqn. 2.9. The parameters  $M$  and  $l$  of Eqn. 2.9 are derived from a log-log plot for  $a$  versus  $\sigma_3$  relation. Figure A.6 shows the variation of  $a$  with  $\sigma_3$  for dense Monterey No.0 sand.

Summary of all nine parameters is provided in Table 7.2.



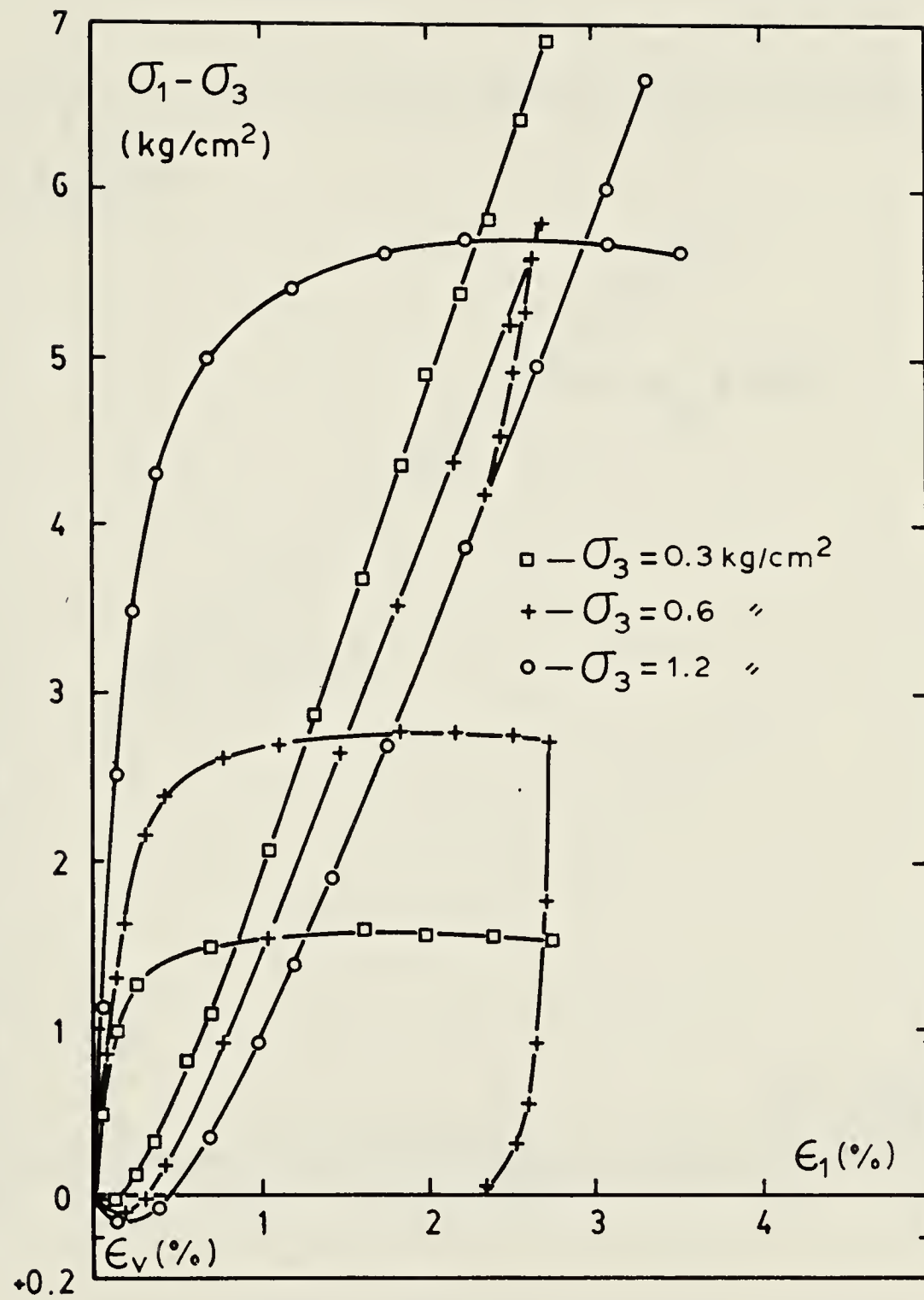


Figure A.1 Three drained conventional triaxial compression tests for dense Monterey No.0 sand. (After Lade, 1972)



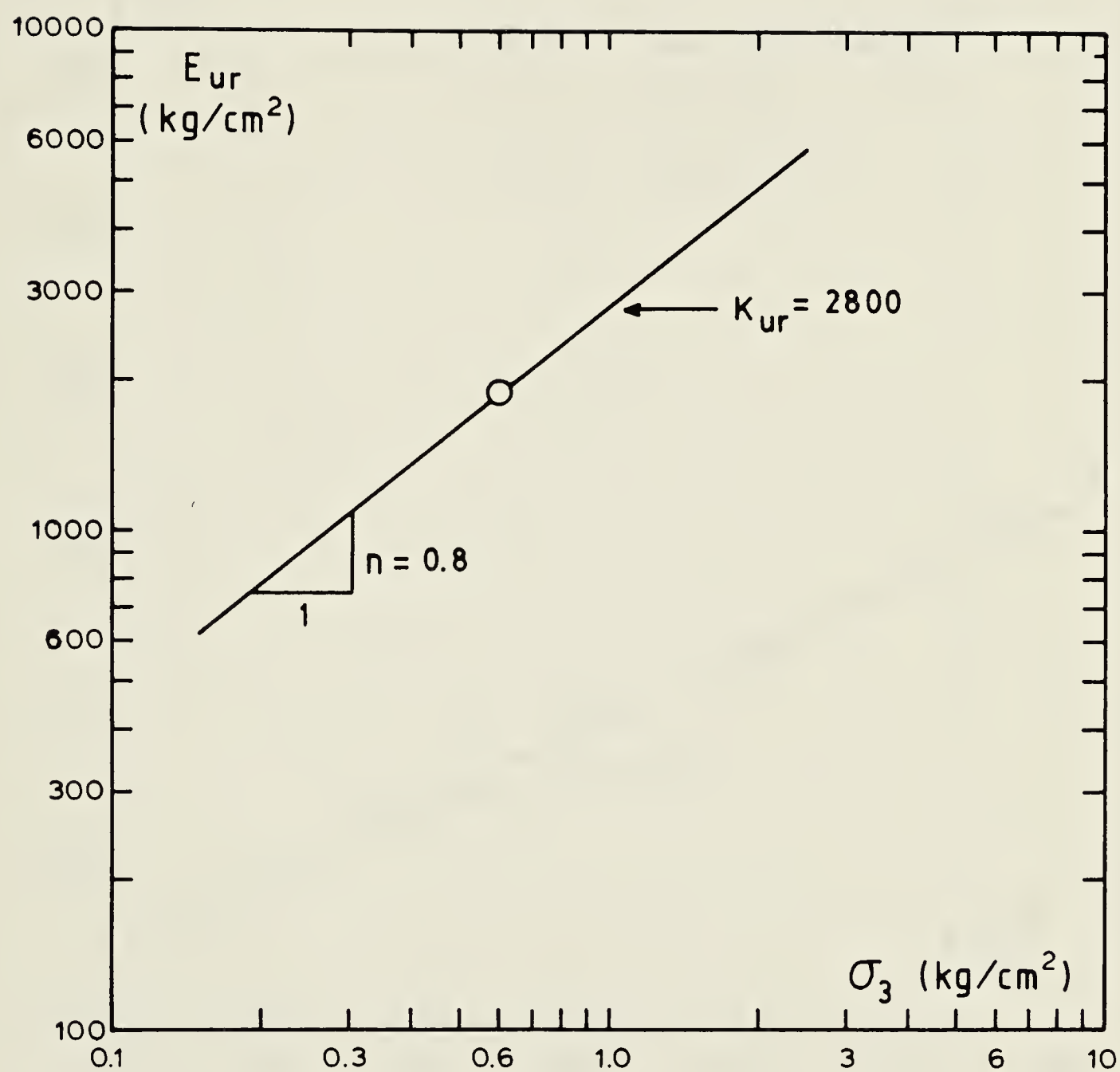


Figure A.2 Derivation of parameters for elastic strains





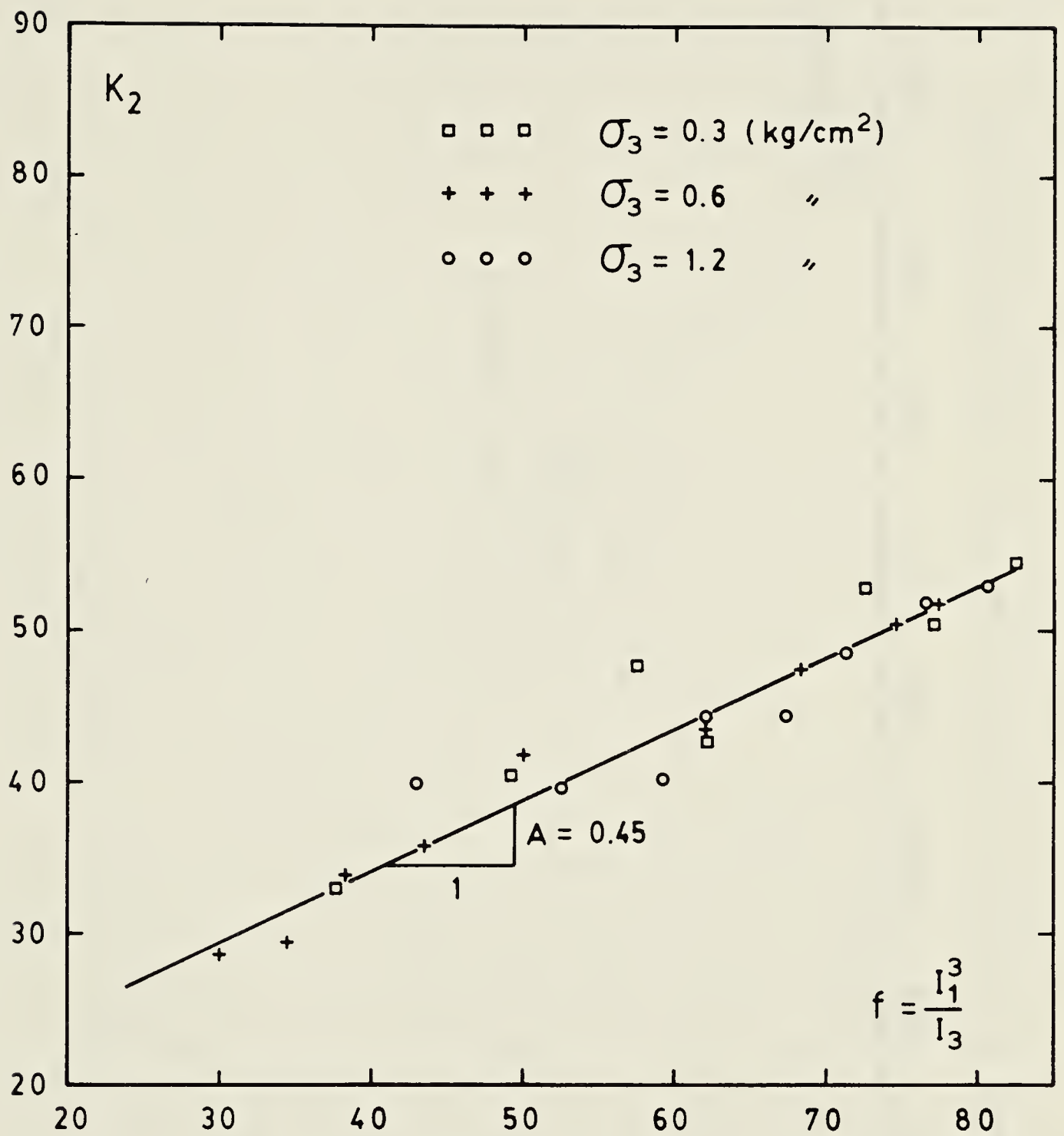


Figure A.3 Variation of  $K_2$  with stress level for dense Monterey No.0 sand.



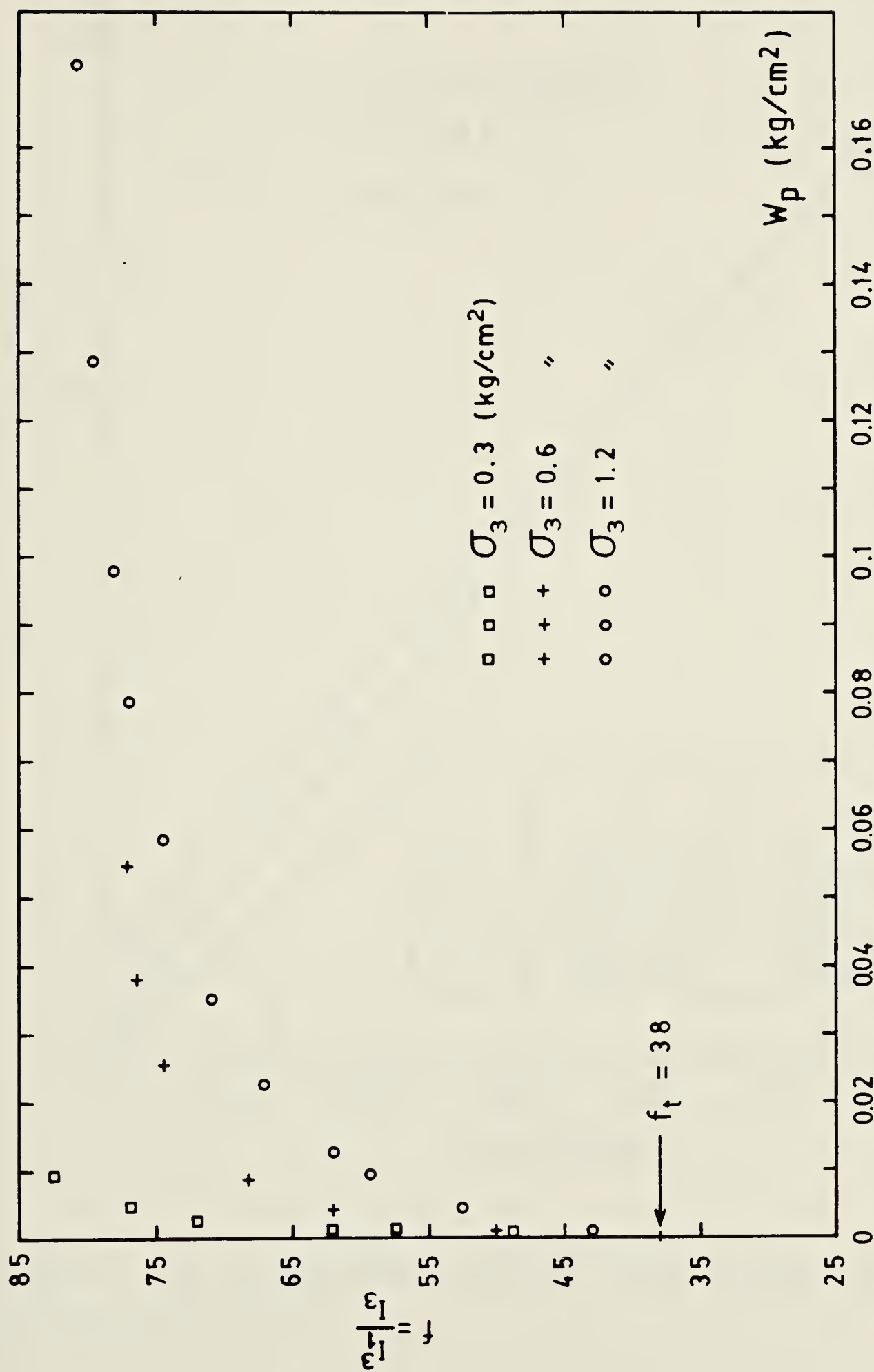


Figure A.4 Variation of plastic work for dense Monterey No.0 sand.



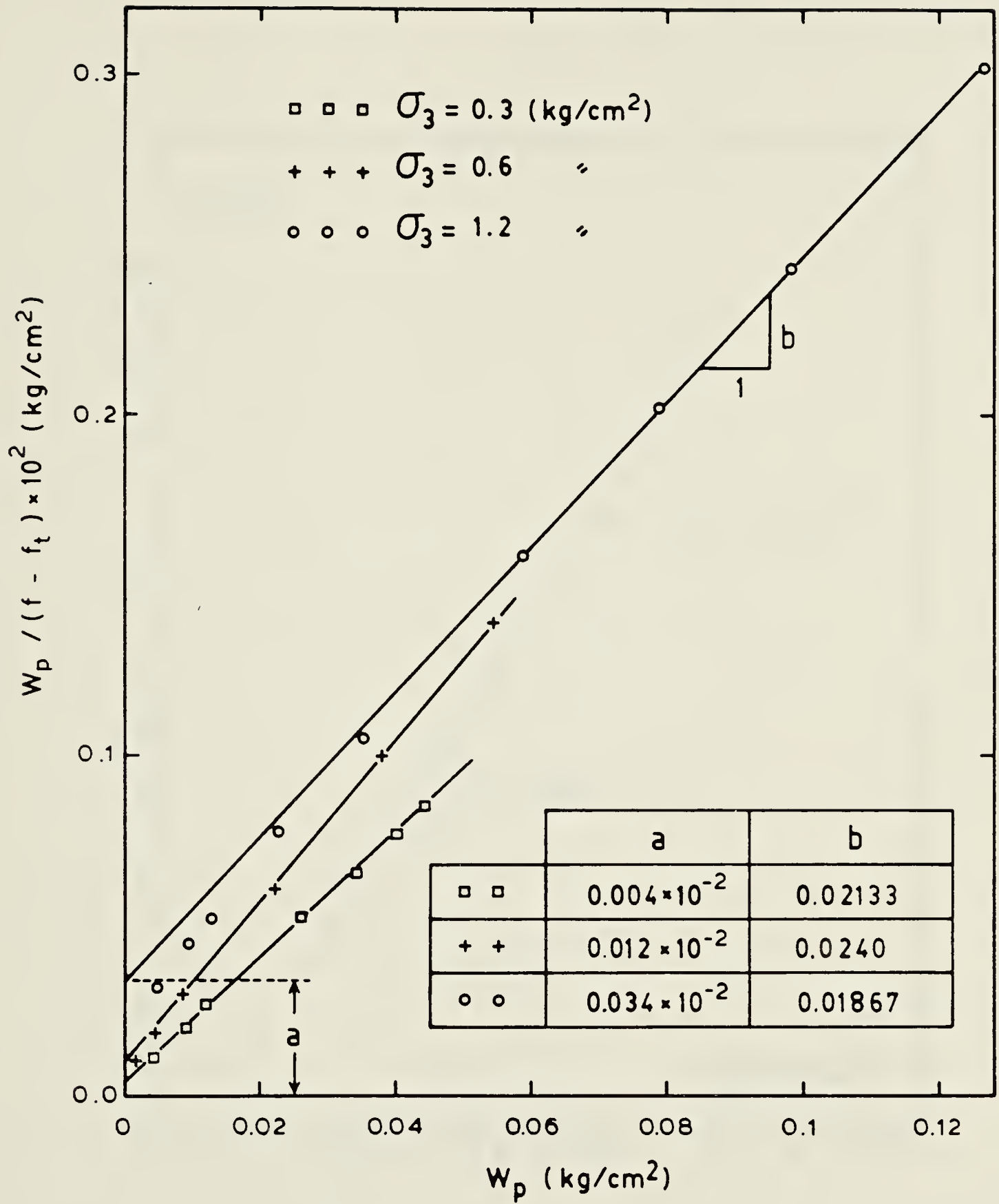


Figure A.5 Transformed plastic work curves for dense Monterey No.0 sand.





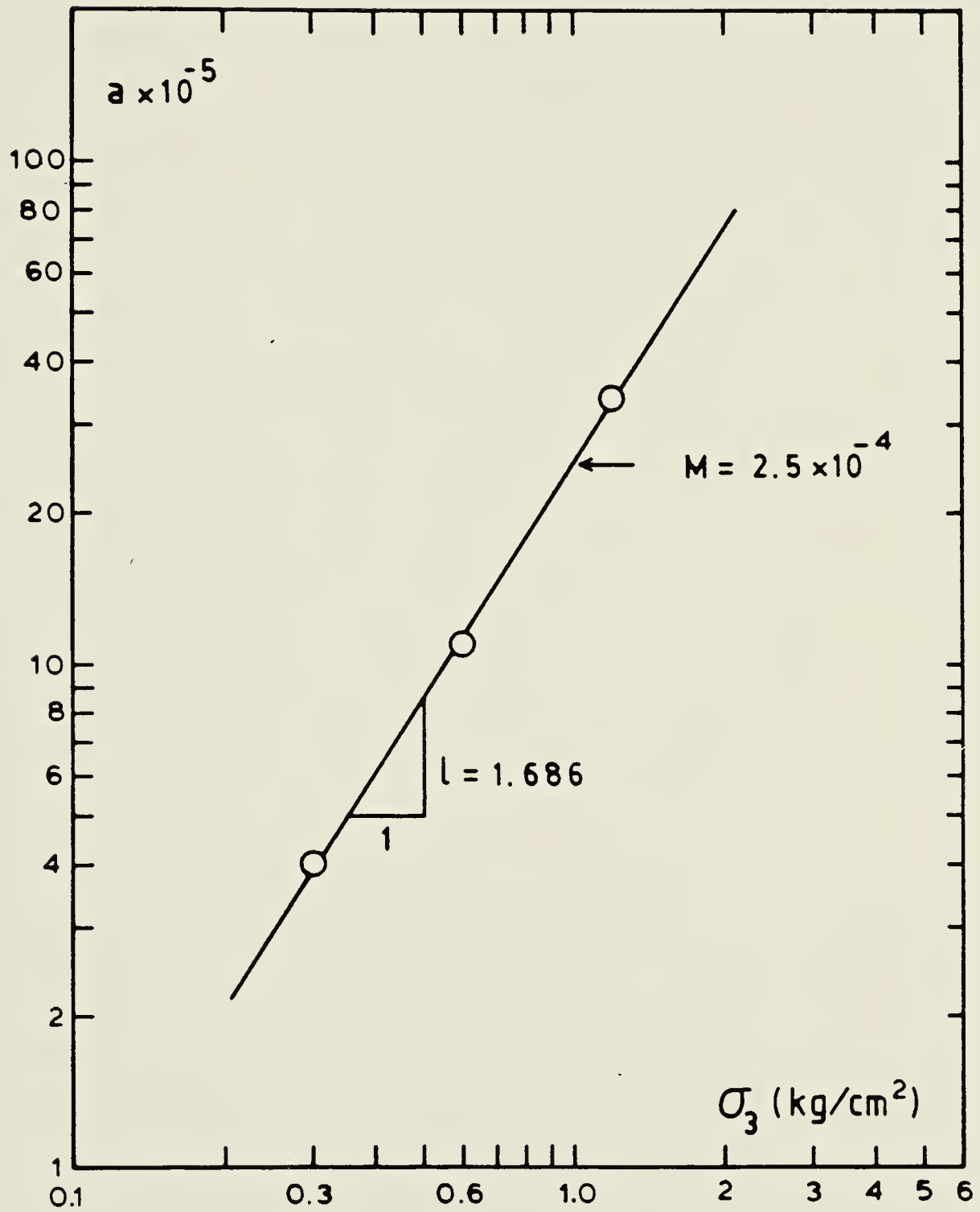


Figure A.6 Variation of initial slope of plastic curves with confining pressure for dense Monterey No.0 sand.







**B30307**